

Reduction of NO₂ by Hydrocarbons over H-form Zeolites

Martin L. Smidt

2003

Ph.D. thesis
University of Twente



Twente University Press

Also available in print:
<http://www.tup.utwente.nl/>

Reduction of NO₂
by Hydrocarbons
over H-form Zeolites

Promotie commissie

Voorzitter/Secretaris:	Prof. C. Hoede	(U Twente)
Promotor:	Prof. dr. J. A. Lercher	(T U München)
Assistent-promotor:	Dr. K. Seshan	(U Twente)
Leden:	Prof. dr. ir. L. Lefferts	(U Twente)
	Prof. dr. D. Blank	(U Twente)
	Prof. dr. J. A. Moulijn	(T U Delft)
	Prof. dr. A. Blik	(U v Amsterdam)
Deskundige	Dr. J. H. Bitter	(U Utrecht)

This work was financed by and carried out in the framework of the project “Research and Development- Program ENV 2C – subprogram: Technologies to Protect and Rehabilitate the Environment - Emission Abatement” of the Commission of European Communities.



Twente University **Press**

Twente University Press, P.O. Box 217, 7500 AE Enschede, www.tup.utwente.nl

Print: Océ Facility Services, Enschede

© Martin L. Smidt, Enschede, The Netherlands 2003

ISBN 90 365 1881 4

REDUCTION OF NO₂ BY HYDROCARBONS OVER H-FORM ZEOLITES

PROEFSCHRIFT

ter verkrijging van
de graad van doctor aan de Universiteit Twente,
op gezag van de rector magnificus,
prof. dr. F. A. van Vught,
volgens besluit van het College voor Promoties
in het openbaar te verdedigen
op vrijdag 14 maart 2003 te 16:45 uur

door
Martin Lucas Smidt
geboren op 9 oktober 1971
te Apeldoorn

Dit Proefschrift is goedgekeurd door de promotor
Prof. Dr. J. A. Lercher
en assistent-promotor
Dr. K. Seshan

To my parents,

Acknowledgements

Many people have in one way or another contributed to the completion of this thesis for which I am very grateful. First I want to thank Professor Johannes Lercher, for offering me the position in his group that enabled me to perform the research described in this thesis. I thank Seshan for being my co-promotor and supervisor, for the fruitful discussions and guidance throughout my PhD. I would like to thank all people that came across my path during my stay in Twente and in Munich. I thank Jan van Ommen, Leon Lefferts for their time and the fruitful discussions, Bert for being the most adorable *chef de cuisine* of in the Twente *gift-mixers* labs. Karin, Cis and Regina for the most efficient assistance through Twente bureaucraties, Louise for the XRF measurements, Herman Koster for the XRD analysis's, Sergio for the introduction into the wonders of lab equipment and the secrets of 'how to keep your boss happy'. I thank the 'old' Twente crew, Marco, Laurent, Laszlo L., Laszlo D., Gautam, Victor, Sheila, Cristina, Jean-Pierre, Katja, Takeshi, Gerhard and Olivier, the many students that came for short or longer time to Twente and made the group even more 'alive and kicking', David, Marta, Isaac and the 'new' people in Twente, Nabeel, Valer, Mujeebur, Zhu, Sepp, Jiang Xu, Li, Babych and Kazu that in the little time that we could share I came to value a lot. I thank the present and former colleagues of the Munich group, Cristina, Hilton for being a wonderful person, Fred for being the best not-always-winning pool partner. Special thanks to Jan-Olaf and Jan K. for the last minute proof reading, to my roommates Anil, Alex G., Shouroung, Xuebing, to Linda, Adam and Florencia for being the best friends one can have, Alex H. for never failing a helping hand, and to all others, Christian S., Andreas F., Jochen, Jenő, Oriol, Stefan G., Krishna, Toshi, Maria, Renate, Su Ru Qing, Christian W., Iker, Hiroaki, Josef, Thomas, Gabriela, Andy, Frau Heike Schüler and Frau Heidi Hermann for their lead through the German bureaucraties, Martin N., Xaver, Andreas M. and the people from the mechanics department for their ready assistance, and Dr. Bratz for the homebrew. Special thanks to Bertha who has been more than a friend and a great help through the hard life of a PhD. The words fail me to express my gratitude to Virginie who has been a great inspiration and motivation and who has given more love and understanding that I am creditable for. 'Merci beaucoup' to Christiane, Janek, Marianna and Alexia for the warm welcome into their family and making me feel at home in France. En als laatste maar zeker niet de minsten wil ik mijn ouders, Stefan en Marieke bedanken voor de onvoorwaardelijke steun, warmte en toeverlaat.

Martin
February 2003

Table of Contents

Chapter 1 Introduction	1
1.1 The NO _x problem	
1.2 NO _x sources	
1.3 Legislation	
1.4 Current NO _x reduction technologies	
1.4.1 NH ₃ Selective Catalytic Reduction	
1.4.2 CO/H ₂ -SCR, three-way catalyst	
1.4.3 Storage Reduction Process	
1.5 HC-SCR	
1.5.1 HC-SCR catalysts	
1.5.2 Zeolite catalysts	
1.5.3 Reaction mechanisms	
1.6 Scope of this thesis	
Chapter 2 Reduction of NO₂ by propene over parent and steamed NaH-Y zeolite	17
2.1 Introduction	
2.2 Experimental	
2.2.1 Materials	
2.2.2 Infrared spectroscopy	
2.2.3 Kinetic activity tests	
2.3 Results	
2.3.1 IR on parent and steamed NaH-Y in contact with C ₃ H ₆ and O ₂	
2.3.2 IR on parent and steamed NaH-Y in contact with NO ₂ , C ₃ H ₆ and O ₂	
2.3.3 Kinetic measurements in the presence and absence of O ₂	
2.3.4 Kinetic measurement using increasing propene feed concentrations	
2.4 Discussion	
2.4.1 Influence of O ₂	
2.4.2 Effect of steaming	
2.4.3 Effect of deactivation by formation of carbonaceous deposits	
2.4.4 Effect of C ₃ H ₆ feed concentration on N ₂ selectivity	
2.4.5 Mechanism and selectivity	
2.5 Conclusions	

Chapter 3 Reduction of NO₂ by C₃H₆ and C₃H₈ over H-form zeolites **45**

- 3.1 Introduction
- 3.2 Experimental
 - 3.2.1 Materials
 - 3.2.2 Infra red spectroscopy
 - 3.2.3 Kinetic activity tests
- 3.3 Results
 - 3.3.1 Reduction of NO₂ by C₃H₆
 - 3.3.2 Reduction of NO₂ by C₃H₈
 - 3.3.3 Influence of C₃H₆ partial pressure on NO₂ conversion
 - 3.3.4 Identification of adsorbed species by IR spectroscopy
- 3.4 Discussion
 - 3.4.1 Influence of C₃H₆ partial pressure
 - 3.4.2 Sensitivity for deactivation
 - 3.4.3 Activity of H-MOR at high temperatures using propene
 - 3.4.4 C₃H₈ activation
 - 3.4.5 On a possible reaction mechanism
- 3.5 Conclusions

Chapter 4 Role of oxygenated intermediates in the reduction of NO₂ by C₃H₆ over NaH-Y zeolite **75**

- 4.1 Introduction
- 4.2 Experimental
 - 4.2.1 Catalyst and reactants
 - 4.2.3 Infrared spectroscopy
 - 4.2.4 Kinetic measurements
- 4.3 Results
 - 4.3.1 Kinetic experiments with NO, NO₂, O₂ and C₃H₆
 - 4.3.2 Kinetic experiments with increasing reductant feed concentration
 - 4.3.3 Characterization of adsorbed species by IR spectroscopy
 - 4.3.4 Reactivity of adsorbed species with NO₂
 - 4.3.5 IR spectroscopy on adsorbed species at 200°C
 - 4.3.6 Reactivity of adsorbed nitriles
- 4.4 Discussion
 - 4.4.1 Formation of oxygenates during NO_x reduction
 - 4.4.2 Identification of adsorbed species
 - 4.4.3 Mechanism for the reaction of NO₂ with C₃H₆ on NaH-Y zeolite
- 4.5 Conclusions

Chapter 5 Kinetic study on the reduction of NO using separated oxidation and reduction steps	107
5.1 Introduction	
5.2 Experimental	
5.2.1 Catalysts and reactants	
5.2.4 Catalytic tests	
5.3 Results and discussion	
5.3.1 Oxidation of NO and reduction of NO ₂	
5.3.2 Catalytic tests using separated oxidation and reduction catalysts	
5.3.3 Reduction of NO/NO ₂ mixtures over γ -alumina	
5.3.4 Reductant efficiency	
5.3.5 Effectiveness of intermediate addition of reductant	
5.4 Conclusions	
Chapter 6 Summary	125
6.1 Summary	
6.2 Samenvatting	
6.3 Zusammenfassung	
6.4 Résumé	
Curriculum Vitae	140
List of Publications	141

Chapter 1

Introduction

Chapter 1

1.1 The NO_x problem

The emission of nitrogen oxides into the atmosphere causes great danger to our environment [1]. In contact with water NO_x forms nitric acid. In the atmosphere this results in acid rains with the corresponding severe damaging affects to flora and fauna. In combination with volatile fossil fuel components and the right weather conditions (sunny, little wind and a temperature inversion layer in the troposphere) photochemical smog is formed. Under the influence of sunlight NO₂ and these organic compounds react to form a wide series of harmful substances such as peroxyacetylnitrates (PAN) and ozone. The exposure to high NO_x concentrations in the air can cause inflammation of lung tissue, bronchitis and pneumonia. Ozone is a useful substance in the ozone layer (about 90 km above earth surface) where it absorbs highly energetic UV light, but closer to the surface ozone is very poisonous giving rise to similar symptoms as NO_x and related irritating and oxidizing substances [2]. NO_x can not only enhance the formation of ozone but also the removal of it and so contribute to the depletion of ozone from the ozone layer. NO_x can, similar to CO₂, absorb long wave infrared light and so, when accumulated in the atmosphere, contribute to the green house effect.

1.2 Sources of NO_x

Nitrogen oxides are formed by the production of nitric acid, combustion of fossil fuels, oxidation of NH₃, biological decompositions of proteins in the soil [3], lightning, and volcanic activity. The latter three are natural sources and thus not under our control. In the 1st half of last century nitric acid plants were producing large amounts of tail gases that colored brown by the high content of NO₂. Such excesses were outlawed in the 1950. The NO_x formed by the combustion of fossil fuels can be divided into three groups; 1: Thermal NO_x,

produced by the oxidation of N_2 by O_2 at very high temperatures ($>1000^\circ C$), 2: Fuel NO_x , which is formed by the oxidation of nitrogen containing fuel compounds and 3: Prompt NO_x which is formed by the oxidation of HCN. HCN is formed as a product of organic compounds reacting with nitrogen radicals. Formation of prompt NO_x is only significant in very fuel-rich flames. The nitrogen (in nitrogen containing organic compounds) can largely be removed from the fuel at the refinery by hydrotreating and thus remains only thermal NO_x as the main source of NO_x formed during the combustion of fossil fuels.

NO_x is a general name for a collection of in total eight neutral oxides of nitrogen (NO , NO_2 , NO_3 , N_2O , N_2O_2 , N_2O_3 , N_2O_4 , N_2O_5) [4]. Even though this many NO_x variations are known the NO_x formed by combustion consists mainly of NO ($>90\%$), NO_2 and traces of N_2O . Other NO_x species are thermodynamically unstable and easily decompose into the former three. Combustion of fossil fuels is used in general to free energy for the propulsion of vehicles such as cars, boats and airplanes or to generate electricity in power plants, heating installations and waste inclinators. The total amount of NO_x produced by these mobile and stationary sources are estimated around 20 million tons per year [5] in the USA and similar amount in Europe [6].

1.3 Legislation

To reduce the amount of NO_x emissions produced from stationary and mobile sources many governments worldwide have installed restrictive legislations. The USA was the first country to install legislation, known as the Clean Air Act, on NO_x production by limiting the NO_x emission of newly build steam boiler heaters to 78 ppm (160 mg/m^3) for 400 MW power stations. Although this limit was not feasible at the time of installation, following amendments to further restrict emissions were installed in 1971, 1977 and 1990

Chapter 1

[6]. Federal legislations in the USA were often preceded by national legislations in especially the state of California. The restrictions set very widely for the many different sources but to indicate the level of NO_x emission for passenger cars in USA at the moment is limited to 0.4 g/mile and will be reduced to 0.2 g/mile in 2004 [7, 8]. In the USA the limits for stationary sources are depending on the ozone level in the area so that in times of serious ozone problems the BACT regulations apply while else the LAER regulations apply. For gas turbines the BACT results in 9-25 ppm of NO_x and the LAER in 3-15 ppm NO_x (both at 15% O₂).

Japan installed in 1973 a limit for the emissions of NO_x, which were gradually lowered until 1979. Nowadays the for large gas-, oil-, and coal-fired power plants are set at 60, 130 and 200 ppm respectively.

In Europe the European economic community installed in 1970 a directive to limit the NO_x emissions of motor vehicles (Directive 70/220/EEC) although until 1988 only Germany (FRG) and Sweden had installed strict limitations on NO_x emissions while other countries had only guidelines (Netherlands) or nothing at all (United Kingdom, Italy, France). In 1998 directive 98/69/EC was published which defined limitation levels for the years 2000 (Euro III), 2005 (Euro IV) and 2008 (Euro V). The Euro III norm limits the NO_x emissions of passenger cars to 0.15 - 0.21 g/km for petrol-fuelled cars and 0.5 - 0.78 g/km for diesel fuelled cars. In the Euro V norm these limitations are further brought down to 0.08 - 0.11 g/km and 0.25 - 0.39 g/km for petrol and diesel fuelled cars respectively [9].

1.4 Current NO_x reduction technologies

In order to meet these legislative restrictions technologies are being developed all around the world one of which is the removal of NO_x from exhaust

gases and is generally referred to as 'DeNO_x'. A brief summary on most common DeNO_x techniques is presented below.

1.4.1 NH₃ Selective Catalytic Reduction

The removal of NO_x from industrial effluents started in the 1950's when nitric acid plants produced large amounts of tail gases containing so much NO_x that they colored brown [19]. Various reductants such as hydrogen, methane and other hydrocarbons were tested with a range of noble metal catalysts. In the 1970's the catalytic reduction using NH₃ as reductant was developed mainly in Japan using a vanadia/titania catalyst [10]. The overall reaction proceeds according to reaction (1).



Although this process is widely applied and many authors have proposed possible mechanistic steps a general consensus on the complete mechanism has not been achieved yet.

1.4.2 CO/H₂-SCR, three-way catalyst

The application of NH₃-SCR on automotive combustion engines causes severe technological problems. Exhaust of these engines operating at stoichiometric Air/Fuel ratio contain enough H₂, CO and hydrocarbons to enable the reduction of all NO_x produced in the combustion chambers. CO and uncombusted hydrocarbons are like NO_x undesired effluents. The removal of NO_x using these available reductants thus handles three problems at once and hence is the catalysts, which enables this process called the three-way catalyst, which is now widely applied. The catalysts contains noble metals such as Pt, Pd

Chapter 1

and Rh and can efficiently operate in stoichiometric conditions determined by the so-called lambda value see figure 1.1 [11]. In fuel-rich conditions ($\lambda < 1$) the unburned hydrocarbons cannot be oxidized while in lean conditions ($\lambda > 1$) the NO_x cannot be reduced.

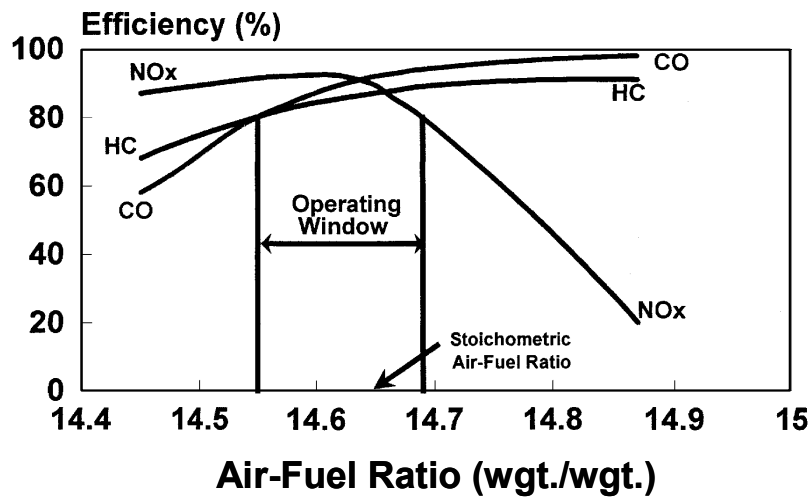


Figure 1.1 Three-Way catalysts conversion efficiency of CO, NO_x and HC as a function of Air-Fuel ratio [10].

1.4.3 Storage Reduction Process

One promising technology forms the so-called NO_x Storage Reduction catalyst [12,13]. The air/fuel ratio applied alternates from between a Lean and a Rich cycle. In the Lean cycle the catalyst oxidizes NO to NO_2 , which is then adsorbed as nitrates on the catalyst. When the catalysts approaches saturation the engine is switched to a fuel rich cycle (slightly below stoichiometric) so that the adsorbed NO_x can be reduced. The catalysts used are in principle a three-way catalyst with an additional NO_x storage function in the form of Barium oxide. Although this principle is still being developed it is far more close to practical application than any hydrocarbon-SCR system. The aim is to keep the rich cycle as short as possible, compared to a long lean cycle, in order to waist a minimum

of hydrocarbons on the combustion of excess of oxygen present in the lean cycle.

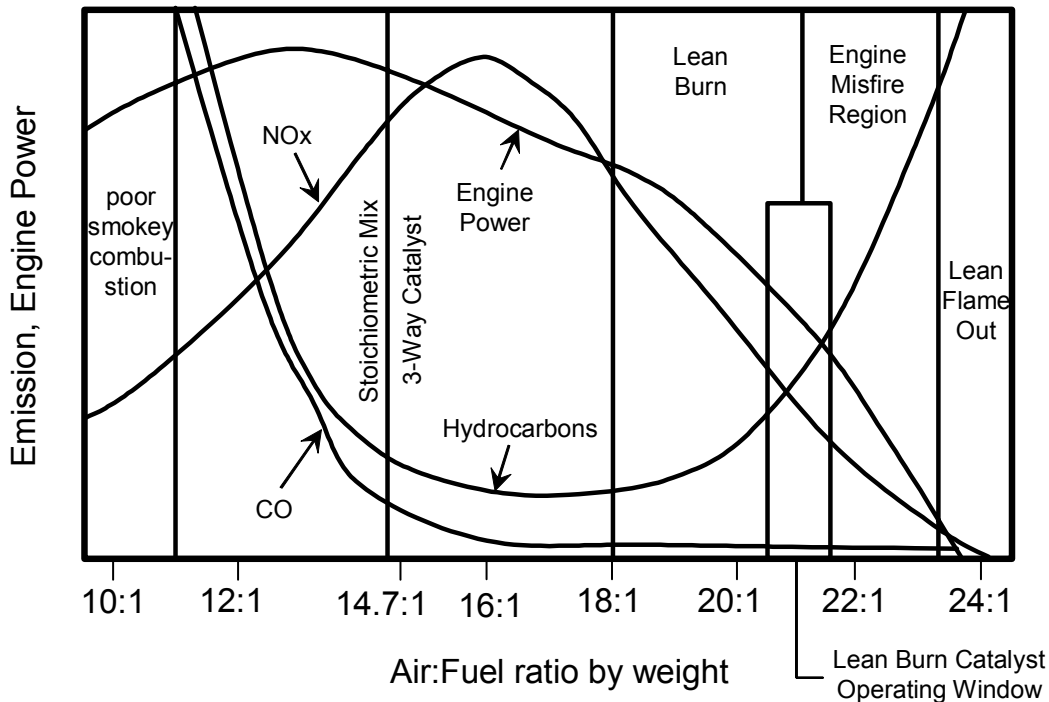


Figure 1.2 Changes in emission and engine power of internal combustion spark-ignited engines, showing three-way and lean-burn operating windows with air/fuel ratio [13, 18]

1.5 HC-SCR, selective catalytic reduction using hydrocarbons

The fuel consumption of an internal combustion engine (Otto engine) that runs with a relative high air/fuel ratio, so called Lean Burn engine, is about 10% below that of an engine running at a stoichiometric air/fuel ratio. Another advantage of running lean is that the NO_x formation is strongly reduced with increasing air/fuel ratio. The increase of air/fuel ratio is though limited since a too high air/fuel ratio will result in misfire and finally a total failure the engine. Figure 1.2 shows the NO_x , CO and hydrocarbon emissions and the engines power as function of the air/fuel ratio [19, 14]. The marked area shows the

Chapter 1

air/fuel-window in which a lean-burn engine has to operate in order to obtain the desired fuel-efficiency. A disadvantage is that in such conditions the three-way catalyst becomes ineffective for NO_x removal. The development of catalysts able to reduce NO_x in oxygen rich conditions is thus desired. The catalytic reduction of NO_x using hydrocarbon reductants may hold a possible solution (HC-SCR). Hydrocarbons are available as they are used for the combustion or can be stored relative easily, as opposed to ammonia, which is not available and also not easily stored. The amount of hydrocarbons needed for the reduction of NO_x may be tuned by the air/fuel ratio as the amount of unburned hydrocarbons increased when approaching the misfire region, see figure 2. Excess of hydrocarbons can also relative easily be removed by an oxidation catalyst while excess of NH_3 will inevitably lead to NH_3 -slip or the oxidation to NO_x .

1.5.1 HC-SCR catalysts

In 1990 Iwamoto *et al.* [15] and Held *et al.* [16], reported simultaneously high NO decomposition activity on Cu-ZSM5 catalysts. Although the decomposition of NO (to N_2 and O_2 without the use of a reductant) is a relative slow process and likely will never lead to an satisfactory solution, decomposition of NO is an important factor in the reduction of NO by hydrocarbons. In the following 5 years Copper containing catalysts were extensively studied and much insight was obtained on the mechanism of NO reduction and on catalytic properties improving the catalysts performance [17-20]. Several mechanisms were proposed for the N_2 formation by decomposition that involve the oxidation and reduction of surface Cu as well as mechanisms which do not contain a redox step and is thus still a matter of debate [21-23]. Copper catalysts showed reduction activity using parafins ($\text{C}>2$), olefins, oxygenates while it was inactive using hydrogen, CO, methane or ethane. The presence of oxygen and water suppresses the catalysts decomposition activity

while the presence of SO₂ leads to a complete deactivation. Increasing the temperature above ~600°C lead to irreversible loss of activity.

Inspired by the partial success of copper supported catalyst many other transition and noble metals were tested [18, 23-25]. Early reports of Li and Armor [26-28] showed that Co/ZSM5 catalyst were active for the SCR of NO by methane. The activity was found to significantly increase in the presence of excess O₂. The presence of H₂O suppressed the activity. Bulk Co₃O₄ or CoO supported on Al₂O₃ or amorphous SiO₂/Al₂O₃ showed completely inactive what indicated that only finely dispersed Co on zeolites and thus emphasizes the role of the zeolite support.

Of all metals tested Platinum supported catalysts showed the highest activity and least sensitive towards the type of support or the presence of SO₂ [29, 30]. The presence of H₂O did not affect the N₂ yield but enhanced the removal of carbonaceous deposits and widen the temperature window in which N₂ can be formed. A major disadvantage of platinum is the high selectivity to N₂O (up to ~50%).

The catalytic function of these catalysts largely depends on the metal. Almost all off the metal supported catalyst show moderate to high activity for the unselective combustion of the reductant by O₂, which limits the temperature up to where the catalyst can be operated in order to reduce NO to N₂. A high reduction activity is usually combined with high oxidation activity so that, severely generalizing, the optimal N₂ yields for different catalysts are relative close although appear at different temperatures.

1.5.2 Zeolite supports

For the support of the metal phases many different oxides have been used such as SiO₂, Al₂O₃, ZrO₂ or zeolites. More active catalysts were obtained using acidic supports. Zeolites are porous alumina-silicates crystals with a

Chapter 1

surface area of 300-1000 m²/g [31, 32]. The aluminum atoms replace a silicium atom in the structure. Aluminum contains one proton less than silicium which thus needs to be compensated by a positively charged ion, such as H⁺ or Na⁺. These ions can be exchanged by any other positively charged ion (provided that the ion fits within the sterical constraints) like metal ions. Metal ions with higher valence than 1 can occupy 2 or more neighboring sites or are compensated with additional hydroxyl groups. Zeolites in the H form show strong Brønsted acidity, which can, often in combination with a metal, be beneficial for the catalysts performance.

1.5.3 Reaction mechanisms

The simplest mechanism for the formation of N₂ from NO is the decomposition, as mentioned earlier, where NO adsorbs on reduced metal ions, oxides or metallic clusters, subsequently decomposes to adsorbed N and adsorbed O atoms. Coupling of two adsorbed N atoms forms N₂, which is thermodynamically very stable and desorbs from the surface. Oxygen is formed in a similar way. Variations of this mechanism were postulated by several authors [21-23, 33, 34]. The decomposition mechanism appears to be particularly significant on platinum supported catalysts. The addition of a reductant can reduce the metallic surface through oxidation by the adsorbed oxygen atoms and so enhancing the N₂ formation.

A mechanism where NO is reduced by coke deposits is proposed by Ansell, Kikuchi and Obuchi *et al.* [35-37]. The latter two authors observed oscillations in the NO removal activity and attributed this to the formation and removal of coke deposits. Ansell performed transient kinetic test where they observed that, using propene and Cu/ZSM-5, independent of the presence of O₂, carbonaceous deposits were formed, which would then enable the reduction of NO. The presence of O₂ enhanced the reduction rate. They suggested that O₂

enabled the formation of adsorbed NO_x species through to formation of NO₂ over Cu sites.

The partial oxidation of the reductant prior to the formation of N₂ was proposed by several authors [38, 39]. Reductant like methanol, ethanol or propanol reacted more easily compared to their corresponding olefins or paraffins with NO. NO₂, which is significantly more reactive, than O₂ or NO possibly enables the oxidation of reductant. NO₂ is often observed in catalytic tests at temperatures outside the window where NO is converted at high rates while it is usually absent when NO is efficiently converted (to N₂ or N₂O) which indicates that NO₂ is converted faster than it is formed and may thus be a crucial intermediate. Misono *et al.* [40] suggested that NO₂ reacts with propene to form organo nitro (R-NO₂) and organo nitrite (R-ONO) compounds which are intermediates in the formation of N₂. Such compounds were observed by Xin *et al.* [41] using DRIFT spectroscopy. Although NO₂ is thermodynamically favored over NO, in excess O₂, the homogeneous formation of NO₂ is too slow to account for the reaction rates and therefore oxidation of NO to NO₂ occurs at catalytically active sites [42].

A typically elegant mechanism has been proposed for the reduction of NO in excess O₂ by methane over Co/ZSM5 type catalyst [43-49], which builds on ideas formulated in earlier work. Cant and Cowan showed by using isotopic labeling experiments that the rate limiting step in this reaction is the abstraction of a hydrogen radical from methane by NO₂ leading to a methyl radical (CH₃•) and HNO₂. The methyl radical reacts with another NO₂ to form nitro methane, which can decompose to CO₂ and ammonia or HNCO and H₂O. Ammonia reacts immediately with NO or NO₂ to form N₂. At temperatures below 300°C HNCO can condensate forming cyanuric acid, which can lead to deactivation of the catalyst. The cyanuric acid is easily hydrolyzed by water at temperatures above 300°C after which the catalyst regains its original activity. The mechanism for

Chapter 1

the decomposition of nitromethane has formed the basis for several other mechanisms that involve light hydrocarbons such as propane and propene [50].

1.6 Scope of this thesis

The oxidation of NO to NO₂ and subsequent reduction of NO₂ to N₂ is believed to be an important step in the selective reduction of NO by hydrocarbons in the presence of excess oxygen. Effective catalysts therefore need to possess oxidation as well as reduction functions. Brønsted acid sites of partially exchanged zeolites are believed to enhance the formation of N₂. Although detailed information of the mechanism by which N₂ is formed remains a subject of discussion. The aim of this thesis is to obtain insight in the functionality of zeolitic Brønsted in the formation of N₂. Brønsted acid sites are known to exhibit low activity for the oxidation of NO. Brønsted acidic zeolites are thus only interesting for the reduction of NO₂ which is therefore used as NO_x feed in this work.

In chapter 2 the activity and selectivity of the reduction of NO₂ by propene over H-Y zeolite and steamed H-Y zeolite are compared and evaluated. Special attention is given to the influence of steaming and the propene feed concentration. In chapter 3 the activity of different Brønsted acidic zeolites is compared using propene and propane. Intermediates observed by infrared spectroscopy are possible mechanistic steps. In chapter 4, a more detailed mechanistic study is deployed. Special attention is given to the importance of oxygenated intermediates in the formation of N₂. In chapter 5 a practical approach to avoid unselective combustion of the reductant is tested by using separate catalysts for the oxidation of NO and reduction of NO₂ with the intermediate addition of propene. Chapter 6 finishes by summarizing the main results and conclusions of this thesis.

References

- 1 “Air Pollution, The Automobile and Public Health”, Watson A.Y., Bates R., Kennedy D., Eds., National Academy Press, Washington DC.
- 2 T. Gow , M. Pidwirny, 1996,
<http://royal.okanagan.bc.ca/mpidwirn/atmosphereandclimate/smog.html>
- 3 “Cleaning our Environment: A Chemical Perspective”, a report by the Committee on Environmental Improvement, American Chemical Society, Washington DC., 2nd ed., 1978.
- 4 A. Striling, I. Pápai, J. Mink, J. Phys. Chem. 100 (1994) 2910.
- 5 J.N. Armor, Cat. Today 38 (1997) 163.
- 6 H. Bosch, F., Janssen, Cat. Today 2 (1988) 369.
- 7 Lox E.S.J., Engler B.H., in “Environmental Catalysis”, Eds.: Ertl G., Knözinger H., Weitkamp J., Wiley-VCF Verlag GmbH, Weinheim, 1999, p. 236.
- 8 Bertelsen B.I., Topics in Catalysis 16 (2001) 15.
- 9 Greening P., Topics in Catalysis 16 (2001) 5.
- 10 Busca APCATB 18.1.1998
- 11 Farrauto R.J., Heck R.M., Catal. Today 51 (1999) 351.
- 12 Miyoshi N., Matsumoto S., Katoh K., Tanaka T., Harada J., Takahashi N., Yokota K., Sugiura M., Kasahara K., SAE Paper 950809 (1995).
- 13 Takahashi N., Miyoshi N., Matsumoto S., Tanaka T., Shonjoh H., Iijima T., Yokota K., Suzuki T., Suzuki H., Yamazaki K., Tanizawa T., Tateishi S., Kasahara K., Catal. Today 27 (1996) 63.
- 14 Truex T.J., Searles R.A., Sun D.C., Platinum Met. Rev. 36 (1992) 2.
- 15 Iwamoto,-M.; Yahiro, H.; Shundo, Y.; Yu-u, Y.; Mizuno, N.; Shokubai (Catalyst) 1990,32, 430.
- 16 Held, W.; Konig, A.; Richter, T.; Puppe, L. SOC. Aut. Eng. 1990, Paper 900496.

Chapter 1

- 17 A. Fritz, V. Pitchon, *Appl. Catal. B* 13 (1997) 1.
- 18 M.D. Amiridis, T. Zhang, R.J. Farrauto, *Appl. Catal. B* 10 (1996) 203.
- 19 M. Shelef, *Chem. Rev.* 95 (1995) 209.
- 20 A.P. Walker, *Catal. Today* 26 (1995) 107.
- 21 Iwamoto, M.; Yahiro, H.; Tanda, K.; Mizuno, N.; Mine, Y.; Kagawa, S. J. *Phys. Chem.* 1991,95, 3727.
- 22 Li, Y.; Hall, W. K. J. *Catal.* 1991, 129, 202.
- 23 Shelef, M. *Catal. Lett.* 1992, 15, 305.
- 24 Traa Y., Burger B., Weitkamp J., *Micro. Meso. Mat.* 30 (1999) 3.
- 25 Parvulescu V.I., Grange P., Delmon B., *Cat. Today* 46 (1998) 233.
- 26 Li Y., Armor J.N., *Appl. Catal. B. Env.* 1 (1992) L31.
- 27 Li Y., Armor J.N., *Appl. Catal. B. Env.* 2 (1993) 239.
- 28 Li Y., Armor J.N., *Stud. Surf. Sci. Catal.* 81 (1994) 103.
- 29 Hirabayashi H., Yahiro H., Mizuno N., Iwamoto M., *Chem. Lett.* (1992) 2235.
- 30 Yahiro H., Hirabayashi H., Shin K.H., Mizuno N., Iwamoto M., *Trans. Mater. Res. Soc. Jpn.*, 18A (1994) 409.
- 31 Depmeier W., in "Handbook of Porous Solids", Eds.: Schüth, Sing K.S.W., Weitkamp J., Wiley-VCH Verlag GmbH, Weinheim, 2002, vol. 2, p. 699.
- 32 Weitkamp J., *Solid State Ionics* 131 (2000) 175.
- 33 A. Obuchi, A. Ogata, K. Mizuno, A. Ohi, M. Nakamura, H. Ohuchi, *J. Chem. Soc., Chem. Commun.* (1992) 247.
- 34 R. Burch, P.J. Millington, A.P. Walker, *Appl. Catal. B* 4 (1994) 65.
- 35 G.P. Ansell, A.F. Diwell, S.E. Golunski, J.W. Hayes, R.R. Rajaram, T.J. Truex, A.P. Walker, *Appl. Catal. B* 2 (1993) 81.
- 36 Kikuchi E., Yogo K., Tanaka S., Abe M., *Chem. Letters* 1063 (1991).
- 37 Obuchi A., Nakamura M., Ogata A., Mizuno K., Ohi A., Ohuchi H., *Chem. Comm.* 16 (1992) 1150.

- 38 Iwamoto M., Mizuno N., Proc. Inst. Mech. Eng. Part D: J. Automob. Eng. 207 (1993) 23.
- 39 Montreuil C.N., Shelef M., Appl. Catal. B Env. 1 (1992) L1.
- 40 C. Yokoyama, M. Misono, J. Catal. 150 (1994) 9.
- 41 M. Xin, I.C. Hwang, S.I. Woo, J. Phys. Chem. B 101 (1997) 9005.
- 42 Burch R., Scire S., Appl. Catal. B Env. 3 (1994) 295.
- 43 Li Y., Slager T.L., Armor J.N., J. Catal. 150 (1994) 338.
- 44 Campbell K.D., Morales E., Lunsford J.H., J. Am. Chem. Soc. 109 (1987) 7900.
- 45 Cowan A., Dumpelmann R., Cant N.W., J. Catal. 151 (1995) 356.
- 46 Cowan A., Cant N.W., Cat. Today 35 (1997) 89.
- 47 Cowan A., Cant N.W., Haynes B.S., Nelson P.F., J. Catal. 176 (1998) 329.
- 48 Lukyanov D.B., Sill G., d'Itri J.L., Hall W.K., J. Catal., 153 (1995) 265.
- 49 Lukyanov D.B., Lombardo E.A., Sill G., d'Itri J.L., Hall W.K., J. Catal., 163 (1996) 447.
- 50 Park S.-K., Park Y.-K., Park S.-E., Kevan L., Phys. Chem. Chem. Phys. 2 (2000) 5500.

Chapter 1

Chapter 2

Reduction of NO_2 by propene over parent and steamed NaH-Y zeolites

Abstract

The reduction of NO_2 by propene over NaH-Y zeolite and steamed NaH-Y zeolite has been studied by in situ IR spectroscopy and kinetic measurements. NaH-Y zeolite is a very active catalyst for this reaction, converting all NO_2 at temperatures between 150 and 600°C. At lower temperatures C_3H_6 readily reacts with NO_2 to oxygenates, CO, CO_2 , water and nitrogen containing organic compounds such as oximes, isocyanates or cyanides and organo-nitro species. The presence of O_2 primarily enhances the formation of carbonaceous deposits and the unselective combustion of C_3H_6 . Results indicate that O_2 does not play a crucial role in the formation of N_2 . Optimal N_2 yields were obtained feeding NO_2 and C_3H_6 in a stoichiometric ratio of 4 to 1. The selectivity to N_2 is determined by the competitive reactions of the formation of coke by oxygen, removal of coke by NO_2 and the partial oxidation of C_3H_6 by NO_2 . Results indicate that an optimal selectivity to N_2 is obtained at infinite low C_3H_6 feed concentration. Extrapolation of N_2 selectivity indicates a maximum N_2 selectivity of 50% can be obtained using an infinitely low propene feed concentration.

2.1 Introduction

The removal of nitrogen oxides from automotive diesel and lean-burn engine exhausts has been of great interest, since regulations worldwide restrict the emissions of NO_x and SO_x . After the reports by Iwamoto *et al.* [1] and Held *et al.* [2], who showed the high activity of copper based catalysts for the reduction of NO in the presence of oxygen, an enormous amount of research has been published using supported transition metal and noble metal catalysts. Typically, zeolites have been used as supports. The role of the Brønsted acid sites have since been subject of several investigations [3-8]. It was often suggested that the presence of Brønsted sites on zeolitic supports has a positive effect on the catalysts performance [9-12]. It has also been reported that the activity of the catalysts increased with the acid site strength of the zeolite [3] and the concentration of acid sites [6, 8]. The presence of sodium cations has been found to slightly decrease the activity of the remaining acidic protons [13, 14, 19]. For the reduction of NO or NO_2 a variety of reductants such as methane, propane, propene, hexane have been used. Among these, methane appeared to be the least and propene the most active [20]. Consensus exists among many authors that the initial step in the formation of N_2 is the oxidation of NO to NO_2 [15-22]. Next to the initial oxidation of NO to NO_2 several other steps have been proposed to be critical for the formation of N_2 . These include the formation of NO^+ or NO_2^+ [4, 23, 24] or the formation of carbenium ions from the hydrocarbons [18, 3].

From the applications point of view, zeolite H-Y would be an interesting choice because (i) of the low Si/Al ratios and, thus, relatively high concentration of acid sites, (ii) its potential to be (hydro)thermally stabilized, and (iii) wide commercial availability. The high concentration of Brønsted acid sites also allows to vary the Brønsted acid site concentration by ion exchange with alkali metals and, hence, monitor the influence of acidity on NO_x reduction. In this study, the

Reduction of NO₂ by propene over parent and steamed NaH-Y zeolite

reduction of NO₂, which is the key intermediate in the reduction of NO, by propene in the presence of oxygen is studied over NaH-Y and steamed NaH-Y zeolite in order to understand the role of Brønsted and Lewis acid sites on the activity and the sensitivity for deactivation.

2.2 Experimental

2.2.1 Materials

Na-Y was obtained from Zeolyst International (CBV100, Na form, Si/Al=2.6). The zeolite was ion-exchanged in a 1.0 M NH₄NO₃ aqueous solution at room temperature for 24 hr (2 g catalyst per 100 ml solution) to the NH₄ form. AAS analysis of Na and Al content showed that a 70% exchange was achieved. The de-aluminated sample was prepared by steaming the NaNH₄-Y at 550°C in a 35% H₂O/He flow for 90 minutes atmospheric pressure. The NaH-form of the zeolites was obtained after activation at 450°C. Brønsted and Lewis acid site concentrations, as determined by pyridine adsorption using *in situ* infrared spectroscopy [25] (for details see Chapter 3), gave for the parent NaH-Y: 630 μmol/g Brønsted acid sites (located in the supercages) and 6.9 μmol/g Lewis acid sites, and for the steamed NaH-Y: 145 μmol/g Brønsted acid sites and 54 μmol/g Lewis acid sites.

2.2.2 Infrared spectroscopy

For IR spectroscopic measurements, approximately 2 mg of catalyst were pressed into a self-supporting wafer and placed into a cell equipped with CaF₂ windows. IR spectra were recorded on a BRUKER IFS88 FTIR spectrometer (resolution 4 cm⁻¹) *in situ* during activation, adsorption and reaction. The cell was

Chapter 2

connected to a flow system, which enabled the recording of transmission spectra of the catalyst in the desired gas mixture at temperatures up to 550°C. The catalysts were activated by heating to 450°C (ramp 10°C/min) for 30 minutes in a flow of Helium (30 ml/min). After activation the temperature was lowered to 120°C, after which the desired gas mixture was fed.

2.2.3 Kinetic activity tests

For kinetic measurements 200 mg of catalyst (particle size range 0.3-0.7 mm), were placed into a tubular reactor and fixed between quartz plugs. The catalyst was activated in a Helium flow of 100 ml/min, increasing the temperature by 10°C/min to 450°C at which it remained for 1 hr. After activation the temperature was lowered to 150°C and the flow was switched to a mixture of NO₂, propene, oxygen with He as balancing gas to a total flow of 100 ml/min. This resulted in a GHSV of 15000 hr⁻¹. The temperature was increased by 25°C per step to a final temperature of 600°C. To ensure steady state conditions catalyst was maintained at each temperature between 50-200 minutes. A Hewlett Packard 6890 GC equipped with a capillary mole sieve column (HP-PLOT-5A) and a porapack (HP-PLOT-Q) column was used to analyze N₂, O₂, CH₄, CO, CO₂, N₂O and C₃H₆. NO and NO₂ were monitored by a 'Thermo Environmental Instruments 42C' chemiluminescence NO/NO₂/NO_x analyzer.

Reduction of NO₂ by propene over parent and steamed NaH-Y zeolite

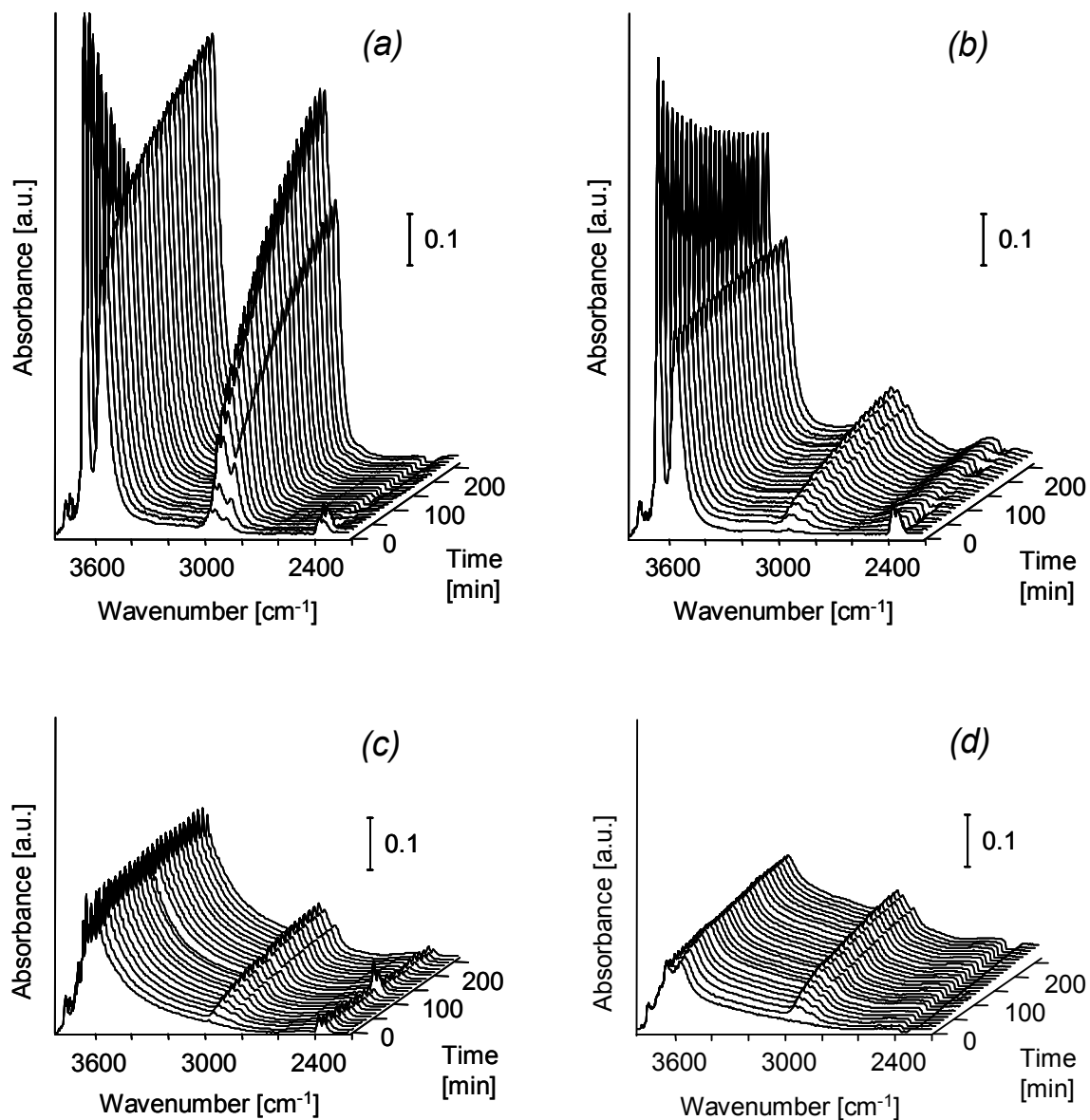


Figure 1. IR absorbance spectra of NaH-Y (a,b) and steamed NaH-Y (c,d) exposed to a mixture of C₃H₆, He (a,c) or C₃H₆, O₂, He (b,d) for 250 minutes.

Chapter 2

2.3 Results

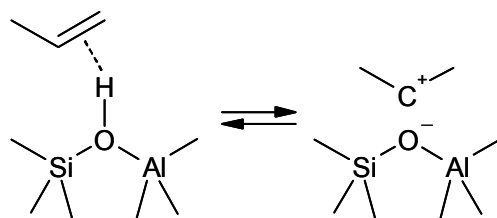
2.3.1 Infrared spectroscopy on parent and steamed NaH-Y in contact with C_3H_6 and O_2 .

Figure 1a-d show the IR absorbance spectra of NaH-Y and steamed NaH-Y during the uptake of propene at 120°C in a flow of Helium containing 3000 ppm propene or a flow of He containing 3000 ppm of propene and 5% oxygen. Feeding only propene to NaH-Y (Figure 1a) resulted in a gradual increase of the bands corresponding to CH stretching vibrations (asym.stretch. CH_3 2958, asym. stretch CH_2 2930 and sym. stretch CH_2 2870 cm^{-1}). Parallel to this, a decrease of the high frequency bridging hydroxyl band (HF) at 3640 cm^{-1} and an apparent increase of the low frequency hydroxyl band (LF) at 3545 cm^{-1} was observed. The HF band is assigned to the Brønsted acid sites located in the super cages accessible through 12-membered rings, while the LF band is assigned to the Brønsted acid sites located in the sodalite cages that are only accessible through 6 membered rings. Propene is adsorbed on the bridging hydroxyl groups in the supercages, which causes the HF SiOHAl band to decrease. The complete absence of $=CH_2$ stretching bands (expected around 3080 and 2997 cm^{-1}) indicates that the double bond character disappears upon adsorption.

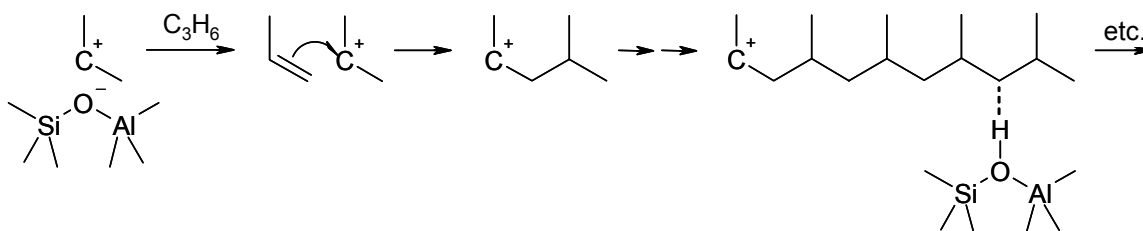
The intensities of the CH_3 and CH_2 stretching bands were remarkably constant (ratio of 1:1) during the whole uptake. A ratio of 1:1 was also observed for n-hexane, 2-methyl-octane, or 2,4-di-methyl-decane, which indicates that propene has oligomerized. Note in this context that Zecchina *et al.* [26] proposed a mechanism for the polymerization of ethene over Brønsted acid sites on H-ZSM5 by consecutive insertion of ethene into the C-O bond of an alkoxy group (carbenium ion). This mechanism may also apply to the oligomerization of propene on NaH-Y as illustrated in Scheme 2. Coordination of the aliphatic group of

Reduction of NO₂ by propene over parent and steamed NaH-Y zeolite

the oligomer to neighboring HF bridging hydroxyl groups causes a shift of this band with about 80-120 cm⁻¹ to lower wavenumbers where it overlaps with the LF bridging hydroxyl group band [26, 27, 28], which therefore increase with increasing propene adsorption. A red shift of the LF band was not observed, indicating that propene did not adsorb on Brønsted sites located in the sodalite cages.



Scheme 1. Adsorption of C₃H₆ on a Brønsted acid site.



Scheme 2. Oligomerization of C₃H₆ on a Brønsted acid site and coordination of the aliphatic group to neighboring bridging hydroxyl groups.

Figure 1b shows the IR absorbance spectra for NaH-Y in the presence of 3000 ppm propene and 5% oxygen. With time on stream, the bands corresponding to CH stretching vibrations reached a much lower intensity compared to the intensities obtained feeding only propene (Figure 1a). Likewise, the band corresponding to HF Brønsted acid sites (3640 cm⁻¹) decreased to about 80% of its original intensity, while feeding only propene (Figure 1a) a near complete removal of this band was observed. In addition to the bands observed while feeding only propene, bands appeared around ~2616 – 3545 and ~2428 cm⁻¹, which indicate the

Chapter 2

adsorption of polar compounds forming hydrogen bonds to the Brønsted acid site giving rise to typical “ABC” bands [29]. The CH deformation bands appeared slightly shifted to higher wave numbers, what may indicate the formation of aromatics or coke like species.

Figure 1c shows the uptake of propene at 120°C on steamed NaH-Y while feeding 3000 ppm. The steaming of the NaH-Y led to a strong decrease of the concentration of Brønsted acid sites, which is clearly shown by the low intensity of the bands corresponding to HF and LF Brønsted sites and the formation of extra-framework aluminum indicated by the presence of additional OH stretching bands. Accordingly, less propene adsorbed what resulted in only a small increase of CH stretching bands. The CH stretching bands appeared at the same position and with the same relative intensities as observed on the parent NaH-Y and, thus, propene may have oligomerized in a similar way as on the parent NaH-Y. The spectra do not show a clear indication of any interaction of propene with the extra framework aluminum. Figure 1d shows the adsorption of propene on steamed NaH-Y in the presence of O₂. The positions of CH stretching bands appear, similar as in Figure 1b, at slightly higher wavenumbers and a small band appears around 2486 cm⁻¹ indicating that, similar as on the parent NaH-Y polar species have adsorbed which are likely to be partially oxidized derivatives of propene. With increasing time the CH stretching bands increased to similar intensities as obtained in the absence of O₂ suggesting that the presence of O₂ hindered the adsorption of propene.

Figure 2 shows the IR absorption spectra in the low frequency region obtained at the end of the experiments described in Figure 1. Bands appearing at 1950 and 1850 cm⁻¹ are assigned to zeolite lattice vibration overtones. In the steamed NaH-Y these bands appeared less intensive. A band appearing at 1710 cm⁻¹ is assigned to a carbonyl group (C=O), possibly arising from acetone. Bands at 1640 and 1593 cm⁻¹ may be assigned to carboxylic groups, possibly stemming from

Reduction of NO₂ by propene over parent and steamed NaH-Y zeolite

acetic or propionic acid. Note that a band at 1640 cm⁻¹ may also be assigned to adsorbed water which can form hydrogen bonding complexes to the Brønsted acid sites of the zeolite and thus result in the typical ABC band formation. A relative wide band appearing around 1720-1520 cm⁻¹ is tentatively assigned to C=C vibrations of carbonaceous deposits. Bands at 1470 and ~1380 cm⁻¹ can be attributed to CH₃ and CH₂ deformation vibrations. It should be emphasized that the bands indicating oxygen containing functional groups and the bands indicating carbonaceous deposits appeared far more intense in the presence of oxygen.

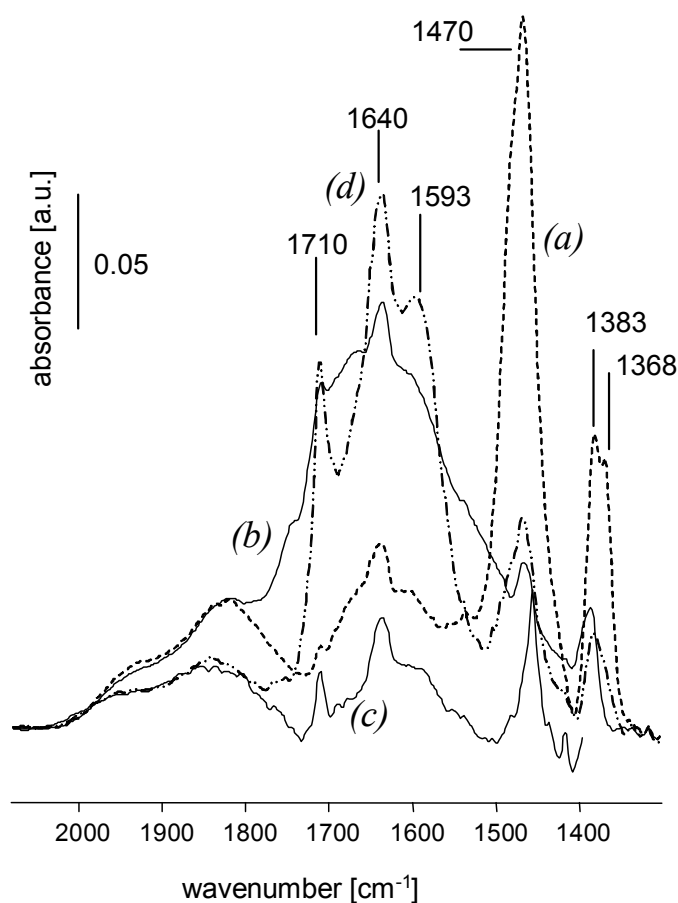


Figure 2. IR absorbance spectra of NaH-Y (a) and steamed NaH-Y (b) in the CH deformation region after exposure to a mixture of C₃H₆, He (a,c) or C₃H₆, O₂, He (b,d) for 250 minutes.

Chapter 2

2.3.2 Infrared spectroscopy of parent and steamed NaH-Y in contact with NO₂, C₃H₆ and O₂.

Figure 3 shows the spectra recorded while feeding 1000 ppm NO₂ plus 3000 ppm C₃H₆ (a,c) and 1000 ppm NO₂, 3000 ppm C₃H₆ and 5% oxygen (b,d) in Helium (30 ml/min) over NaH-Y (a,b) and steamed NaH-Y (c,d) at 5 minute intervals for 250 minutes at 120°C. Feeding NO₂ and propene to HY (Figure 3a) resulted in the rapid disappearance of the HF Brønsted site band (3640 cm⁻¹). Strong narrow bands appear at 1724, 1635, 1567 cm⁻¹ and a broad bands around 3545 – 2620 cm⁻¹ and 2450 cm⁻¹ with a shoulder around 2243 cm⁻¹. Less intensive bands appeared at 3124, 2990, 2945, 1486, 1453, 1434, 1416, 1382 and 1347 cm⁻¹. The broad band between 3545 – 2620 cm⁻¹ and the bands at 2450 cm⁻¹ and 1640 cm⁻¹ are speculated to be related to the adsorption of a relative large amount of water. The bands at 2990, 2945 cm⁻¹ are attributed to CH₃ and CH₂ stretching bands respectively, which correspond to the CH deformation bands appearing at 1453 cm⁻¹ (CH₃, CH₂) and 1382 cm⁻¹ (sym. stretch CH₃). The band at 1724 cm⁻¹ can be attributed to carboxylate groups. Misono *et al.* [30] observed a band at 1561 cm⁻¹ after the adsorption of nitro methane on Pt/SiO₂. Thus, we attribute the band at 1567 cm⁻¹ to organo nitro species. The bands at 3124 cm⁻¹ and 1486 cm⁻¹ are assigned to NOH group of an oxime compound [31], bands around 2243 cm⁻¹ can be assigned to isocyanate or cyanide species [32]. The band at 1347 cm⁻¹ could indicate the presence of weakly sorbed propene [33].

Figure 3b shows the absorption spectra of NaH-Y in contact with C₃H₆, NO₂ and O₂. Similar bands appeared in the absence of O₂ (Figure 3a) although the increase of these bands was significantly slower. Figures 3c and 3d show the spectra of steamed NaH-Y in a flow of (c) NO₂ + C₃H₆ and (d) NO₂ + C₃H₆ + O₂. The bands observed on NaH-Y also appeared on the steamed NaH-Y although the

Reduction of NO₂ by propene over parent and steamed NaH-Y zeolite

3545 – 2620 cm⁻¹ band, assigned to sorption of water, and the 1716 cm⁻¹ band, assigned to a carbonyl group, appeared with a significantly lower intensity.

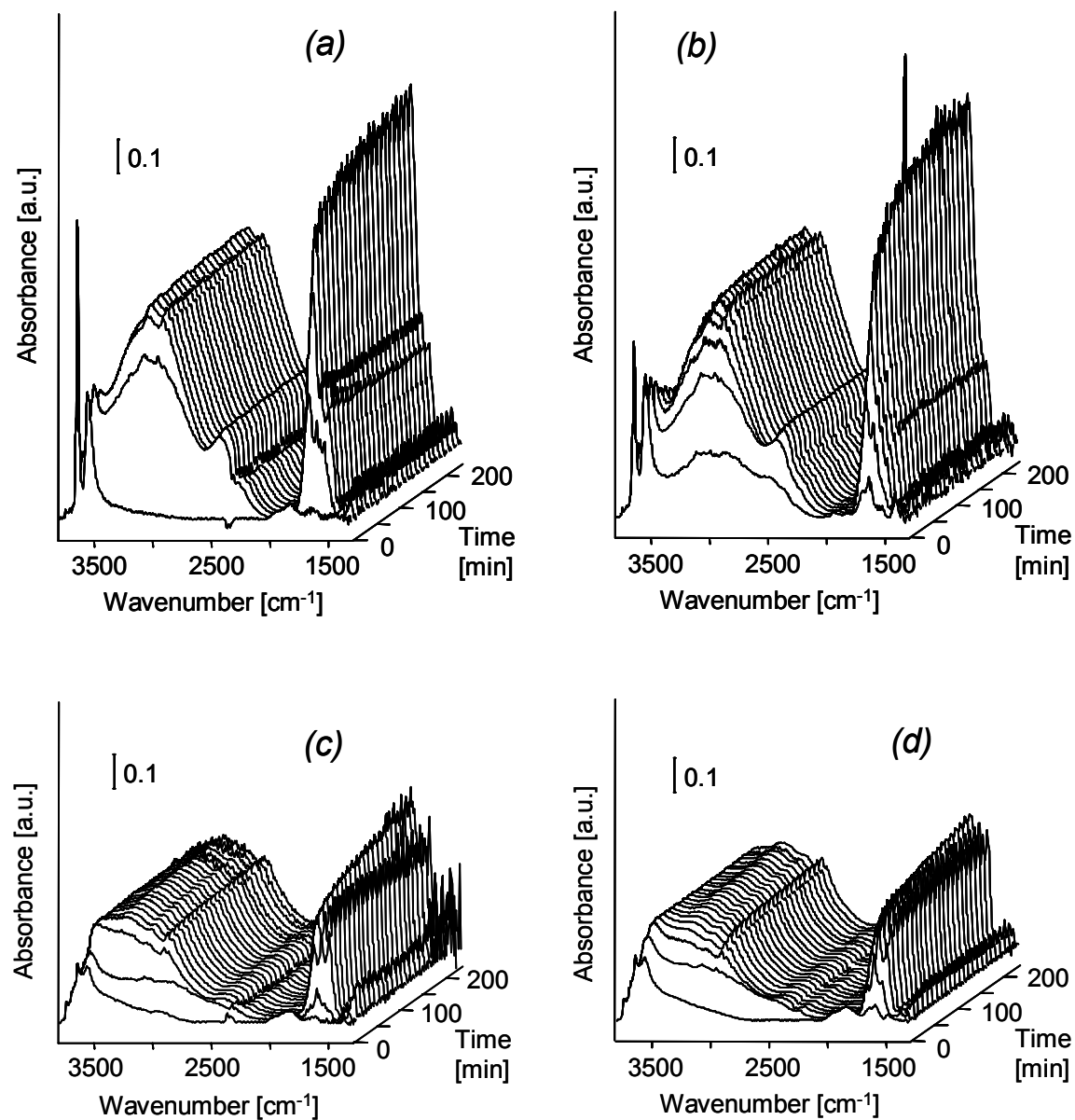


Figure 3. IR absorbance spectra of NaH-Y (a,b) and steamed NaH-Y (c,d) exposed to a mixture of NO₂ + C₃H₆ (a,c) or NO₂ + C₃H₆ + O₂ (b,d) for 250 minutes.

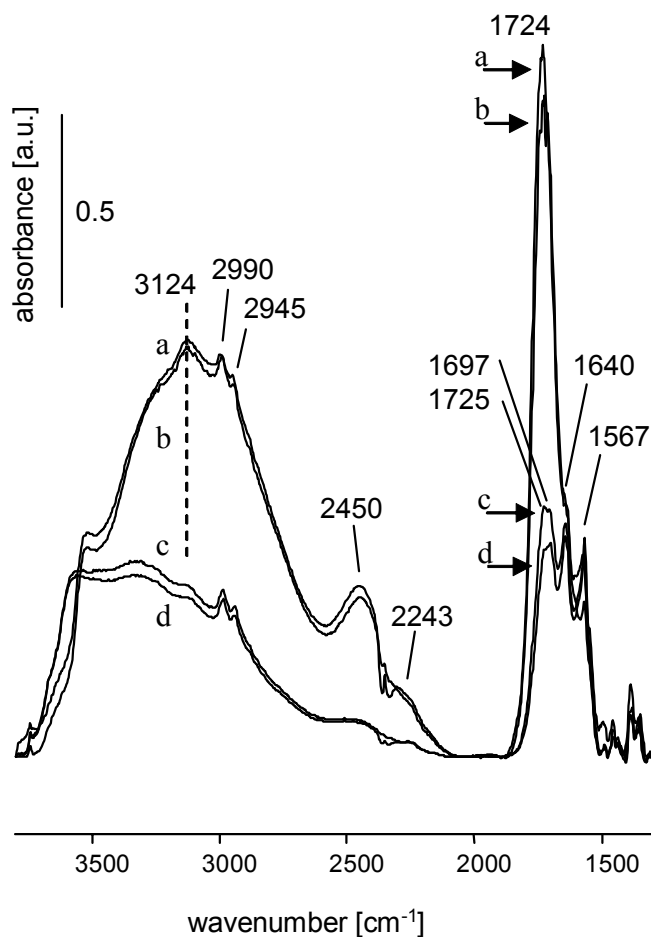


Figure 4. IR absorbance spectra of NaH-Y (a,b) and steamed NaH-Y (c,d) after 250 minutes exposure to a mixture of NO_2 , C_3H_6 , He (a,c) and NO_2 , C_3H_6 , O_2 , He (b,d).

Figure 4 shows the spectra obtained at the end of each NO_2 , C_3H_6 , (O_2) uptake experiments shown in Figure 3 including the low frequency region. The differences between the parent NaH-Y and the steamed NaH-Y zeolite appeared mainly in the water ($3545 - 2620 \text{ cm}^{-1}$) and the carbonyl group ($\sim 1724 \text{ cm}^{-1}$) bands, which both were significantly less intense on the steamed NaH-Y. In the presence of O_2 all bands appear at slightly lower intensity ($\sim 10\%$). Ukisu *et al.* [34] and Sumiya *et al.* [35] assigned bands around 1674 cm^{-1} to the presence of organo nitro or nitrate species. Although the stability of such species under the given conditions is questionable, it remains possible that the band around $\sim 1720 \text{ cm}^{-1}$ is a composite

Reduction of NO_2 by propene over parent and steamed NaH-Y zeolite

of carboxylates and organo nitro or nitrate species. This in addition to the observed oxime and cyanide or isocyanate bands strongly suggests that nitrogen-containing surface species have been formed.

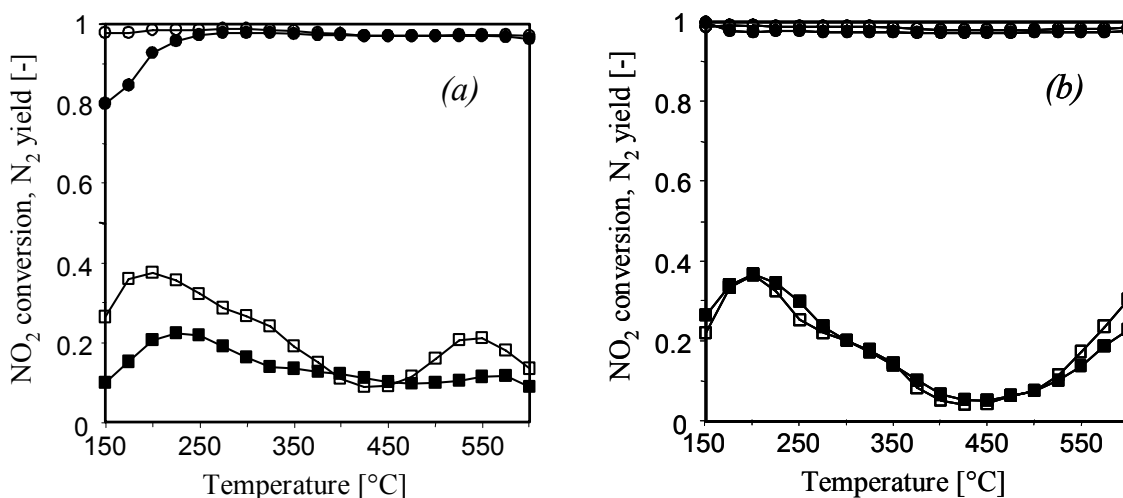


Figure 5. NO_2 conversions and N_2 yields obtained during SCR over NaH-Y and steamed NaH-Y using a mixture of 1000 ppm NO_2 , 1000 ppm C_3H_6 and 5% O_2 (a) and without O_2 (b). The marks represent: (○) NO_2 conversion on NaH-Y, (□) N_2 yield on NaH-Y, (●) NO_2 conversion on steamed NaH-Y, (■) N_2 yield on steamed NaH-Y.

Figure 5 shows the NO_2 conversion and N_2 yield obtained using NaH-Y and steamed NaH-Y in a feed of (a) 1000 ppm NO_2 , 1000 ppm C_3H_6 , 5% O_2 and (b) 1000 ppm NO_2 and 1000 ppm C_3H_6 . In the presence of O_2 the NO_2 conversion was constant at 100% with NaH-Y, while it was slightly below 100% on the steamed NaH-Y at temperatures below 200 °C. The N_2 yields showed a similar trend reaching a maximum at 200 °C of ~40% on the NaH-Y and ~25% on the steamed NaH-Y. The N_2 yields decreased with increasing temperature to a minimum of nearly 10%. For NaH-Y the N_2 yield increased again above 450 °C to reach a second maximum at 550 °C of ~25%. The main product of NO_2 conversion was NO and about 5-10% N_2O . The carbon and nitrogen balance were up to 20%

Chapter 2

lower than expected at temperatures below 300°C while small excess is obtained at higher temperatures. In the absence of O₂ (Figure 5b) the NO₂ conversions (constant at 100%) and N₂ yields were practically identical for the two materials. The N₂ yield showed a maximum at 200°C of nearly 40%, which is also similar to what, was obtained on NaH-Y in the presence of O₂. With increasing temperature the N₂ yields decreased to about 5% at 450°C from where the N₂ yields increase again.

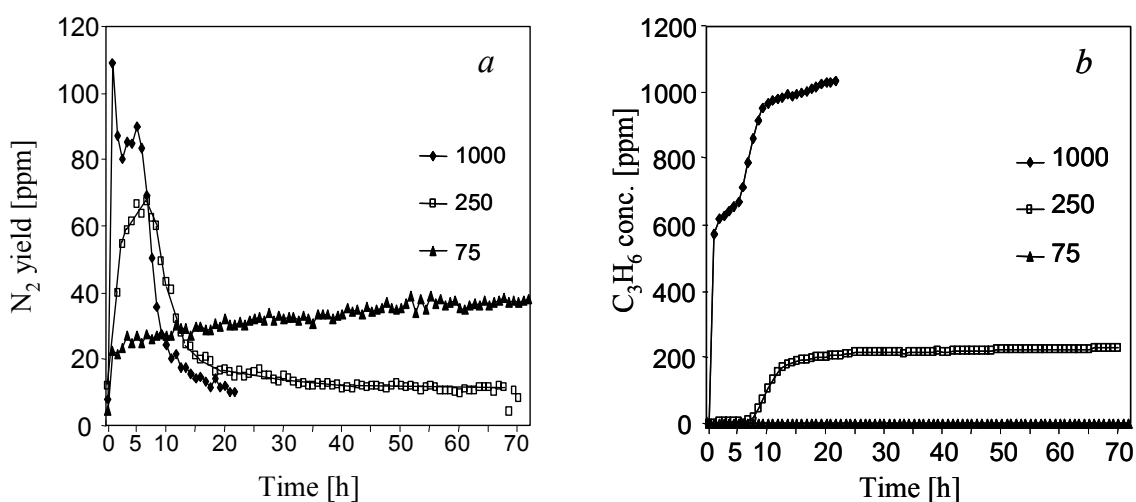


Figure 6. (a) N₂ yield and (b) C₃H₆ concentration after the reactor, measured at 150°C using 75, 250 and 1000 ppm of C₃H₆, 5% O₂ and 1000 ppm of NO₂.

2.3.4 Kinetic measurements using increasing propene feed concentrations

The main reactions with propene are oligomerization, dehydrogenation and aromatization to form carbonaceous deposits, unselective combustion to CO and CO₂ and selective oxidation by NO₂. By reducing the propene feed concentration the usage of propene for the formation of N₂ may be enhanced at the expense of coke formation.

Reduction of NO_2 by propene over parent and steamed NaH-Y zeolite

Figure 6a,b show the (a) N_2 yield and (b) C_3H_6 concentration after the reactor in time at 150°C using a C_3H_6 feed concentration of 75, 250 and 1000 ppm. Using 1000 ppm of C_3H_6 the N_2 yield and C_3H_6 conversion remained practically constant for nearly 6 hours after which the N_2 yield and C_3H_6 conversion decreased strongly. Using 250 ppm of C_3H_6 a similar trend was observed. The C_3H_6 conversion was constant at 100% for nearly 8 hours, during this time the N_2 yield was about 60%. After this period the C_3H_6 concentration measured in the product stream strongly increased to reach a stable level after further 8 hours. Using a C_3H_6 feed concentration of 75 ppm deactivation of the catalysts was not observed for 70 hours. During this period the N_2 yield increased slowly from 20 to 40 ppm.

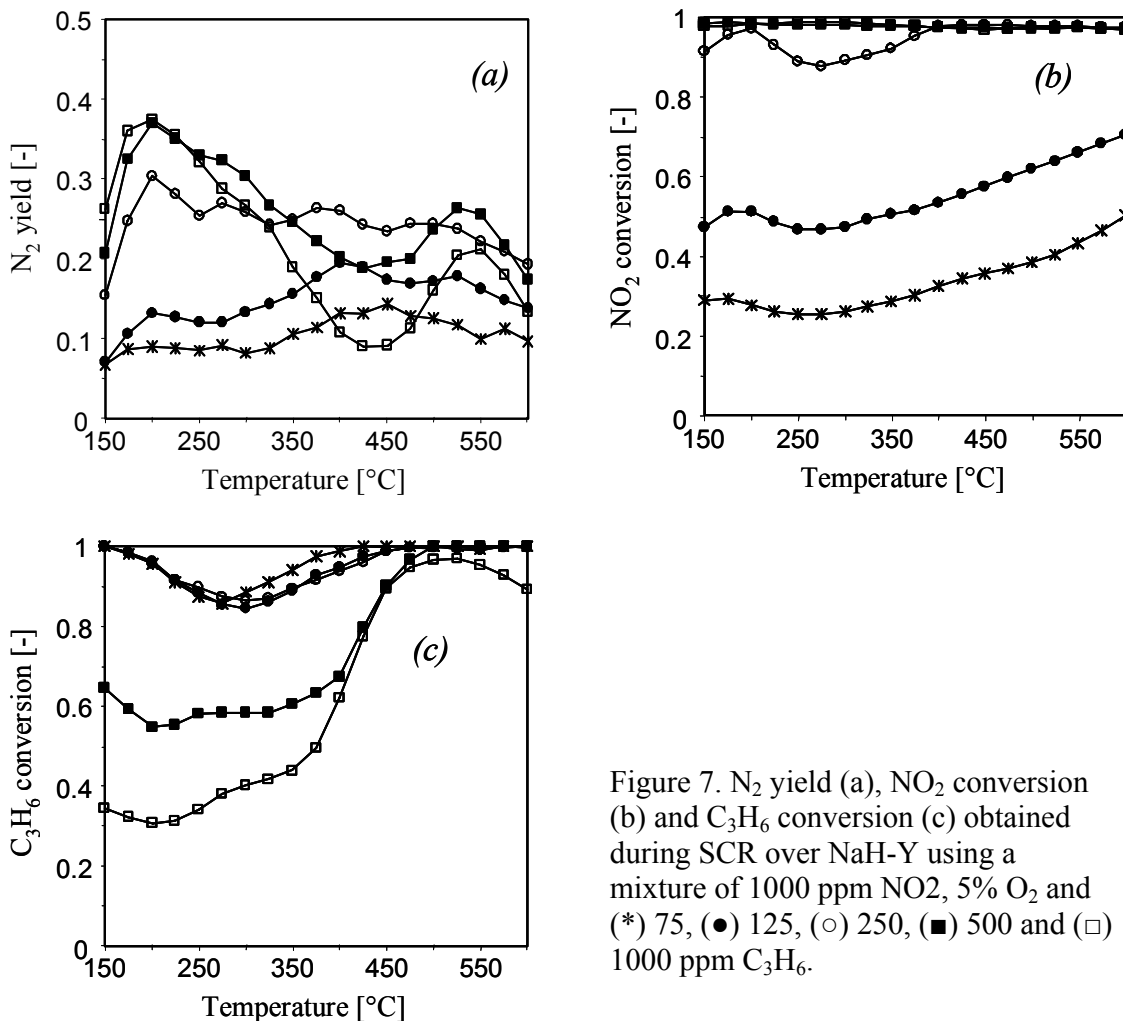


Figure 7. N_2 yield (a), NO_2 conversion (b) and C_3H_6 conversion (c) obtained during SCR over NaH-Y using a mixture of 1000 ppm NO_2 , 5% O_2 and (*) 75, (●) 125, (○) 250, (■) 500 and (□) 1000 ppm C_3H_6 .

Chapter 2

Figure 7a-c shows the N_2 yield, NO_2 conversion and propene conversion as a function of temperature from a mixture of 1000 ppm NO_2 , 5% O_2 and 75, 125, 250, 500 and 1000 ppm propene over the parent NaH-Y catalyst. Figure 7a shows that the N_2 yields obtained never exceeded the maximum of 37% obtained at 200°C using 1000 ppm of C_3H_6 . At 200°C, the N_2 yield strongly decreased below 500 ppm of C_3H_6 . With increasing temperature the N_2 yield decreased while using 1000 ppm of C_3H_6 resulting in a minimum around 425°C. Using lower C_3H_6 feed concentrations this decrease gradually changed into a small increase. Above 525°C the N_2 yield strongly decreased for all C_3H_6 feed concentrations used. This indicates that excess of propene leads to deactivation of the catalysts and that this can be partially prevented by using lower C_3H_6 feed concentration.

Figure 7b shows the corresponding NO_2 conversions obtained. At C_3H_6 feed concentrations of 1000 and 500 ppm all NO_2 was converted between 150-600°C. With increasing temperature the NO_2 conversion showed an initial increase and then decreased to a minimum around 250-275°C, from where it increased slowly with increasing temperature. This trend in NO_2 conversions with temperature is typical for most operating conditions. The NO_2 conversion is increased stepwise with increasing propene feed until a NO_2 conversion of 100%. Besides N_2 , the main products formed were NO and N_2O of which the latter reached a maximum selectivity of nearly 20% at 150°C and decreases strongly with increasing temperature (Selectivity < 6% above 300°C).

Figure 7c shows the corresponding C_3H_6 conversions. With propene feed concentrations of 500 and 1000 ppm, the propene conversion remained around 60% and 40%, respectively, until about 350°C. Above 350°C temperature the propene conversions increased strongly and approached 100% at 500°C. The increase in propene conversion coincided with a strong increase in CO_x yield and, thus, can be concluded that unselective combustion was significantly accelerated above 350°C. The propene conversions obtained using propene feed concentrations

of 75, 125 and 250 ppm showed nearly identical values over the whole temperature range. The conversions initially decreased from 100% at 150°C to a minimum of about 85% at 300°C and approached 100% around 425-475°C.

2.4 Discussion

2.4.1 Influence of O₂

Figure 1 shows that propene readily adsorbs on the Brønsted acid sites of NaH-Y located in the supercages, while the sites located in the sodalite cages appear unreachable for propene. The uptake of propene on NaH-Y was strongly influenced by the presence of O₂. In its presence the HF SiOHAl band decreased to only 80% of its original intensity, while it nearly completely disappeared in the absence of O₂. On steamed NaH-Y this decrease in uptake was not observed. IR spectra showed that in the presence of O₂ partially oxidized species and a relative large amount of coke species were formed on both parent and steamed NaH-Y, while in the absence of O₂ propene may have oligomerized to a minor extent. We speculate that the absence of C=C double bonds in the aliphatic oligomers renders them less reactive with NO₂ than propene. Apparently, the presence of O₂ strongly enhances the formation of carbonaceous species via oxidative dehydrogenation leading to severe obstruction of the diffusion of propene and/or partial blocking of the pores. On steamed NaH-Y similar species are formed, although they do not severely hinder the adsorption of propene on the available supercage-Brønsted acid sites. Note that steaming leads to the partial removal of aluminum from the framework and decreases the concentration of Brønsted acid sites. The zeolite structure is hereby largely maintained. The large number of structure defects gives the zeolite mesoporous properties which is speculated to prevent the pore system from blocking upon coke formation. The formation of coke and partially oxidized

Chapter 2

species in the presence of O_2 was clearly shown in Figure 2. The intensity of the “coke bands” was similar for the parent and the steamed material, suggesting that steaming does not decrease the formation of coke species, but offers more space to accommodate the coke and provides access for propene to diffuse through the zeolite.

Figure 3 shows the accumulation of surface species on contacting parent and steamed NaH-Y with mixtures of NO_2 , C_3H_6 and O_2 . The increase of the intensity of these bands was even faster than the increase of bands of propene adsorption in Figure 1. This indicates the high reactivity of NO_2 and propene on both zeolites. Figure 3a and 3b show that the presence of O_2 does not significantly influence the type of species formed on the surface, while the uptake of these species appears to have slowed down, which indicates that in the presence of NO_2 the influence of O_2 (enhanced formation of carbonaceous deposits) remains unaltered. In the presence of O_2 the bands appear about 10% less intensive as in the absence of O_2 , which is explained by the enhanced formation of carbonaceous deposits and thus confirms the influence of O_2 . Figure 3 also shows that the concentration of sorbed water and carboxylates are significantly lower on the steamed NaH-Y and, thus, that the sorption capacity and/or formation of these species depends on the concentration of Brønsted acid sites. Note that the differences in the spectra are explained by the number of Brønsted acid sites and presence of oxygen, which in turn suggests that these sites dominate the main chemical pathways occurring at the catalysts surface.

Figure 5 shows that the presence of O_2 leads to a lower N_2 yield and NO_2 conversion on the steamed NaH-Y while the yields and conversion remain nearly unaffected on the parent material. The influence of O_2 is concluded to enhance the formation of carbonaceous deposits. These deposits are likely to accumulate on Brønsted acid sites leading ultimately to a deactivation of the catalyst. The concentration of Brønsted acid sites is significantly lower on the steamed NaH-Y

Reduction of NO₂ by propene over parent and steamed NaH-Y zeolite

which is why this material will deactivate faster. In the absence of O₂ the N₂ yields and NO₂ conversions show no signs of deactivation of the catalyst.

2.4.2 Effect of steaming

Steaming of a zeolite leads to the irreversible removal of framework aluminum forming extra framework aluminum. As a result the concentration of bridging hydroxyl groups decreases and, thus, the number of Brønsted acid sites. The concentration of Lewis acid sites is hereby increased what is related to the formation of extra framework aluminum. As a consequence, a large concentration of structure defects sites are formed what result in a mesoporous character and facilitates the diffusion of reactants [36]. On adsorption of propene in the presence and absence of O₂ large differences are observed on the parent zeolite while the steamed NaH-Y appears to accumulate a similar amount of carbonaceous deposits what is thus related to the increased diffusivity of propene through the zeolite pore system. Figure 5b shows that identical N₂ yields and NO₂ conversions can be obtained using the parent or the steamed material, indicating that the low concentration of Brønsted acid sites available on the steamed sample remains sufficient for a total conversion of NO₂ and that a low Brønsted acid site concentration does not influence the N₂ selectivity. The increase of mesoporosity by steaming may thus enhance the catalysts activity as the limitations by diffusion are reduced. Note that no indications were found that can be related to an influence of the increased concentration of extra framework aluminum and Lewis acidity.

2.4.3 Effect of deactivation by formation of carbonaceous deposits

Figure 8 is derived from results presented in Figure 7 and shows the N₂ yield, N₂ selectivity and NO₂ conversion as function of the C₃H₆ feed concentration

Chapter 2

at (a) 200°C and (b) 450°C. Figure 8 shows that 250 ppm of propene suffices to convert 1000 ppm of NO₂. Using higher propene feed concentrations thus result in an excess of propene which are likely to form carbonaceous deposits assisted by the presence of O₂ and thus enhance the deactivation of the catalyst. Figure 6 shows a decrease of the N₂ yields and propene conversion using 250 or 1000 ppm of propene after 8-10 hours on stream at 150°C, while no deactivation occurs using a feed of only 75 ppm propene.

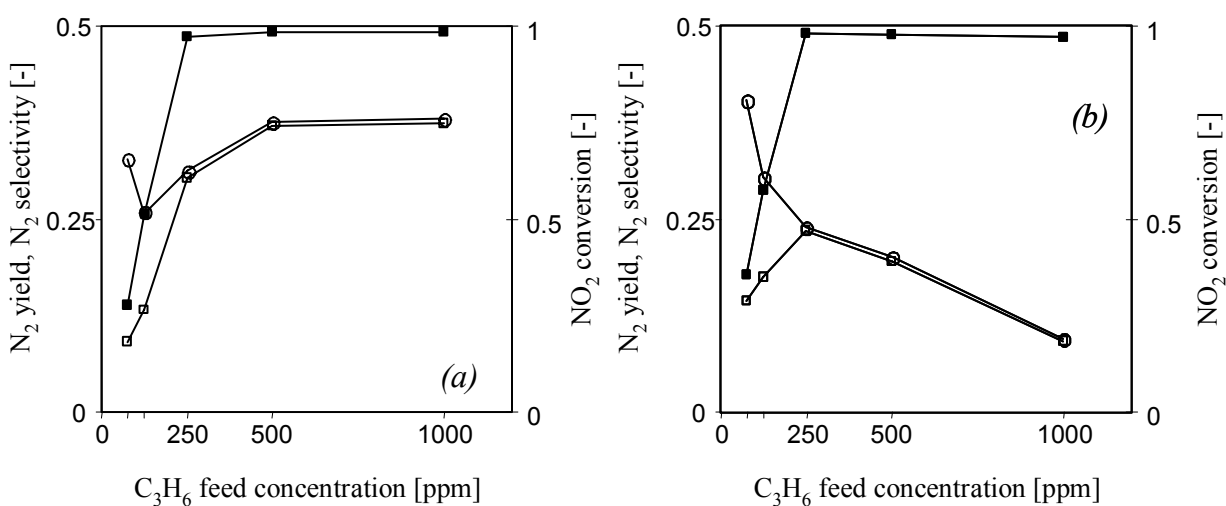


Figure 8. N₂ yield (□), N₂ selectivity (○) and NO₂ conversion (■) (right y-axis) versus C₃H₆ feed concentration obtained during SCR of NO₂ and C₃H₆ over NaH-Y at (a) 200°C and (b) 450°C.

The deactivation using 250 ppm of propene, as shown in Figure 6, thus indicates that the formation of carbonaceous deposits is not prevented using this concentration. The deactivation results in a loss of activity of about 80% which thus includes that the deactivation is not complete and some activity remains. Figure 7c shows that using propene feed concentrations of 250 ppm and below nearly identical propene conversions were obtained while large differences in NO₂ concentrations are obtained. This indicates that the propene conversion in these conditions does not depend on the NO₂ concentration (which is present in excess to

Reduction of NO₂ by propene over parent and steamed NaH-Y zeolite

the concentration of propene). For propene and NO₂ to react it is necessary that propene is activated on the surface after which it can react with NO₂. Removal of carbonaceous deposits by NO₂ could in principle keep a fraction of the Brønsted acid sites available for the reaction of propene with NO₂ although this would suggest that higher NO₂ concentrations would result in higher rates which appear to contradict the observations. Possibly, the catalysts surface in a state of near complete deactivation and thus largely covered by carbonaceous deposits still remains some activity for the activation of propene which then is able to react with NO₂. The adsorption and activation of propene on a surface covered by carbonaceous deposits is most probably not a particularly fast process and thus becomes the rate limiting step. Such a mechanism may explain the remaining low activity on extensive deactivation and includes that propene conversion in such conditions become independent from the NO₂ concentration.

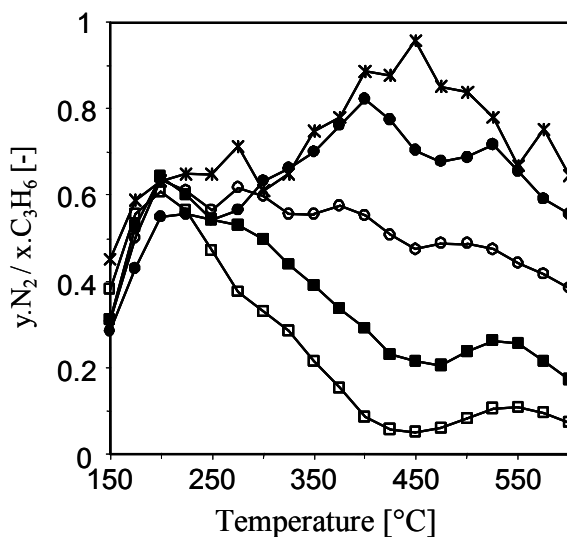


Figure 9. N₂ yield to C₃H₆ conversion ratio (N₂/C₃) obtained during SCR over NaH-Y using a mixture of 1000 ppm NO₂, 5% O₂ and (*) 75, (●) 125, (○) 250, (■) 500 and (□) 1000 ppm C₃H₆.

Chapter 2

2.4.4 Effect of C_3H_6 feed concentration on the N_2 selectivity

Figure 7a shows that the N_2 yield obtained is influenced by the C_3H_6 feed concentration, the temperature and the presence of O_2 . Figure 9 shows the ratio between N_2 yield and C_3H_6 conversion. Apparently, at low temperatures the amount of N_2 formed per C_3H_6 converted is independent of the C_3H_6 feed concentration, while at temperatures above $225^\circ C$ more N_2 molecules were formed per converted C_3H_6 with lower C_3H_6 feed concentrations. Extrapolation of this trend to infinite low C_3H_6 feed concentration would result in a N_2/C_3 ratio of approximately 1. The maximum reductant efficiency to the formation of N_2 is, thus, obtained at minimum C_3H_6 feed concentration and around $450^\circ C$.

Figure 8 shows that at $200^\circ C$ and $450^\circ C$ the NO_2 conversions reach 100% at 250 ppm of C_3H_6 . Below 250 ppm the NO_2 conversion correlates linearly with the C_3H_6 feed concentration indicating that the stoichiometry with which NO_2 and C_3H_6 react remains constant. Note that the NO_2 feed concentration was always kept constant at 1000 ppm and, thus, 1 C_3H_6 reacts with 4 NO_2 molecules. At $200^\circ C$, the selectivity to N_2 shows no clear relation to the C_3H_6 feed concentration, while at $450^\circ C$ the N_2 selectivity increases with decreasing C_3H_6 feed concentration and approaches approximately 0.5 at infinitely low C_3H_6 feed concentrations. Figure 6 shows that even when NO_2 and C_3H_6 are fed at the ratio of 4 to 1 the catalyst still deactivated, thus, using this feed concentrations does not prevent the formation of carbonaceous deposits. The N_2 yield obtained feeding 75 ppm of C_3H_6 did not exceed 40 ppm, which is rather low compared to the 75 ppm of C_3H_6 consumed and thus also indicates that C_3H_6 is consumed by other reactions than N_2 formation.

2.4.5 Mechanism and selectivity

IR spectroscopy at 120°C shows that in the combination of C₃H₆ with NO₂, oxygenates and nitrogen organic compounds were formed on the zeolite, while the combination of C₃H₆ with O₂ resulted in the generation of hydrogen poor carbonaceous species and, thus, no oxygenates were formed. In the literature mechanisms are suggested in which ammonia is produced *via* a complex sequence of steps after which ammonia and NO or NO₂ react to form N₂ in a way similar to NH₃-SCR. In order to form ammonia, NO or NO₂ reacts with the hydrocarbon to form an organo nitro or nitrite, which rearranges to an oxime. The presence of an oxime is concluded from a weak band observed at 3124 cm⁻¹. In the following step the oxime is dehydrogenated to an iso-cyanate or cyanide [4, 16-18, 21, 37-40]. Figures 3 and 4 show bands assigned to oxygenates and NCO intermediates giving support to the conclusion that the reactions of NO₂ proceed in a similar sequence. The 1724 cm⁻¹ band appears relative strong compared to bands assigned to nitrogen containing species, indicating that partial oxidation of propene is an important reaction occurring. The partial oxidation of propene by NO₂ lead to NO as product which is in turn limits the formation of N₂. Results presented in this study clearly show that NaH-Y zeolites catalyze the reaction of propene with NO₂ which is related to the Brønsted acid sites. The fact that H-form zeolites have this ability is known from literature although a mechanism with which NO₂ and propene react remains unknown.

NO₂ is known to react with alkenes via a homogenic mechanism forming organo nitro and nitrite species [40]. Adsorption of propene (see Scheme 1) results in the formation of a propyl carbenium ion and the loss of the π -system as shown in Figure 1. A carbenium ion is likely to react with NO₂ according to a heterogenic mechanism, which would thus require an alternative explanation. Gerlach *et al.* [4] suggested that the Brønsted acid sites enable the formation of a nitrosium ion with

Chapter 2

which propene reacts forming a propenaloxime species. Our results show that propene readily adsorbs on Brønsted acid sites and are as such reactive with O₂ and NO₂. It thus appears likely that NO₂ reacts with an adsorbed propene. On adsorption of propene on a Brønsted acid site propene forms a carbenium ion in the form of a stable alkoxy group. NO₂ may attack *via* a nucleophilic addition on the positively charged secondary carbon of the alkoxy group forming either an organo nitro or nitrite species (see Scheme 3). The nitrite is known to be extremely unstable, especially in the presence of oxygen, and will readily decompose to NO and an oxygenate (such as acetone) and may thus explain the observed oxygenates. The organo nitro species are assumed to be relatively stable and may thus enable the formation of N₂.

2.5 Conclusions

The reduction of NO₂ by propene over partially exchanged NaH-Y and steamed NaH-Y zeolite has been studied by kinetic activity test and infrared spectroscopy. *In situ* IR spectroscopy using mixtures of C₃H₆, O₂ and NO₂ showed that propene readily adsorbs and, in the absence of O₂ or NO₂, oligomerizes on nearly all Brønsted acid sites located in the supercages, while propene does not adsorb on the sites located in the sodalite cages. Propene adsorption experiments showed that the presence of O₂ leads to the formation of bulky coke like species which blocked the zeolites pores of the parent NaH-Y zeolite and disabled propene from interacting with approximately 80% of the supercage Brønsted acid sites. Kinetic and IR experiments show that NaH-Y catalyzes the reaction of propene with NO₂. Pore blocking, due to the formation of bulky carbonaceous species, was not observed in the presence of NO₂ indicating that NO₂ either is able to oxidize these carbonaceous deposits or that these deposits form at a low rate. Pore blocking was absent with the steamed NaH-Y sample which was concluded to be resulting

Reduction of NO₂ by propene over parent and steamed NaH-Y zeolite

from the mesopores induced by steaming. Co-feeding C₃H₆ and oxygen did not lead to the formation of CO_x although small amounts of oxygenates were observed on the catalysts surface. Kinetic measurements with and without O₂ only showed lower N₂ yields in the presence of O₂ on steamed NaH-Y. Therefore, we conclude that O₂ does not play a significant role in the formation of N₂, but solely enhances the formation of carbonaceous deposits and, at temperatures above ~350°C, the unselective combustion of C₃H₆. IR measurements show that co-feeding NO₂ and C₃H₆ results in the formation of nitrogen containing species, which are generally accepted to be intermediates in the formation of N₂. The yield and selectivity to N₂ are determined by competitive reactions of NO₂ reacting with coke (formed mainly by C₃H₆ reacting with O₂), partial oxidation of C₃H₆ by NO₂ to form NO and oxygenates and the formation of organo nitro or nitroso compounds. Optimal N₂ yields were obtained feeding C₃H₆ and NO₂ in the stoichiometric ratio of 1 to 4, respectively. Extrapolation of the N₂ selectivity towards infinitely low C₃H₆ feed concentrations suggests a limit of the N₂ selectivity of 50%.

References

- 1 M. Iwamoto, H. Hamada, *Catal. Today* 10 (1991) 57.
- 2 W. Held, A. König, T. Richter, L. Puppe, SAE Tech. Paper 900496.
- 3 J.T. Miller, E. Gusker, R. Peddi, T. Zheng, J.R. Regalbuto, *Cat. Lett.* 51 (1998) 15.
- 4 T. Gerlach, U. Illgen, M. Bartoszek, M. Baerns, *Appl. Cat. B Env.* 22 (1999) 269.
- 5 A. Satsuma, K. Yamada, T. Mori, M. Niwa, T. Hattori, Y. Murakami, *Catal. Lett.* 31 (1995) 367.

Chapter 2

- 6 V. Indovina, M.C. Campa, B.I. Iacono, D. Pietrogiacomì, *Catal. Lett.* 66 (2000) 81.
- 7 K. Yogo, M. Umendo, H. Watanabe, E. Kikuchi. *Catal. Lett.* 19 (1993) 131.
- 8 H. Hamada, Y. Kintaichi, M. Sasaki, T. Ito, *Appl. Catal.* 64 (1990) L1.
- 9 A. Giroir-Fendler, P. Denton, A. Boreave, H. Praliaud, M. Primet, *Topics in Cat.* 16/17 (2001) 237.
- 10 A. Baiker, C. Wögerbauer, M. Maciejewski, U. Göbel, *Topics in Cat.* 16/17 (2001) 181.
- 11 S. Vergne, A. Berreghis, J. Tantet, C. Canaff, P. Magnoux, M. Guisnet, N. Davias, R. Noiroto, *Appl. Catal. B Env.* 18 (1998) 37.
- 12 S.E. Maisuls, K. Seshan, S. Feast, J.A. Lercher, *Appl. Catal. B Env.* 29 (2001) 69.
- 13 Y. Li, J.N. Armor, *Appl. Catal. B* 1 (1992) L31.
- 14 Y. Li, J.N. Armor, *Appl. Catal. B* 2 (1993) 239.
- 15 K. Yogo, E. Kikuchi, *Stud. Surf. Sci. and Catal.*, vol 84 (Elsevier, Amsterdam, 1994) p. 1547.
- 16 C. Yokoyama, M. Misono, *J. Catal.* 150 (1994) 9.
- 17 J.N. Armor, Y.J. Li, T.L. Slager, *J. Catal.* 150 (1994) 388.
- 18 N.W. Cant, A.D. Cowan, R. Dumpelmann, *J. Catal.* 151 (1995) 356.
- 19 M.C. Campa, S. de Rossi, G. Ferraris, V. Indovina, *Appl. Catal. B Env.* 8 (1996) 315.
- 20 D.B. Lukyanov, E.A. Lombardo, G.A. Sill, J. d'Itri, W.K. Hall, *J. Catal.* 163 (1996) 447.
- 21 B.J. Adelman, T. Beutel, G.-D. Lei, W.M.H. Sachtler, *J. Catal.* 158 (1996) 327.
- 22 A.Y. Stakheev, C.W. Lee, S.J. Park, P.J. Chong, *Catal. Lett.* 38 (1996) 271.
- 23 T.E. Hoost, K.A. Laframboise, K. Otto, *Catal. Lett.* 33 (1995) 105.

Reduction of NO₂ by propene over parent and steamed NaH-Y zeolite

- 24 J. Szanyi, M.T. Paffett, *J. Catal.* 164 (1996) 232.
- 25 C.A. Emeis, *J. Catal.* 141 (1993) 347.
- 26 A. Zecchina, S. Bordiga, G. Spoto, D. Scarano, L. Carnelli, *J. Chem. Soc. Faraday Trans.* 89 (1993) 1843.
- 27 F. Eder, M. Stockenhuber, J.A. Lercher, *Stud. Surf. Sci. Catal.* 97 (1995) 495.
- 28 F. Eder, M. Stockenhuber, J.A. Lercher, *J. Phys. Chem B* 101 (1997) 5414.
- 29 A.G. Pelmenschikov, R.A. van Santen, *J. Phys. Chem.* 97, 1993 10678.
- 30 T. Tanaka, T. Okuhara, M. Misono, *Appl. Catal. B Env.* 4 (1994) L1.
- 31 S.-K. Park, Y.-K. Park, S.-E. Park, L. Kevan, *PCCP* 2, (2000) 5500-5509.
- 32 M. Trombetta, G. Busca, S. Rossini, V. Piccoli, U. Cornaro, A. Guercio, R. Catani, Willey R.J., *J. Catal* 179, (1998) 581-596.
- 33 G. Centi, A. Galli, S. Perathoner, *J. Chem. Soc. Faraday Trans.* 92 (1996) 5129.
- 34 Y. Ukisu, S. Sato, A. Abe, K. Yoshida, *Appl. Catal. B Env.* 2 (1993) 147.
- 35 S. Sumiya, H. He, A. Abe, N. Takasawa, K. Yoshida, *J. Chem. Soc. Faraday Trans.* 94 (1998) 2217.
- 36 van Bokhoven J.A., Koningsberger D.C., Kunkeler P., van Bekkum H., *J. Catal* 211 (2002) 540.
- 37 N.W. Hayes, W. Grunert, G.J. Hutchings, R.W. Joyner, E.S. Shpiro, *J. Chem. Soc. Commun.* (1994) 531.
- 38 S. Vergne, A. Berreghis, J. Tantet, C. Canaff, P. Magnoux, M. Guisnet, N. Davies, R. Noiro, *Appl. Catal. B Env.* 18 (1996) 37.
- 39 C. Yokoyama, M. Misono, *Catal. Today* 22 (1994) 59.
- 40 J. March, *Advanced Organic Chemistry*, 3rd ed. Wiley, New York, 1985, p. 739-740.

Chapter 2

Chapter 3

Reduction of NO_2 by C_3H_6 and C_3H_8 over H-form zeolites

Abstract

The reduction of NO_2 by C_3H_6 and C_3H_8 over NaH-Y, H-USY, H-MOR and H-ZSM5 has been investigated by kinetic measurements and in situ IR spectroscopy. Using propene, the stronger acidic zeolites, H-MOR and H-ZSM5, quickly deactivated at low temperatures, while the weaker acidic zeolites NaH-Y and H-USY remained active for a significantly longer period. This insensitivity of NaH-Y and H-USY for deactivation is related to the tendency to form oxygenates on these zeolites, while inactive carbonaceous deposits are the dominating products on H-MOR and H-ZSM5. The activity of H-MOR is largely regained with increasing temperature, while for the other zeolites the activity remains relatively low. It is speculated that the confinement of the MOR side pockets prevent the formation of stable coke species enabling the high activity. Using propane, H-MOR and H-ZSM5 show significantly higher activities than NaH-Y and H-USY, which is tentatively attributed to the ability to dehydrogenate propane to propene. The reaction mechanisms, using propene and propane, are thus concluded to be largely similar. A mechanism is proposed in which propene adsorbs on Brønsted acid sites, where it reacts with NO_2 to form organo nitro compounds that are converted in a complex sequence of reaction steps to N_2 .

3.1 Introduction

In the search for effective NO_x reduction for lean burn or diesel engines many catalytic systems have been tested and reported. The majority of the literature has focused on supported transition metal based catalysts, initiated by the early work of Iwamoto *et al.* [1] and Held *et al.* [2]. The mechanisms describing the reduction of NO to N₂ can be roughly divided into two groups [3, 4]. According to the first, NO decomposes on a reduced metal surface and N₂ is formed by the recombination of two adsorbed N atoms. The reductant maintains in this case the metal in a reduced state by reacting with adsorbed oxygen atoms. The second group of mechanism utilizes the reaction of NO or NO₂ with a hydrocarbon yielding nitrogen containing intermediates, which after several steps lead to the formation of amines or ammonia. Subsequently, a reaction similar to NH₃-SCR leads to the formation of N₂. In this case, the metal primarily catalyzes the oxidation of NO to NO₂ [5-13]. NO₂ is more reactive than NO [5] and plays an important role for the formation of nitrogen containing intermediates.

Kinetic and mechanistic aspects of the reduction of NO or NO₂ [9, 14-17] by methane, C₃H₆, C₃H₈ and iso-butane have been studied by several authors. Zeolites have been frequently used as support. In their acidic form, zeolite based supported metal catalysts have been shown to be able to catalyze the formation of N₂ at significantly lower temperature than most other metal supported catalysts [5,18-22]. It has been found that H-MOR and H-ZSM5 are more reactive than NaH-Y or H-USY [18, 23, 24]. While using methane as reductant, the activity of the Brønsted acidic zeolites was shown to be related to the acid site concentration [19, 23] and/or acid strength [25]. For the reaction of NO₂ to N₂, N₂O and/or NO, clear relations have not been reported between the type of zeolite and selectivity. Among the possible reductants, alkenes (such as propene and ethene) have been found to be more reactive than alkanes (such as propane and ethane). However,

alkenes also lead to the formation of carbonaceous deposits, which may deactivate the catalyst.

H-form zeolites have a relatively low activity for the oxidation of NO to NO₂ [25-28]. Since NO reduction is thought to proceed *via* intermediate NO₂ formation, we here compare different zeolites in their Brønsted acidic form for the reduction of NO₂ by C₃H₆ in order to understand the role of the support. Being a strong oxidizing agent, NO₂ may minimize or prevent the deposition of carbonaceous species and, thus, the performance of the zeolites can be compared at optimized conditions.

3.2 Experimental

3.2.1 Materials

H-ZSM5 was obtained from Alsi Penta Zeolith GmbH and has a Si/Al ratio of 10.2 and was used as supplied. The H-MOR used is a dealuminated mordenite [29] with a Si/Al ratio of 5.1 and was supplied by the Japanese Catalysis Society. Na-Y (CBV100) and H-USY (CBV740) were obtained from Zeolyst International. The CBV100 has a Si/Al ratio of 2.6 while CBV740 is a dealuminated sample with a Si/Al ratio of 25. The H-MOR and H-ZSM5 zeolite were obtained in the NH₃ form, CBV100 was obtained in the Na form while CBV740 was supplied in the H-form. To obtain the NH₃ form of Na-CBV100, the zeolite was ion exchanged in NH₃NO₃ aqueous solution for 24 hours at room temperature. AAS measurements for Na, K, Al and Si confirmed the given Si/Al ratios and showed that an exchange of 70% was achieved on the CBV100 while no Na and K was found in the H-MOR, H-ZSM5 or H-USY samples. The Brønsted and Lewis acid site concentrations were measured by *in situ* IR spectroscopy during the adsorption of pyridine [30]. For this, the catalysts were activated in vacuum (10⁻⁵ mbar) at 450°C

Chapter 3

(MOR at 550°C) for 30 minutes after which the temperature was lowered to 150°C. The catalysts were then exposed to pyridine at initially 10^{-2} mbar, gradually increasing to 10^{-1} mbar. Spectra were recorded during adsorption for 30-60 minutes. Finally, the samples were outgassed for 30 minutes at 10^{-5} mbar, what, however, did not result in a decrease of the pyridine bands. On the NaH-Y and H-MOR samples a complete coverage of all Brønsted acid sites was not obtained within the given time span, which may be related to increasing diffusion constraints, or in case of H-MOR, the narrow access to the sites located in the side pockets. The integrated areas of Brønsted acid and pyridinium bands showed linear correlation for all samples. The values reported for NaH-Y and H-MOR were obtained by extrapolation of the linear correlation. Note that on NaH-Y pyridine appeared to adsorb preferentially on the HF SiOHAl sites, which correspond to Brønsted acid sites located in the supercages, and the value obtained, thus, represents only these Brønsted acid sites. On H-MOR, pyridine may have preferentially adsorbed on the main-channel sites what could explain the relative low value obtained. The corresponding Brønsted and Lewis acid site concentrations are listed in Table 1.

Table 1. Brønsted and Lewis acid site concentrations

	Si/Al ratio	Brønsted acid sites [$\mu\text{mol/g}$]	Lewis acid sites [$\mu\text{mol/g}$]
NaH-Y	2.6	630	7
H-USY	25.6	150	25
H-ZSM5	10.2	692	0
H-MOR	5.1	624	16

3.2.2 Infrared spectroscopic measurements

For *in situ* IR measurements, approximately 2 mg catalyst was pressed into a self-supporting wafer of 1 cm diameter. The wafer was placed into a circular oven and was fixed between two gold rings. The oven was placed into a stainless steel cell equipped with CaF₂ windows. The maximum temperature that could be achieved in the cell was 550°C. The cell was connected to a flow system that allows the catalyst to be exposed to the desired gas mixture. Spectra were recorded on a BRUKER IFS 88 spectrometer using a resolution of 4 cm⁻¹. Prior to exposure to the gas mixture the catalysts were activated *in situ* in He at 450°C (10°C/min) for 30 minutes. During activation, water and NH₃ desorbed and the zeolite in H-form was obtained.

3.2.3 Kinetic measurements

For the kinetic measurements the catalyst was pressed to pellets, crushed and sieved to obtain particles of 0.3-0.6 mm diameter. Typically 200 mg of catalyst particles were mounted in a quartz tube reactor and held between quartz wool plugs. A thermocouple, shielded by a closed quartz tube, measured the temperature inside the catalyst bed. The catalyst was activated *in situ* by heating to 450°C (20°C/min) in a He flow of 100 ml/min, where it remained for 1 hour after which the reactor was cooled down to the initial reaction temperature. The feed mixture were composed using BROOKS 5850S massflow controllers and gasmixtures of 1.0% NO₂/He, 1.0% C₃H₆/He or C₃H₈/He, 100% O₂ and He as balancing gas. Typically a flow of 200 ml/min was used which resulted in a GHSV of about 15000 h⁻¹. Gasmixtures were supplied by Messer Griesheim GmbH, Germany. Products were analyzed by a HP gas chromatograph equipped with a MS 5A and PLOT Q capillary columns (N₂, N₂O, O₂, CO, CO₂, CH₄, C₃H₆ and C₃H₈) and

Chapter 3

Thermo Environmental Instruments Inc. model 42C NO_x analyzer equipped with an EPM diluting stack sampler (NO, NO₂). For steady state activity measurements the temperature was increased by 25°C per step from 150°C to 600°C. The time at which the reaction was left to equilibrate varied from 200 minutes at low temperature to 50 minutes at high temperatures. In some experiments, the C₃H₆ concentration was stepwise increased from 75 ppm to 125, 250, 500 and 1000 ppm. Chromatograms were taken after a stabilization period of 50 and 100 minutes at each step.

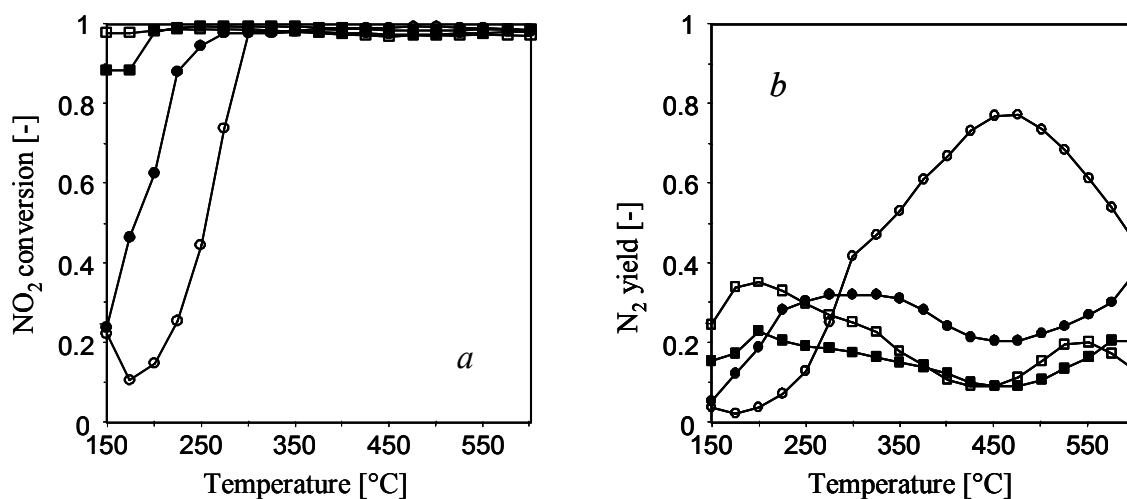


Figure 1: (a) NO₂ conversion and (b) N₂ yield versus temperature using 1000 ppm NO₂, 1000 ppm C₃H₆, 5% O₂ over (□) NaH-Y, (■) H-USY, (○) H-MOR and (●) H-ZSM5

3.3 Results

3.3.1 Reduction of NO₂ by C₃H₆

Figure 1 shows the NO₂ conversion and the N₂ yield as function of temperature for NaH-Y, H-USY, H-MOR and H-ZSM5 catalysts in a flow containing 1000 ppm C₃H₆, 1000 ppm NO₂ and 5% O₂. For NaH-Y, the NO₂ conversion was 100% at all temperatures measured (150-600°C). On H-USY, the

NO₂ conversion reached 100% only above 175°C. With H-MOR the NO₂ conversion was 10% at 175°C and increased to 100% at 300°C. On H-ZSM5 the NO₂ conversion was about 24% at 150°C from where it increased to 100% at 275°C.

Figure 1b compiles the corresponding N₂ yields obtained. NaH-Y showed a maximum N₂ yield of ~35% at 200°C from where it slowly decreased with increasing temperature. H-USY showed a similar pattern of activity. With H-MOR the N₂ yield was only 2% at 175°C, but strongly increased to reach about 42% at 300°C (this is the temperature where NO₂ conversion reaches 100%), it further increased to a maximum of about 77% at 475°C. Further increasing temperatures caused a decrease of the N₂ yield to 45% at 600°C. With H-ZSM5, the N₂ yields were initially low, but varied between 38% and 22% with temperature. Note that NaH-Y, H-USY and H-ZSM5 showed a minimum in the N₂ yield around 450°C.

The main products of NO₂ conversion were N₂, NO and N₂O. At lower temperatures, the last was found in concentrations of up to 20%. The nitrogen balance during the experiments was incomplete varying between 60 and 100%, which suggests that part of the nitrogen is retained on the catalyst surface.

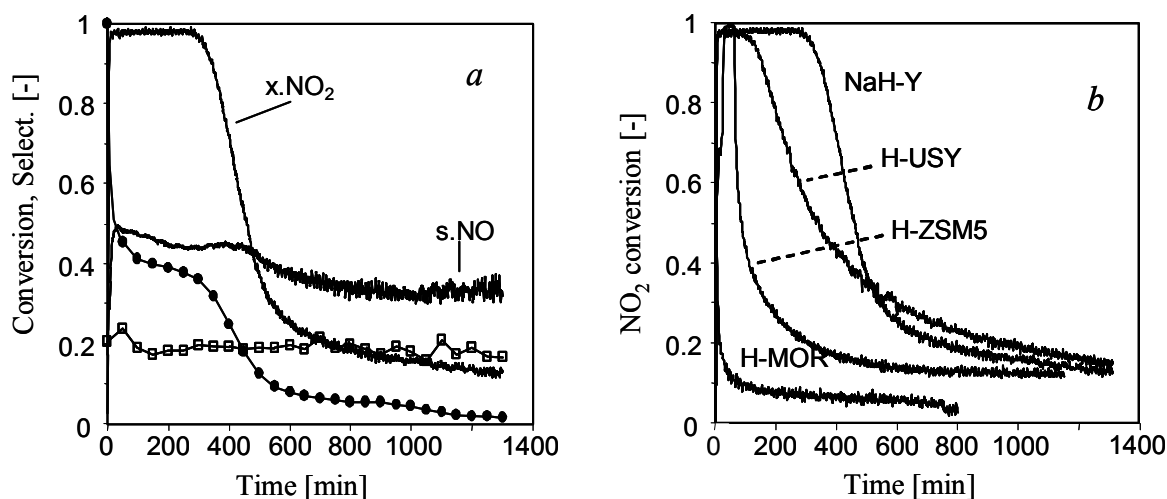


Figure 2: (a) NO₂ conversion (x.NO₂), C₃H₆ conversion (●), N₂ selectivity (□) and NO selectivity (s.NO) at 150°C using 1000 ppm NO₂, 1000 ppm C₃H₆, 5% O₂ over NaH-Y, (b) NO₂ conversion in time over different catalysts.

Chapter 3

Figure 2a shows conversions, and selectivities obtained as a function of time over NaH-Y in a flow containing 1000 ppm of NO₂, 1000 ppm of C₃H₆ and 5% oxygen at 150°C. NO₂ and C₃H₆ conversions remained stable for about 5 hours after which the catalysts deactivated and the conversions decreased to about 10% of their original values. The selectivity to NO was relatively constant at ~45% during the first 5 hours and decreased to about 30% afterwards. The N₂ selectivity was nearly constant at about 20% during the whole 21 hours. This trend in selectivity was similar for the other catalysts.

Figure 2b shows the NO₂ conversions of all zeolites studied as function of time on stream. With H-USY the NO₂ conversion remained at 100% for about 2 hours, after which it decreased to about 15% during the next 21 hours. With H-MOR, NO₂ conversion decreased immediately and stabilized after about 1 hour to a constant level of about 5%. With H-ZSM5, the NO₂ conversion was unstable within the first 30 minutes. After 30 minutes it stabilizes to show the 'normal' transient behavior with typically 100% conversion of NO₂. Although variations in the first 30 minutes appear rather unexpected, these variables were highly reproducible. H-ZSM5 strongly deactivated after 65 minutes and the NO₂ conversion stabilized at about 10%.

3.3.2 Reduction of NO₂ by C₃H₈

Figure 3 shows the NO₂ conversion and N₂ yield, over NaH-Y, H-USY, H-ZSM5 and H-MOR between 150 - 600°C in a flow containing 1000 ppm NO₂, 1000 ppm C₃H₈ and 5% O₂. The NO₂ conversion (Fig 3a) increased with increasing temperature in a similar fashion on all zeolites. The temperature at which this increase occurred was the lowest for H-ZSM5 reaching 50% conversion at ~200°C followed by H-MOR at 290°C, H-USY at 425°C and NaH-Y at 445°C. These variations of NO₂ conversion as a function of the reaction temperature were very

different from those obtained using C₃H₆ and clearly show that C₃H₈ is much less reactive than C₃H₆. The N₂ yields obtained (Fig 3b) using NaH-Y and H-USY increased with increasing temperature until 500°C. Then, the N₂ yields leveled off at 17% and 28%, respectively. With H-ZSM5, a maximum of ~84% was obtained at 450°C, while with H-MOR a maximum of ~74% was achieved around 500°C. Besides N₂, NO was the other major product. N₂O was only obtained over H-ZSM5 and H-MOR. On all zeolites, a good nitrogen balance (~100%) was achieved indicating that in contrast to the situation with C₃H₆ as a reductant, nitrogen was not retained in surface species.

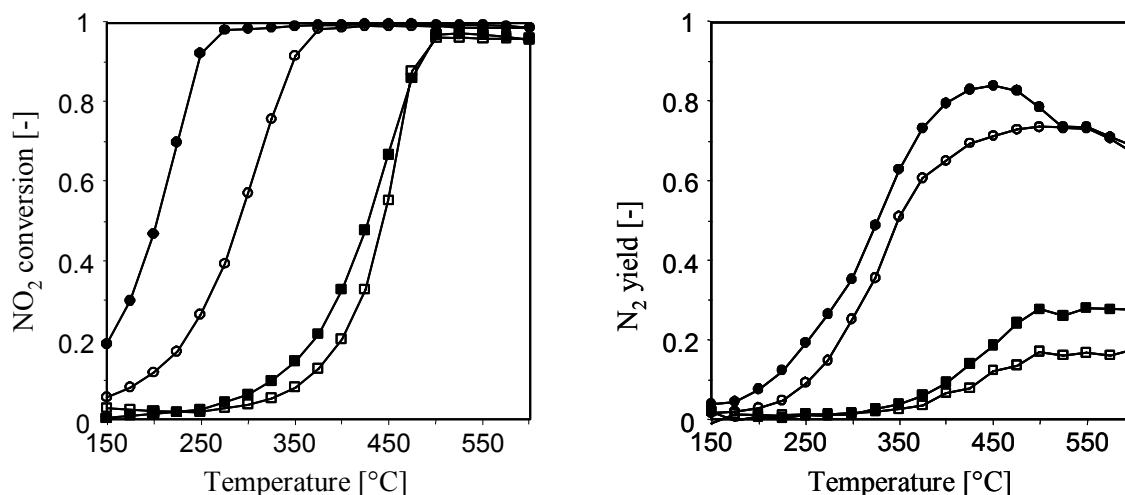


Figure 3: (a) NO₂ conversion and (b) N₂ yield versus temperature using 1000 ppm NO₂, 1000 ppm C₃H₈, 5% O₂ over (□) NaH-Y, (■) H-USY, (○) H-MOR and (●) H-ZSM5

3.3.3 Influence of C₃H₆ partial pressure on NO₂ conversion

Figure 4a shows the NO₂ conversion as a function of feed C₃H₆ concentration at 200°C for the four zeolites used. With NaH-Y, the NO₂ conversion increased with increasing C₃H₆ concentration to reach nearly 100% at 250 ppm of C₃H₆ and remained 100% at higher C₃H₆ concentrations. On H-USY and H-ZSM5 the increase in NO₂ conversion with increasing C₃H₆ feed concentration was less

pronounced compared to NaH-Y and reached 100% NO₂ conversion at 500 ppm of C₃H₆. With H-ZSM5, the NO₂ conversion dropped below 100% with further increase of the C₃H₆ feed concentration. The NO₂ conversion with H-MOR at 75 ppm C₃H₆ was nearly identical to that found on other zeolites and slightly decreased to about 15% with increasing C₃H₆ concentration.

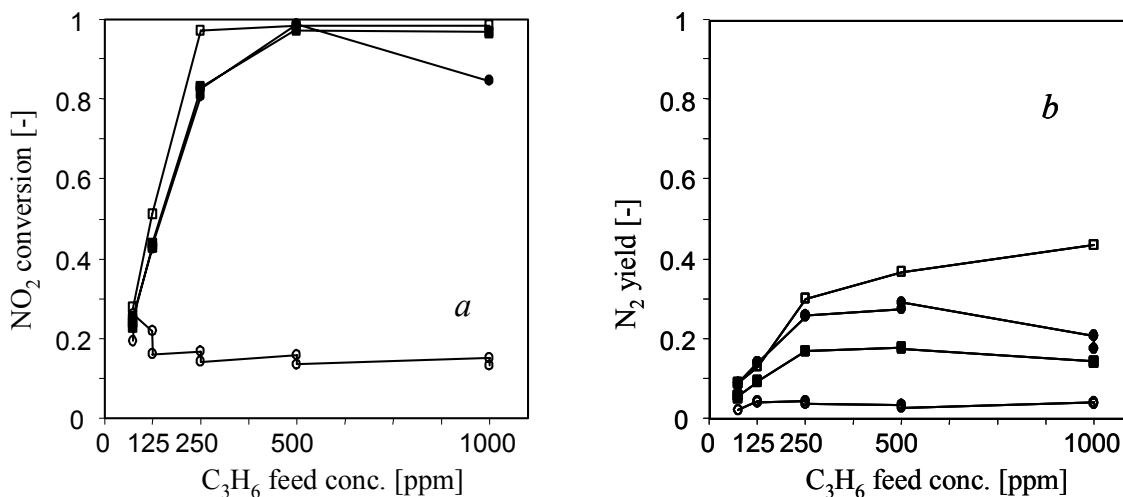


Figure 4: (a) NO₂ conversion and (b) N₂ yield versus C₃H₆ feed concentration using 1000 ppm NO₂, 5% O₂ at 200°C over (□) NaH-Y, (■) H-USY, (○) H-MOR and (●) H-ZSM5.

Figure 4b shows the corresponding N₂ yields obtained. With increasing C₃H₆ concentration the N₂ yields increased almost linearly until 250 ppm except with H-MOR, for which the N₂ yield remained extremely low. The linearly increasing NO₂ conversion and N₂ yields in this region, suggest that the selectivity for N₂ is constant until 250 ppm. Above 250 ppm C₃H₆, the N₂ yield changes only weakly with further increasing C₃H₆ feed concentration, while the NO₂ conversion has reached 100% under these conditions. In these experiments, for NaH-Y, H-USY and H-ZSM5, propene conversions were close to 100% using 75 to 250 ppm propene, and decreased gradually to below 40% with increasing propene feed to

500 and 1000 ppm. For H-MOR, propene conversion was initially high (~100%) but rapidly decreased to ~10% with increasing propene concentration (>125 ppm).

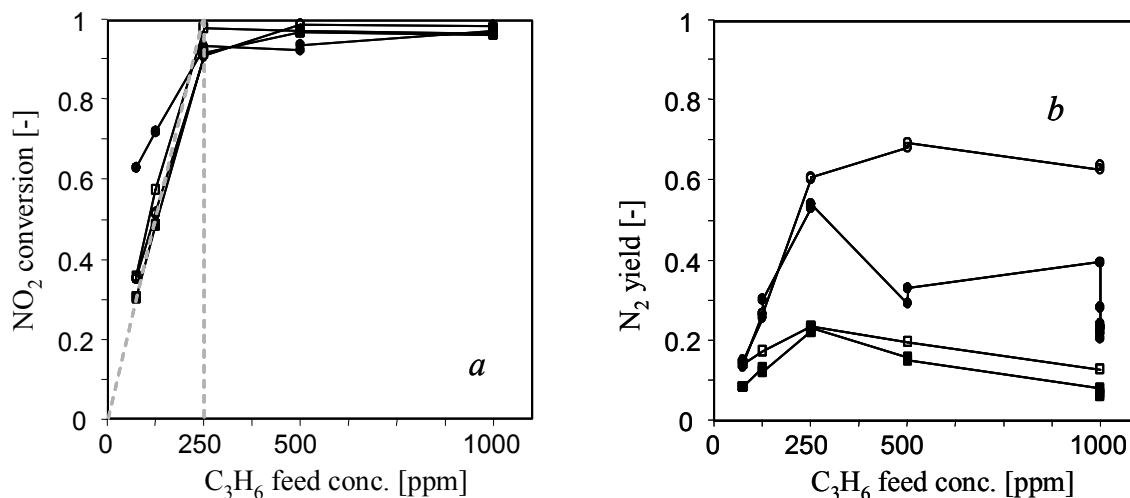


Figure 5: (a) NO₂ conversion and (b) N₂ yield versus C₃H₆ feed concentration using 1000 ppm NO₂, 5% O₂ at 450°C over (□) NaH-Y, (■) H-USY, (○) H-MOR and (●) H-ZSM5.

Figure 5a shows the NO₂ conversion as a function of C₃H₆ concentration at 450°C. Between 75 and 250 ppm C₃H₆ the NO₂ conversions linearly increased and reached 100% at 250 ppm of C₃H₆. H-ZSM5 differed slightly from the other three zeolites in that the NO₂ conversion remained low. Figure 5b shows the N₂ yields obtained. Below 250 ppm C₃H₆, the N₂ yields linearly increased with increasing C₃H₆ concentration, although H-ZSM5 and H-MOR produced much more N₂ than NaH-Y and H-USY. Above 250 ppm C₃H₆ the N₂ yields slowly declined. Apparently, the optimal N₂ yields are obtained at the stoichiometric ratio of 1 mol C₃H₆ to 4 mol NO₂. This ratio was already observed for NaH-Y in chapter 2 of this thesis but now appears valid for the 3 other Brønsted acidic zeolites. H-MOR was the least affected by the excess of C₃H₆, as the N₂ yield remained nearly constant during all experiments. Note that during these experiments, propene conversions were close to 100 % using 75 to 250 ppm propene, and decreased gradually to

Chapter 3

values between 60 and 40% when increasing the propene concentration to 500 and 1000 ppm.

3.3.4 Identification of adsorbed species by *in situ* IR spectroscopy

Figure 6 shows IR difference spectra (the spectra of the catalyst in contact with the reactants after subtracting spectra for the activated catalyst) of adsorbed species in a flow containing (1) C_3H_8 , (2) C_3H_6 , (3) $C_3H_6 + O_2$ and (4) $C_3H_6 + NO_2$ for (a) NaH-Y, (b) H-MOR and (c) H-ZSM5 at 120°C. Spectrum 1 in Figures 6 a, b and c were recorded after flowing C_3H_8 and subsequently flushing with He. The complete absence of CH stretching and deformation bands indicates that C_3H_8 was not retained on the materials after purging. The IR spectra of H-MOR and H-ZSM5 showed traces of sorbed water, which is tentatively attributed to feed impurities. After sorption of C_3H_6 (Spectrum 2), strong bands of CH stretching (2957, 2934, 2868 cm^{-1}) and deformation vibrations (1468, 1382, 1366 cm^{-1}) appeared on all three zeolites. Simultaneously a strong negative band appeared at the wavenumber of the Brønsted acidic bridging hydroxyl group (NaH-Y 3642 cm^{-1} , H-MOR 3603 cm^{-1} and H-ZSM5 3607 cm^{-1}) indicating that C_3H_6 is sorbed on the Brønsted acid site. In addition, all zeolites showed a band at 80-120 cm^{-1} wavenumbers lower from the Brønsted acid site band, which indicates that a part of the bridging OH groups are interacting with saturated alkane fragments, presumably generated by oligomerizing propene. With H-ZSM5, Spectra 2.1 and 2.2 in Figures 6c, recorded after 3 and 360 minutes respectively, show that the CH bands nearly reached their final intensity within 3 minutes, while a band at 1508 cm^{-1} continued to increase during prolonged exposure. The band at 1508 cm^{-1} is typical for the ring stretching vibration in para-substituted aromatic species and, thus, indicates that aromatic species were formed. A small band at 3090 cm^{-1} is assigned to the CH stretching vibration of aromatic species.

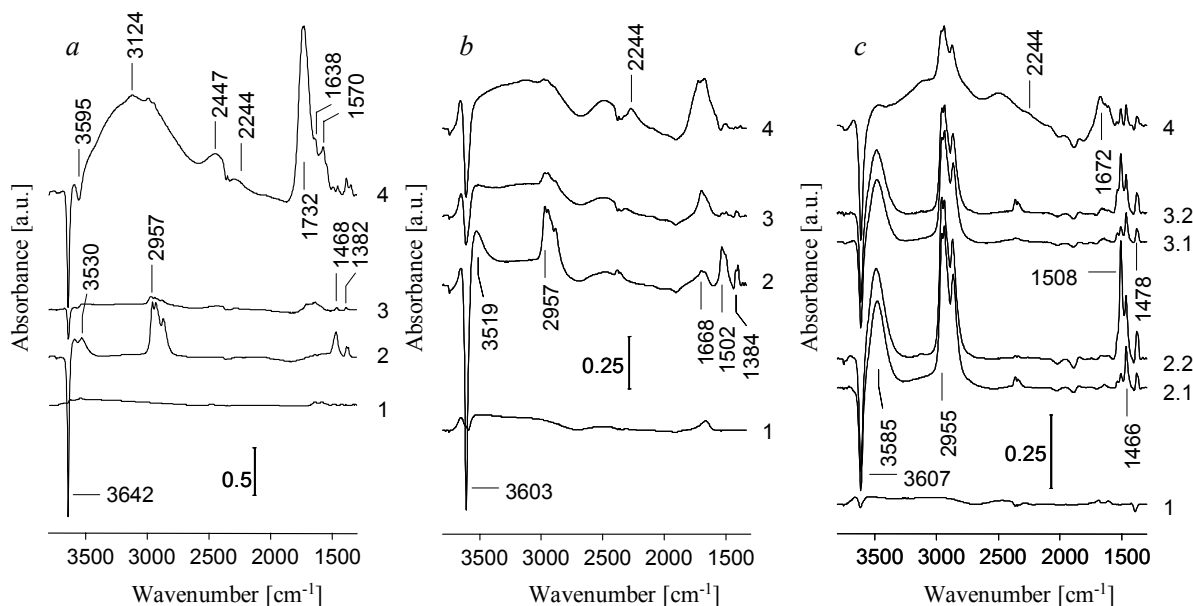


Figure 6: IR difference of (a) NaH-Y, (b) H-MOR and (c) H-ZSM5 after contacting with (1) C_3H_8 , (2) C_3H_6 , (3) $\text{C}_3\text{H}_6/\text{O}_2$, (4) $\text{C}_3\text{H}_6/\text{NO}_2$ at 120°C .

The formation of aromatic species under comparable reaction conditions is also reported in the literature [31-33]. The band at 3090 cm^{-1} , appeared with a much lower intensity on H-MOR, while it was not observed on NaH-Y. Exposing the zeolites to a mixture of C_3H_6 and oxygen led to Spectrum 3 in Figures 6a-c. On NaH-Y and H-MOR the CH the bands appeared with a much lower intensity as compared to those in the absence of oxygen (Spectra 2). Instead, the band at 1668 cm^{-1} appeared with an increased intensity indicating the presence of conjugated π -systems. The presence of oxygen seems to enable the formation of oligomers. Note that H-ZSM5 appears to be nearly unaffected by the presence of oxygen.

Spectra 4 in Figures 6a-c were recorded in a flow of C_3H_6 and NO_2 . On NaH-Y an intense band between $3595\text{--}2447\text{ cm}^{-1}$ and the bands at 2447 cm^{-1} and 1638 cm^{-1} indicate that a large amount of water was adsorbed under these conditions. This water is probably the result of the oxidation of C_3H_6 by NO_2 as it appeared on the introduction of NO_2 and, thus, cannot be attributed to feed

Chapter 3

impurities. At 1732 cm^{-1} a very strong band appeared, which indicates the presence of carbonyl groups. The bands at 1570 cm^{-1} are assigned to carboxylate or organic nitro compounds [34]. The relative weak band at 2244 cm^{-1} might indicate the presence of cyanide or isocyanate species. The weak band at 3124 cm^{-1} , in combination with bands characteristic of cyanide or iso-cyanate functions, is assigned to the -OH stretching vibration in an oxime, aci-nitro or hydroxamic acid.

Gerlach *et al.* [35] observed a band at 2280 cm^{-1} after adsorption of acrylonitrile on H-MOR and assigned it to the CN stretching vibration of the nitrile. In the literature, cyanide groups are usually associated with a band appearing around $2120\text{-}2170\text{ cm}^{-1}$ while bands of isocyanate species are reported to appear around $2230\text{-}2290\text{ cm}^{-1}$ [36-40]. As the present spectra were measured at 120°C and, thus, at a lower temperature than in the experiments of Gerlach *et al.* (300°C) and our band appears in the area commonly associated with isocyanate species it seems more likely that the band we observe at 2244 cm^{-1} should be assigned to isocyanate species.

On H-MOR similar bands appeared, the carbonyl band, however, was reduced to a shoulder of the water and carboxylate band. The isocyanate band (2244 cm^{-1}) appeared more intense than on NaH-Y. On H-ZSM5 the CH bands were relatively intense compared to those on NaH-Y and H-MOR. In addition, the mixture of C_3H_6 and oxygen was less reactive on H-ZSM5 than on NaH-Y and H-MOR. Kinetic results in Figure 3 showed H-ZSM5 to be more active than H-MOR and NaH-Y and, which thus appears to be in conflict with the surface chemistry as shown by the IR results.

Figure 7 shows the spectra obtained at 450°C , for (a) NaH-Y, (b) H-MOR and (c) H-ZSM5 in a flow of, (1) C_3H_6 , (2) $\text{C}_3\text{H}_6 + \text{O}_2$, (3) $\text{C}_3\text{H}_6 + \text{NO}_2$ and (4) NO_2 . In all cases a practically stable spectrum was obtained after equilibration for 30 minutes. Feeding only C_3H_6 (Spectrum 1) resulted in a band around 1580 cm^{-1} ,

which in the absence of oxygen indicates polyaromatic or graphite like coke species. The practically absent CH bands indicate that the coke formed contains nearly no hydrogen. The negative band around 3640 cm⁻¹ indicates that the coke formed blocks the Brønsted acid sites.

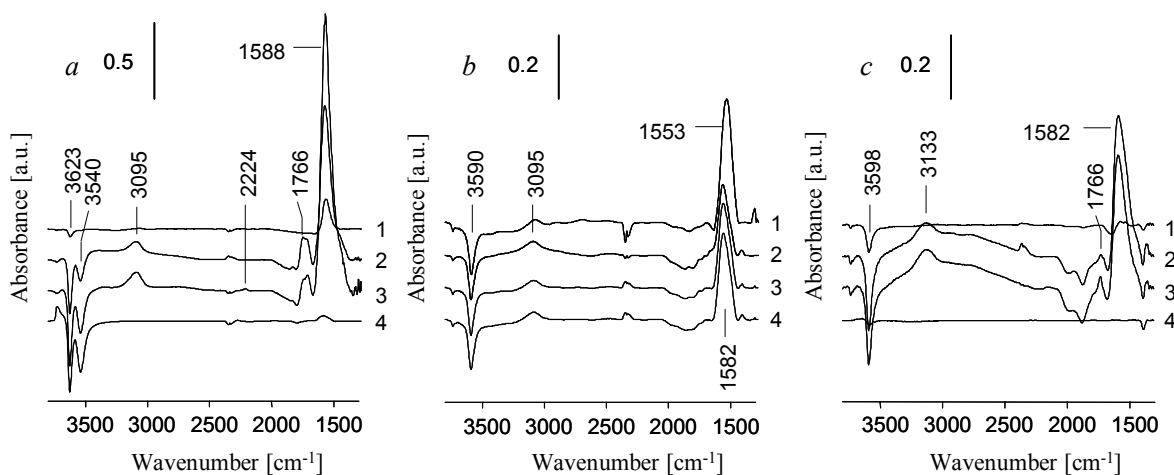


Figure 7: IR difference spectra of (a) NaH-Y, (b) H-MOR and (c) H-ZSM5 at 450°C after contacting with (1) C₃H₆, adding oxygen (2) C₃H₆/O₂, removing oxygen and adding NO₂ (3) C₃H₆/NO₂ and removing C₃H₆ (4) NO₂.

On addition of 5% oxygen (Spectrum 2) the coke band increased on NaH-Y and H-ZSM5, while it decreased slightly on H-MOR. Simultaneously, the negative bands for the bridged hydroxyl groups increased in intensity. Note that on NaH-Y also species have adsorbed on the sodalite cage Brønsted acid sites as indicated by the second negative band at 3540 cm⁻¹. A relative broad band at 3095 cm⁻¹ appeared, which is probably due to a coordinated hydroxyl group, possibly from a zeolite lattice bridging hydroxyl group or an alcohol group on the coke. On NaH-Y, and with a lower intensity on H-ZSM5, bands appeared at 1766 and 1732 cm⁻¹ indicating the presence carbonyl groups. On H-MOR a small band at 1432 cm⁻¹ was assigned to a deformation of a carboxylate or coke species. The band appeared with H-ZSM5 and NaH-Y only as shoulder below the wide and intense coke band. Apparently, the presence of oxygen has led to an increase in the amount

of coke and the formation of some partially oxidized species. On H-ZSM5 a very wide band is found, stretching from ~ 3250 to 2236 cm^{-1} , indicating the adsorption polar compounds forming hydrogen bondings to the Brønsted acid sites. This band appeared with a smaller intensity on NaH-Y and H-MOR.

Spectra 3 in Figures 7a-c were recorded after replacing oxygen with NO_2 . The spectra obtained are very similar to those obtained in the presence of C_3H_6 and O_2 . On NaH-Y the coke band increased significantly with time on stream, while on H-ZSM5 only a small increase of the 1726 cm^{-1} carbonyl band was observed and practically no changes were observed on H-MOR. We speculate that on NaH-Y and H-ZSM5, the formation of coke is enhanced by the presence of an oxidizing agent such as O_2 or NO_2 , while on H-MOR the presence of O_2 or NO_2 does not significantly influence coke formation. Only on NaH-Y a small band appeared at 2224 cm^{-1} indicating the presence of isocyanate or cyanide species. Spectra 4 in Figures 7a-c were recorded after stopping the flow of C_3H_6 , and maintaining only the stream of NO_2 in He. On NaH-Y and H-ZSM5 practically all adsorbed species were removed, while on H-MOR changes were not observed.

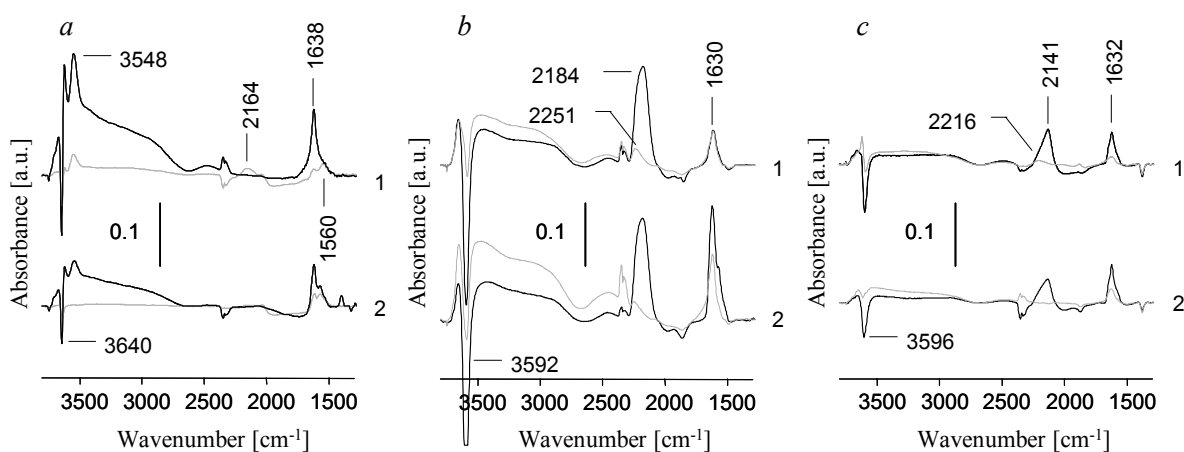


Figure 8: IR difference of (a) NaH-Y, (b) H-MOR and (c) H-ZSM5 in contact with (1) NO and flushing with He and (2) NO_2 and flushing with Helium at 120°C .

Figure 8 shows the IR difference spectra obtained in a flow of NO or NO₂ and after flushing with He on (a) NaH-Y, (b) H-MOR and (c) H-ZSM5 at 120°C. In the presence of NO or NO₂ a band indicating the presence of NO⁺ or NO₂⁺ [41-44] appeared at 2170 cm⁻¹ on NaH-Y, 2184 cm⁻¹ on H-MOR and 2141 cm⁻¹ on H-ZSM5. This band was most significant on H-MOR and H-ZSM5, while on NaH-Y it had only very low intensity and disappeared after prolonged exposure (3-5 minutes) to NO or NO₂. Simultaneously, a negative band appeared at 3640 cm⁻¹ on NaH-Y, at 3592 cm⁻¹ on H-MOR and at 3596 cm⁻¹ on H-ZSM5 indicating that the Brønsted acid sites formed hydrogen bonds to sorbed species. The band at 1638 cm⁻¹ indicates sorption of water and a weak band at 1560 cm⁻¹ indicates the formation of nitrates. After flushing with He, the NO_x⁺ bands on H-MOR and H-ZSM5 rapidly decreased to a fraction of their previous intensities. This indicates that the majority of the NO_x⁺ species is only weakly adsorbed. Consequently, the remaining bands at 2164 cm⁻¹ on HNaH-Y, 2251 cm⁻¹ on H-MOR and at 2216 cm⁻¹ on H-ZSM5 stem from stable NO_x⁺ species. As Brønsted acid sites on H-MOR and H-ZSM5 are reported to be stronger than those on NaH-Y [25] it is speculated that only the strongest Brønsted acid sites allow the formation of stable NO_x⁺ species.

3.4 Discussion

3.4.1 Influence of C₃H₆ partial pressure

The kinetic experiments clearly show that Brønsted acidic zeolites are able to catalyze the reactions of NO₂ with propene. Depending on the conditions, it results in the formation of N₂, NO and N₂O. Steady state experiments (see Figure 1) using a relatively high propene partial pressure showed that the selectivity to N₂ remained low on NaH-Y, H-USY and H-ZSM5, while over H-MOR the selectivity reached a maximum of nearly 80%.

Chapter 3

By decreasing the propene partial pressure (see Figures 4 and 5) the selectivity to N₂ can be optimized. Maximum N₂ selectivities were obtained using a propene partial pressure of 250 ppm (and 1000 ppm of NO₂). Experiments with varying propene concentrations (see Figures 4 and 5) allows us to conclude that NO₂ and propene react with a constant stoichiometry of 1 C₃H₆ to 4 NO₂. At propene partial pressures below this ratio the selectivity to N₂ is constant. At propene partial pressures below this ratio the carbon balance was practically 100%, while at higher propene concentrations the carbon balance had a deficit of up to 40% indicating that carbonaceous deposits are formed on the surface.

3.4.2 Sensitivity for deactivation

Figure 2 shows that H-MOR is readily deactivated at low temperatures when using propene. With increasing temperature the activity was regained and N₂ yields of nearly 80% were obtained at 475°C (see Figure 1). H-ZSM5 deactivated slightly slower, what allowed it to reach higher N₂ yields at low temperatures although the activity was not regained with increasing temperature. NaH-Y and H-USY deactivated even far slower, but it was also not possible to restore their activity with increasing temperature. Using propane (see Figure 3), catalytic activity was not observed at 150°C, while at 450°C high N₂ yields (>80%) were obtained using H-MOR and H-ZSM5. The maximum N₂ yields obtained on NaH-Y and H-USY were obtained above 500°C and remained below 30%. The deactivation is attributed to the formation of carbonaceous deposits on Brønsted acid sites, as concluded from the IR spectra in Figure 7. The formation of carbonaceous deposits from propene is enhanced by the presence of oxygen (see also chapter 2 of this thesis). Figure 6c indicates that on H-ZSM5 the formation of carbonaceous deposits from propene is not significantly enhanced by the presence of O₂. This is speculated to enable the high N₂ yields obtained on H-ZSM5 using

propane. We believe that in a first step propane is dehydrogenated to propene from where the reaction proceeds similar to the situation with propene. The dehydrogenation of propane is certainly one of the slowest steps, what in combination with the fast reaction of propene with NO₂, will result in extremely low propene concentrations in the pores of H-ZSM5.

The reaction of propene with NO₂ is speculated to be faster than the formation of carbonaceous deposits so that deactivation is largely inhibited. The Brønsted acid sites of NaH-Y and H-USY are less strong compared to those of H-MOR and H-ZSM5. From Figure 2 we conclude that H-MOR deactivates practically instantaneously upon contact with propene, closely followed by H-ZSM5, while NaH-Y and H-USY remain active for much longer. Deactivation occurs when propene adsorbs, oligomerizes and/or dehydrogenates to inactive coke species. Higher acid site strength results in faster deactivation. The NO₂ conversion in Figure 2 shows the characteristics of a break through curve which indicates that a front of deactivation moves progressively through the catalysts bed. The NO₂ conversion remains thereby 100% until this front reaches the end of the bed after which the conversion strongly decreases. The sequence of deactivation is difficult to explain. In this context it is interesting to know that NaH-Y was most sensitive to form carbonaceous deposits in the presence of O₂, followed by H-MOR and H-ZSM5, the latter being particularly insensitive. This suggests that stronger acid sites do not favor coking. Therefore, we conclude that the intrinsic tendency to coke is not the primary and sole reason for deactivation. Spectra 4 in Figures 6a-c show relative intense oxygenate bands (1732 cm⁻¹) on NaH-Y, which appear to be far less intense on H-MOR and H-ZSM5. Possibly, the Brønsted sites of relative low acid strength allow for the formation of these oxygenates while on the stronger acid sites these oxygenates are hardly formed in favor of carbonaceous deposits and thus enable relative long life times for NaH-Y and H-USY.

Chapter 3

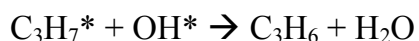
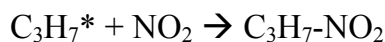
3.4.3 Activity of H-MOR at high temperatures using propene

Figure 7 shows that only on H-MOR the concentration of coke decreases upon introduction of O₂, while it increased on NaH-Y and H-ZSM5. Apparently, the reactivity of carbonaceous species differs strongly among the zeolites. On H-MOR (see Figure 7b), carbonaceous deposits appear inert to NO₂ while all coke species were oxidized and removed by NO₂ on NaH-Y and H-ZSM5 (see Figures 7a,c). The oxidation of coke by NO₂ selectively forms NO [45], thus, on NaH-Y, H-USY and H-ZSM5 coke is continuously being formed and removed converting NO₂ to NO, which influences the N₂ selectivity negatively. We speculate that the reason for the persistence of coke in H-MOR is the limited accessibility in the one-dimensional channel system. Thus, the steric constraint after blocking of a significant fraction of the pores allows the selective pathways to dominate in the alkene/NO₂ reaction. The presence of unreactive deposits in the pores suggests that most of the mordenite pore system is blocked and only the narrow zone at the outside of the particle are active. It can, however, not be excluded that the special pore geometry of the mordenite side-pockets also supports this trend as they prevent formation of bulkier carbonaceous deposits keeping at least the entrances to the pore system free of deposits and active for selective catalysis.

3.4.4 Propane activation

Overall, it is observed that the catalytic activity increased in the sequence NaH-Y < H-USY < H-MOR < H-ZSM5 (see Figure 3). It is interesting to note that this sequence does not follow the concentration of Brønsted or Lewis acid sites, but rather the expected strength of acid sites in the investigated materials. Note also that it is not only the catalytic activity which changes strongly as a function of the zeolite, but the temperature at which NO₂ and C₃H₈ begin to react. If we accept that

the reaction between NO₂ and an activated olefin or alkane is one of the critical steps in the reduction of NO₂ to N₂, one possible route of the alkane activation is related to the reaction of NO₂ with C₃H₈ removing an H* radical and forming C₃H₇* and HONO (reaction 1) [9]. Such a mechanism is analogous to the normal mechanism of nitration of alkanes [46]. The C₃H₇* radical formed is proposed to react with a second NO₂ molecule forming an organonitro radical (reaction 2), which can be stabilized by H radical abstraction. It is speculated that the Brønsted acid sites facilitates the abstraction by stabilizing it as radical cation. Alternatively dehydrogenation of propane can be visualized by a similar mechanism. In a pure Brønsted acidic zeolite propane is hydrogen bonded to the Brønsted acid sites and is, therefore, available for attack by physisorbed NO₂ and OH· radicals forming propene (reaction 3), which reacts further.



Because C₃H₆ is more reactive towards NO₂ than C₃H₈, the propene concentration remains always close to zero. Results with varying propene concentrations showed that at low propene concentrations the selective reaction with NO₂ is strongly favored over the formation of coke or unselective combustion by O₂, which accounts for the fact that the reaction of NO₂ with C₃H₈ does practically not lead to coke formation and high selectivities to N₂

3.4.5. On a possible reaction mechanism

In the literature several reaction steps have been proposed in which NO or NO₂ reacts with hydrocarbons. It is possible to divide the mechanism in two groups

Chapter 3

[3, 4]. The dissociation mechanism (1), in which NO adsorbs on reduced metal surfaces and is dissociated into N(ads) and O(ads). The reductant serves to keep the metal surface in a reduced state by removing adsorbed oxygen in order to enable the formation of N₂ by recombination of two adsorbed N atoms. The second class of mechanisms can be labeled the reductive mechanism (2), in which the reductant reacts with NO_x to form nitrogen containing intermediates. In many cases it is found that NO₂ rather than NO reacts with the hydrocarbon to form a nitrogen containing intermediate such as an organo-nitro (R-NO₂) or -nitrite compounds (R-ONO) [47, 48]. NO₂ is formed by oxidation of NO, which can be catalyzed by a supported metal or zeolites [49]. Note that NO₂ is thermodynamically favored over NO at temperatures below ~380°C. After forming the organo nitro or nitrite compounds, this intermediate is believed to be converted to cyanide or isocyanate species, which can be hydrolyzed to form amines and ammonia. The further reaction pathway to N₂ is thought to be similar to NH₃-SCR reaction.

The exact route and intermediates in these reactions remain yet unclear although many mechanistic steps have been reported. For instance, Cant [9] *et al.* have shown by isotopic labeling experiments that using methane, the initial step is the abstraction of a hydrogen while for iso-butane another, not specified, reaction is rate limiting. The rearrangement of nitromethane to isocyanic acid and hydrolysis to ammonia were concluded to be relatively fast and, thus, these intermediates were seldomly observed. Gerlach *et al.* [35] suggested that the initial step in the reduction of C₃H₆ by NO₂ over H-MOR is the formation of nitrosonium (NO⁺) or nitronium (NO₂⁺) ions on Brønsted acid sites. Our results (see Figure 8) show that NO⁺ or NO₂⁺ species formed on Brønsted acid sites are extremely weakly adsorbed and sensitive to water. Adsorption of propene or its derivatives on Brønsted acid sites forms relatively stable complexes and, thus, strongly suggest that all Brønsted sites are occupied by sorbed organic species, which is in agreement with our

Chapter 3

results in a primary nitro group [50]. In principle this would result in a free radical on the α -carbon, which could be neutralized by the addition of a second NO_2 to give a nitro or nitrite (R-ONO) (see Scheme 2). Hydrolysis of organo nitro compounds following the *Nef reaction* [51] is known to yield ketons and N_2O . N_2O was obtained during all reaction of propene or propane with NO_2 and thus may indicate that organo nitro species were formed. Alternatively, N_2O can be formed from a reaction of NO or NO_2 with ammonia. Nitrite compounds are very unstable and in the presence of oxygen and/or water immediately rearrange to nitrates, generating a carbonyl or alcohol group. This reaction pathway to a carbonyl group is tentatively used to explain the intense carbonyl band found on NaH-Y in the presence of C_3H_6 and NO_2 . The IR spectra observed show relatively little evidence for the presence of nitrogen containing species, partly because less reactive side products appear most abundant on the surface. Bands were observed that suggest the presence of nitrogen containing functional groups such as oximes, isocyanates and/or cyanides whereas remaining functional groups of the intermediates may include oxygenated and aliphatic groups. The influence of possible oxygen containing and aliphatic groups on the reactivity of these possible intermediates is beyond the scope of this study. The proposed mechanism (see Scheme 1) proceeds in a similar way as proposed for nitro-methane by Cowan *et al.* [14] and Lombardo *et al.* [15] and includes the nitrogen containing intermediates observed. The primary nitro group rearranges to an aci-nitro compound. Unlike with nitromethane, now the ethyl (or derivative of this group) enables the formation of a cis (II) and a trans (I) form of the aci-nitro compound. The corresponding hydroxamic acids (III and IV) can be formed *via* a *Beckmann* rearrangement [52]. This mechanism does not proceed *via* an oxime (R-C=NOH) and thus the band observed at 3124 cm^{-1} is more probable assigned to an aci-nitro or hydroxamic acid compound, both of which contain an N-OH group. Elimination of water from structure III will yield an isocyanate, which can be hydrolyzed to an amine, alcohol

mixture and ammonia. Structure IV could reduce to a cyanide *via* structure V and subsequent elimination of water and a hydrogen atom. IR measurements after adsorption of C₃H₆ together with oxygen leads to hydrogen poor coke species at 120°C indicating that abstraction of hydrogen or hydride transfer from intermediate species is relatively easy at reaction conditions. Hydrolysis of the cyanide leads to an amide and ammonia from where an NH₃-SCR type reaction may proceed.

Isocyanates and cyanides are often reported as observed and assigned to be critical intermediate to yield ammonia with which N₂ can be formed by an NH₃-SCR similar reaction. Amines, amides or related species are the intermediates of the hydrolysis to ammonia and it is conceivable that already before the formation of ammonia, NO or NO₂ attacks on the amine or amide by electrophilic substitution at the nitrogen yielding a diazonium or diazo compound which readily eliminates N₂ [53].



This reaction is known to precede using nitrous acid and may possibly occur on the zeolite catalyzed by the Brønsted acid site. This reaction may provide a shortcut to the formation of N₂ bypassing the hydrolysis of an amine or amide to form ammonia. The selectivity at which N₂ is formed thus depends on three competitive reactions; (1) removal of coke species by NO₂, (2) conversion of organic nitro groups to oxygenates, NO and N₂O and (3) the selective formation of N₂.

3.5 Conclusions

The reduction of NO₂ by C₃H₈ and C₃H₆ over Brønsted acidic zeolites has been investigated. With propene as reductant, the main reaction was the sorption of propene on Brønsted acid sites (formation of propyl alkoxy groups / propyl

Chapter 3

carbenium ions) and the subsequent oligomerization and aromatization. NO_2 supports the process *via* stoichiometric dehydrogenation (formation of NO). This causes rapid deactivation with all zeolites investigated. Only with H-MOR, the selectivity to N_2 was at acceptable levels (80 % at 450°C), all other zeolites showed N_2 yields lower than 40% at 100 % NO_2 conversion. With propane as reductant the activity of the zeolites increased with their expected acid strength and the decreasing average pore size. The differences in the reactivities are related to the activation of propane, which is speculated to occur *via* dehydrogenation. It is concluded that the main pathway proceeds with physisorbed propane and mobile physisorbed NO_2 . It not clear, however, if propene is formed truly as intermediate product or if propyl nitrate forms in a concerted reaction step. The similarities in the product distributions observed suggests convincingly that propene is formed as true intermediate. NO_2 and C_3H_6 react with a constant stoichiometry of 4 to 1 and the highest N_2 yields and rates are obtained with this ratio. At lower fractions of C_3H_6 in the feed, the selectivity to N_2 is unaffected and the coke formation is minimized. With H-MOR and H-ZSM5 the selectivity to N_2 approached 75% at optimal conditions. At higher C_3H_6 feed concentrations, the excess of C_3H_6 leads to enhanced coke formation and unselective combustion. We conclude that H-MOR is the least sensitive to excess of C_3H_6 , because carbonaceous deposits built up in mordenite pores cannot react with NO_2 because of diffusional constraints. This leads ultimately to selective reactions (high N_2 selectivity) at presumably side pocket sites at the outer shell of the zeolite particles, which simultaneously prevent formation of carbonaceous deposits. With all other zeolites investigated, excess of C_3H_6 at 450°C caused the selectivity to N_2 to decline sharply. This is explained with a dynamic balance of the carbon forming reactions and the carbon removal by NO_2 (leading mostly to NO).

Unfortunately, the mechanistic details can only be explained on a plausibility level. The mechanism proposed describes an ionic pathway for the

formation of primary organo nitrates and a series of transformations of these nitrates catalyzed by Brønsted acid sites. It is interesting to note that the alternative route via NO₂⁺ would be compatible with the sequence of activities of the zeolites tested, which seems to depend upon the strength of the Brønsted acid sites. Overall it is clearly shown by the present study that three reactions influence the yield to N₂ in the system investigated. With propene the most crucial factor seems to be the reversible formation of carbonaceous deposits and the oxidation of these deposits by NO₂ with the parallel formation of NO. With propane, the oxidative dehydrogenation of the alkane limits the yield to N₂ even under a situation that does not lead to the formation of carbonaceous deposits. Finally, the formation of organonitrate compounds that are transformed to isocyanates and eventually hydrolyzed to ammonia determines the yields to N₂.

References

- 1 M. Iwamoto, H. Hamada, *Catal. Today* 10 (1991) 57.
- 2 W. Held, A. König, T. Richter, L. Puppe, SAE Tech. Paper 900496 (1990) 209.
- 3 M.D. Amaridis, T. Zhang, R.J. Farrauto, *Appl. Catal. B Env.* 10 (1996) 203.
- 4 H. Hamada, *Cat. Today* 22 (1994) 21.
- 5 K. Yogo, E. Kikuchi, *Stud. Surf. Sci. and Catal.*, vol 84, p. 1547, Elsevier, Amsterdam, 1994.
- 6 K. Yogo, M. Umeno, H. Watanabe, E. Kikuchi, *Cat. Lett.* 19 (1993) 131.
- 7 C. Yokoyama, M. Misono, *J. Catal.* 150 (1994) 9.
- 8 J.N. Armor, Y.J. Li, T.L. Slager, *J. Catal.* 150 (1994) 388.
- 9 N.W. Cant, A.D. Cowan, R. Dumpelmann, *J. Catal.* 151 (1995) 356.

Chapter 3

- 10 M.C. Campa, S. de Rossi, G. Ferraris, V. Indovina, *Appl. Catal. B Env.* 8 (1996) 315.
- 11 D.B. Lukyanov, E.A. Lombardo, G.A. Sill, J. d'Itri, W.K. Hall, *J. Catal.* 163 (1996) 447.
- 12 B.J. Adelman, T. Beutel, G.-D. Lei, W.M.H. Sachtler, *J. Catal.* 158 (1996) 327.
- 13 A.Y. Stakheev, C.W. Lee, S.J. Park, P.J. Chong, *Catal. Lett.* 38 (1996) 271.
- 14 A.D. Cowan, N.W. Cant, B.S. Haynes, P.F. Nelson, *J. Catal.* 176 (1998) 329.
- 15 E.A. Lombardo, G.A. Sill, J.L. d'Itri, W.K. Hall, *J. Catal.* 173 (1998) 440.
- 16 C. J. Blower, T.D. Smith, *Zeolites* 13 (1993) 394.
- 17 T. Gerlach, U. Illgen, M. Bartozek, M. Baerns, *Appl. Catal. B Env.* 22 (1999) 269.
- 18 H. Hamada, Y. Kintaichim, M. Sasaki, T. Ito, *Appl. Catal.* 64 (1990) L1-L4.
- 19 A. Satsuma, K. Yamada, T. Mori, M. Niwa, T. Hattori, Y. Murakami, *Catal. Lett.* 31 (1995) 367.
- 20 H.K. Shin, H. Hirabayashi, H. Yahiro, M. Watanabe, M. Iwamoto, *Catal. Today* 26 (1995) 21.
- 21 M.D. Amaridis, K.L. Roberts, C.J. Pereira, *Appl. Catal. B Env.* 14 (1997) 203.
- 22 R. Burch, P.J. Millington, A.P. Walker, *Appl. Catal. B Env.* 4 (1994) 65.
- 23 M.C. Campa, B. Iacono, D. Pietrogiacomini, V. Indovina, *Catal. Lett.* 66 (2000) 81.
- 24 K. Yogo, M. Umeno, H. Watanabe, E. Kikuchi, *Catal Lett.* 19 (1993) 131.
- 25 J.T. Miller, E. Glusker, R. Peddi, T. Zheng, J.R. Regalbuto, *Catal. Lett.* 51 (1998) 15.
- 26 A.Y. Stakheev, C.W. Lee, S.J. Park, P.J. Chong, *Catal. Lett.* 38 (1996) 271.
- 27 I. Halasz, A. Brenner, K.Y.S. Ng, Y. Hou, *J. Catal.* 161 (1996) 359.
- 28 K.A. Bethke, C. Li, M.C. Kung, H.H. Kung, *Catal. Lett.* 31 (1995) 287.

- 29 G.I. Kapustin, T.R. Brueva, A.L. Klyachko, S. Beran, B. Wichtelova, *Appl. Catal.* 42 (1988) 239.
- 30 C.A. Emeis, *J. Catal.* 141 (1993) 347.
- 31 F.C. Meunier, L. Domokos, K. Seshan, J.A. Lercher, *J. Catal.* 211 (2002) 366.
- 32 P. Andy, N.S. Gnep, M. Guisnet, E. Benazzi, C. Travers, *J. Catal.* 173, 322 (1998).
- 33 C. Pazé, B. Sazak, A. Zecchina, J. Dwyer, *J. Phys. Chem. B* 103, 9978 (1999).
- 34 T. Tanaka, T. Okuhara, M. Misono, *Appl. Catal. B Env.* 4 (1994) L1.
- 35 T. Gerlach, F.-W. Schütze, M. Baerns, *J. Cat.* 185 (1999) 131.
- 36 N. Bion, J. Saussey, C. Hedouin, T. Seguelong, M. Daturi, *Phys. Chem. Chem. Phys.* 3 (2001) 4811.
- 37 G.R. Bamwenda, A. Ogata, A. Obuchi, J. Oi, K. Mizuno, J. Skrzypek, *Appl. Catal. B Env.* 6 (1995) 311.
- 38 A. Obuchi, C. Wögerbauer, R. Köppel, A. Baiker, *Appl. Catal. B Env.* 19 (1998) 9.
- 39 N.W. Hayes, W. Grünert, G.J. Hutchings, R.J. Joyner, E.S. Shpiro, *J. Chem. Soc. Chem. Commun.* 531 (1994)
- 40 Y. Ukisu, S. Sato, G. Muramatsu, K. Yoshida, *Catal. Lett.* 16 (1992) 11.
- 41 T. Hoost, K. Laframboise, K. Otto, *Catal. Lett.* 33 (1995) 105.
- 42 M. Iwamoto, H. Yahiro, N. Mizuno, W. Zhang, Y. Mine, H. Furukawa, S. Kagawa, *J. Phys. Chem.* 96 (1992) 9360.
- 43 K.I. Hadjiivanov, J. Saussey, J.L. Freysz, J.C. Lavalley, *Catal. Lett.* 52 (1998) 103.
- 44 K.I. Hadjiivanov, *Catal. Rev.-Sci. Eng.* 42 (2000) 71-144
- 45 K. Tabor, L. Gutzwiller, M.J. Rossi, *J. Phys. Chem.* 98 (1994) 6172.
- 46 J. March, "Advanced Organic Chemistry", 3rd ed., p. 637-638, Wiley, New York, 1985.

Chapter 3

- 47 C. Yokoyama, M. Misono, *J. Catal.* 150 (1994) 9.
- 48 C. Yokoyama, M. Misono, *Catal. Today* 22 (1994) 59.
- 49 C.U.I. Odenbrand, L.A.H. Andersson, J.G.M. Brandin , S. Järås, *Cat. Today* 4 (1989) 155.
- 50 J. March, “Advanced Organic Chemistry”, 3rd ed., p. 739, Wiley, New York, 1985.
- 51 J. March, “Advanced Organic Chemistry”, 3rd ed., p. 786-789, Wiley, New York, 1985.
- 52 J. March, “Advanced Organic Chemistry”, 3rd ed., p. 946, 987-989, Wiley, New York, 1985.
- 53 J. March, “Advanced Organic Chemistry”, 3rd ed., p. 570, Wiley, New York, 1985.

Chapter 4

Role of oxygenated intermediates in the reduction of NO_2 by propene and propane over NaH-Y

Abstract

The role of oxygenate intermediates in the reduction of NO_2 by propene over NaH-Y zeolite catalysts has been studied by kinetic and infrared spectroscopic measurements. At lower temperatures, selective oxidation of propene can lead to formation of oxygenates. These, together with NO_2 , form azo type intermediates, where N-N coupling occurs and their further decomposition leads to the formation of N_2 . Non selective consumption of the hydrocarbon reductant occurs via oxygenates to carbon oxides, efficiency of which determines the overall efficiency of the conversion of NO_x to N_2 . A mechanism is proposed for the reaction of NO_2 and propene over Brønsted acidic zeolites, via the abstraction of an allylic hydrogen radical leading to the formation of oxygenates and primary nitro compounds

4.1 Introduction

The emission of nitrogen oxides from stationary and mobile sources causes serious environmental problems. Minimization of nitrogen oxide emissions is thus of keen interest currently. For automobiles, attention has now shifted to lean-burn mode from the point of view of efficient fuel use. The three-way catalysts developed for controlling the emissions (NO_x , CO, HC) from cars is unsuitable for lean burn engines. Thus, new solutions are needed for the removal of NO_x when present together with excess oxygen. Reduction of NO_x to N_2 by hydrocarbons is suggested to be an attractive possibility. After the early work by Iwamoto *et al.* [1] and Held *et al.* [2] with Cu/ZSM5 catalysts, a wealth of work has been reported for the reduction of NO_x with hydrocarbons.

In the studies reported, zeolites are often applied as supports for metal catalysts, however, in some cases, the H-form by itself adds an important catalytic function [3-10]. Li and Armor [11-13] showed that H-ZSM5, H-MOR and H-Y were active for the reduction of NO by methane although activities measured were lower as compared to metal loaded (Co, Mn, Ni, Ga) catalysts. Similar results were also found by Campa [14, 15] who used H-, Na-, Co-, H/Co- and H/Na-ZSM5. Miller [16] found the activity for NO_2 reduction by propene or methane to increase with increasing acid site strength of the zeolite used.

Hamada *et al.* [17, 18] found that NO is reduced by propene and propane in excess of oxygen over H-ZSM5, H-MOR and H-Y zeolites. They observed that the catalytic performance was greatly enhanced in the presence of small concentrations of oxygen [18, 19] and proposed that propene or propane was partially oxidized (oxygenates) before a reaction with NO leading to N_2 . Sachtler [20], Iwamoto [21], Gulunski [22] and Shelef *et al.* [23] came to a similar conclusion using metal supported catalysts. Halasz *et al.* [24] found, over H-ZSM5, that partial oxidation by oxygen would lead to oxygenates only above 400°C .

Misono *et al.* [25] proposed that oxygenates could be formed from nitro or nitrite compounds derived from the reaction of hydrocarbon with NO₂ over Pt/SiO₂. Myadera [26] found that reduction of NO with oxygenates over H-Y was less sensitive to the presence of water than when using propene. This may be significant since presence of water normally affects HC deNO_x catalysts negatively. Thus, oxygenates seem to play a key role during the reduction of NO_x to nitrogen.

The formation of N₂ over metal exchanged zeolite catalysts is believed to proceed *via* a variety of intermediate species, for e.g., nitro, nitrite, oxime, isocyanate, cyanide, diazo, amine, ammonia species [27-37]. These types of intermediates have been found over H-form of zeolites. For H-MOR, Gerlach *et al.* [38, 39] proposed a mechanism with the formation of allylic cyanide. Using H-FER, Nanba *et al.* [40] showed that HCN was formed, which could be hydrolyzed to ammonia and subsequently reacted with NO_x to form N₂. The same authors [41] also showed that the reaction of NO₂ with ethene led to the formation of nitroethane, which caused the formation of N₂, HCN, HNCO and NH₃ in the presence of O₂. Thus, a role of these intermediates can be expected in the formation of N₂ over H-form zeolites. It is known [17, 18] that relatively high N₂ yields can be obtained during the reduction of NO₂ with propene over H-form zeolites.

The aim of this study was to investigate the role of oxygenates, if any, in the reduction of NO₂ with hydrocarbons over NaH-Y zeolite. Specifically, the experiments carried out aimed at identifying if oxygenates, derived from propene, are crucial for the formation of nitrogen containing species which lead to the formation of N₂.

Chapter 4

4.2 Experimental

4.2.1 Material and reactants

Zeolite Y was obtained from Zeolyst International (CBV100) in the Na form. This zeolite is a faujasite type with a Si/Al ratio of about 2.6. To obtain the NH_4^+ form, the catalyst was ion exchanged in a 1.0 M NH_4NO_3 aqueous solution at room temperature for 24 hours. The catalyst was then filtered, washed with de-ionized water and dried at 120°C for another 24 hours. AAS measurements of obtained zeolite for Na, Al and Si indicated that about a 70% exchange to NH_4^+ was obtained. The Brønsted and Lewis acid site concentrations were measured by *in situ* IR spectroscopy during adsorption of pyridine (see Chapter 3). Concentrations obtained were 630 $\mu\text{mol/g}$ Brønsted acid sites (attributed to supercage positions) and 6.9 $\mu\text{mol/g}$ Lewis acid sites.

Gas mixtures used were 1.0% NO_2/He , 1.0% $\text{C}_3\text{H}_6/\text{He}$, 1.0% $\text{C}_3\text{H}_8/\text{He}$ and 100% O_2 and were all obtained from Messer Griesheim GmbH. Liquid reactants used were 1-propanol, 2-propanol, acetone, formic acid, acetic acid, propionic acid, propylamine, 2-nitropropane, acetonitrile and propionitrile, all of high purity and obtained from Sigma-Aldrich Chemie GmbH.

4.2.2 Infrared spectroscopy

IR spectroscopic measurements were performed using a BRUKER IFS 88 equipped with a MCT detector and using a resolution of 4 cm^{-1} . The catalyst was pressed into a self-supporting wafer (~2 mg, 7 mm diameter) placed in a circular oven where it was fixed between two gold rings. The oven was then placed in a stainless steel cell equipped with CaF_2 windows. The cell was connected to a flow system which allowed the catalysts to be exposed to desired gas mixtures. Prior to

sorption and reaction experiments, the catalyst was activated *in situ* by increasing the temperature to 450°C (10°C/min) in helium. During activation, NH₃ desorbed and the NaH-form of the zeolite was obtained.

4.2.3 Kinetic measurements

Catalysts were pressed into tablets, crushed and sieved to particles of 0.3-0.6 mm diameter. 200 mg of catalyst particles was then mounted in a tubular reactor where it was fixed between quartz wool plugs. The catalysts were then activated at 450°C and 20°C/min ramp in a He flow for 1 hour and next cooled to 150°C. In a typical kinetic test, the catalyst was exposed to a 100 ml/min flow containing 1000 ppm NO₂, 1000 ppm C₃H₆ and 5% O₂. The temperature was subsequently increased stepwise (25°C per step) to 600°C. The time at which the temperature was kept constant varied between 200 and 50 minutes (low to high T, respectively). The products were analyzed by gas chromatography using an HP 6910 gas chromatograph equipped with MS5A column and PLOT Q capillary columns for the analysis of O₂, N₂, CO, CO₂, N₂O, CH₄, C₃H₆, C₃H₈. A chemiluminescence analyzer (Thermo Environmental Instruments Inc. model 42C) was used for the analysis of NO and NO₂.

4.3 Results

4.3.1 Kinetic experiments with NO_x, O₂ and C₃H₆

Feeding NO₂ (Figure 1a) results in a relatively high N₂ yield at 225°C, which gradually decreases with increasing temperature to a minimum at 425°C. Above 425°C, the N₂ yield increased and reached a maximum of ~100 ppm at 525°C. A NO₂ conversion of 100% was obtained over the whole temperature range

resulting mainly in the formation of NO and a small amount of N₂O (< 5 %). Feeding NO resulted in a very low N₂ yield below 375°C, while above this temperature the N₂ yield increased and reached a maximum of about 65 ppm (~13 %) at 525°C. Using NO, N₂ was the main product and small amounts of NO₂ (< 5 %) and traces of N₂O (< 2 %) were observed.

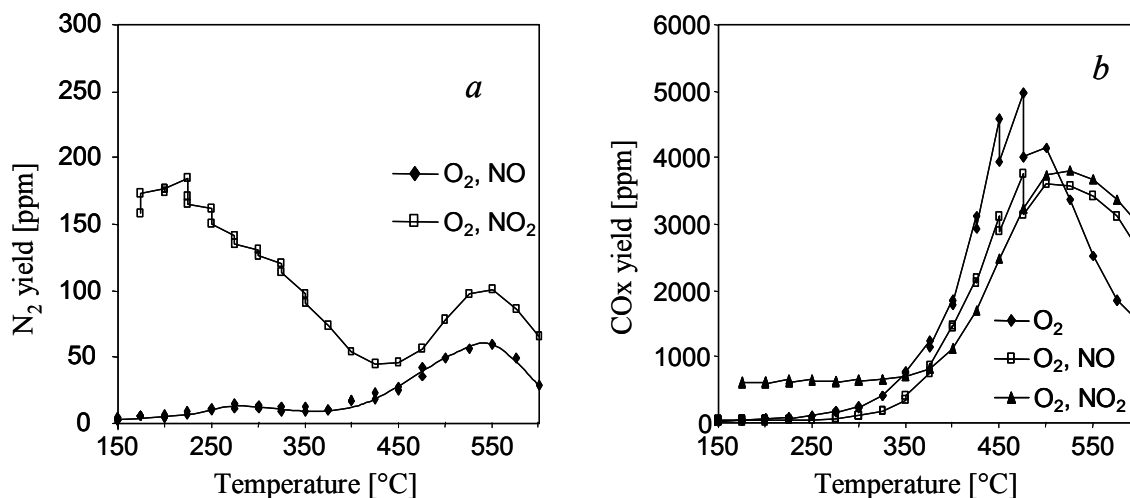


Figure 1: (a) N₂ yield and (b) CO_x yield versus temperature feeding (x) 5% O₂, (■) 5% O₂, 1000 ppm NO and (□) 5% O₂, 1000 ppm NO₂ over 200 mg NaH-Y.

The CO_x yields (Figure 1) showed a strong increase with temperature for all three feed mixtures above 350°C. Only in the presence of NO₂, CO_x (~600 ppm) was formed below 350°C. The maximum CO_x yields obtained are higher than the theoretical maximum of 3000 ppm, which can be formed from 1000 ppm C₃H₆. These high yields indicate that carbonaceous deposits have accumulated at lower temperatures and are removed through oxidation by NO_x and O₂ at temperatures above 350°C. The CO_x yields in the presence of pure O₂ are similar to those in the presence O₂ and NO or NO₂, hence, it is concluded that the CO_x formed is a result of unselective combustion in all three cases. The carbon balance showed an increasing deficit up to ~350°C from where it increased to a surplus. This confirms the assumption that carbonaceous deposits, formed at low temperatures, were

removed by oxidation at higher temperatures. The decrease in CO_x yield above 500°C may indicate that the surface was depleted from carbonaceous deposits.

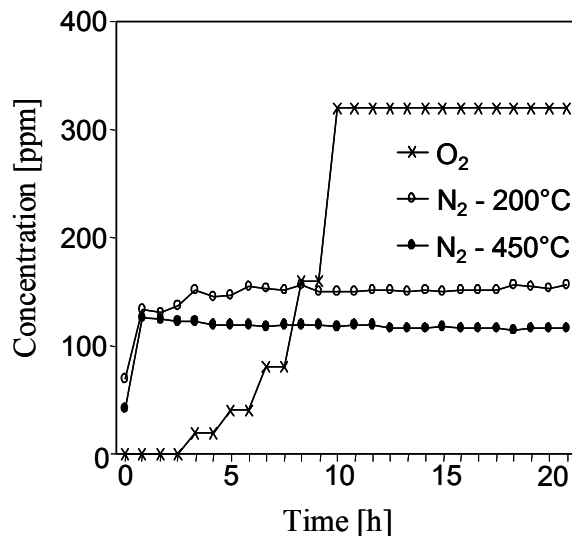


Figure 2: N₂ yield in time with increasing O₂ feed concentration at (□) 200°C and (■) 450°C feeding 250 ppm of C₃H₆ and 1000 ppm NO₂ over 200 mg NaH-Y.

Concentrations of 1000 ppm NO₂ and 250 ppm C₃H₆ were used (Figure 2) correspond to a stoichiometric ratio of 4 to 1. Previous results (see Chapters 2 and 3) showed that NO₂ and C₃H₆ react most efficiently at this ratio. A reaction of C₃H₆ and O₂ can lead to the formation of carbonaceous deposits or partially oxidized species. These species may react with NO₂ what may result in changes in the observed yields. Both, at 200°C and 450°C no changes in the yields were observed in any of the shown components, which thus shows that the presence of O₂ did not significantly influence the reaction of NO₂ with C₃H₆.

4.3.2 Kinetic experiments with increasing concentration of reductant feed

Figure 3 shows the (a) NO₂ conversion and (b) N₂ selectivity obtained at 200°C, using a feed of 1000 ppm of NO₂, 5% O₂ and an increasing concentration of

reductant. The reductants used were propene, propane, acetone, 1-propanol and 2-propanol. The last three are typical oxygenates that can be formed by partial oxidation of propene. The NO_2 conversion reached practically 100% when the propene concentration was increased to 250 ppm. Acetone, 1- and 2-propanol were less reactive. Propane is practically unreactive under these reaction conditions.

The selectivities to N_2 were relatively constant with increasing reductant feed concentration, except 1-propanol for which the selectivity to N_2 showed a maximum around 500 ppm. With regard to the efficiency of the reductant, the selectivity to N_2 was 50% for acetone, 30-40% for propene and 2-propanol and 20% for 1-propanol. For all reductants (except propane), the carbon balance was around 85% which suggests that carbonaceous deposits were formed. NO was the most abundant product while the N_2O yields remained below 15% for all reductants. The CO_2/CO ratio remained relatively constant around 1.0-2.0 and unaffected by the reductant feed concentration.

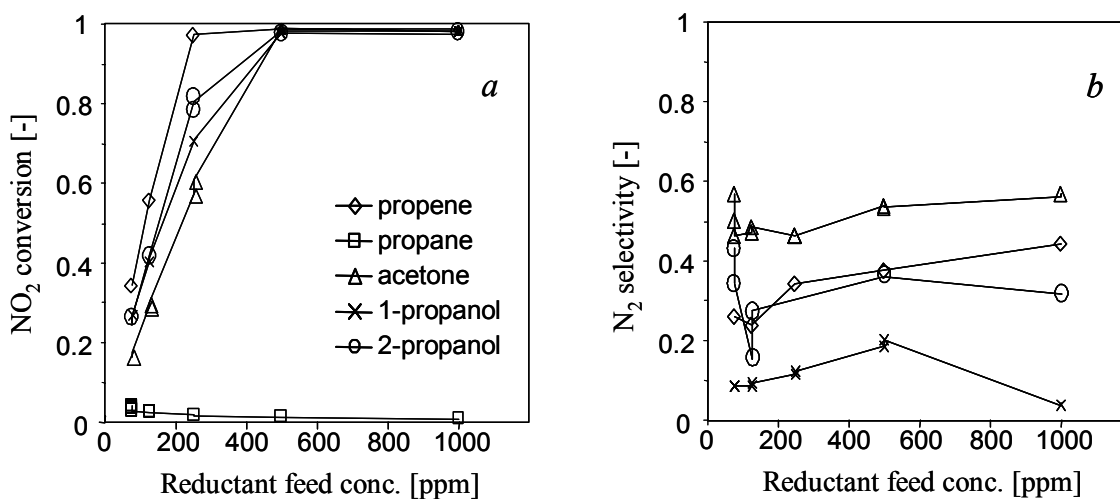


Figure 3: (a) NO_2 conversion and (b) N_2 selectivity with increasing reductant feed concentration at 200°C over 200 mg NaH-Y. (◇) propene, (□) propane, (△) acetone, (×) 1-propanol and (○) 2-propanol.

Figure 4 shows the (a) NO_2 conversion, (b) N_2 selectivity and (c) CO_2/CO ratio obtained at 450°C with increasing reductant feed concentration. The NO_2

Role of oxygenated intermediates in the reduction of NO_2 ...

conversion reached 100% at 250 ppm of reductant feed, except for propane. The selectivities to N_2 varied between 10% and 35% and decreased gradually with propene and acetone concentration and showed a weak maximum at 500 ppm with propane and 1- and 2-propanol. Note the relatively low selectivity to N_2 that was obtained using acetone at 450°C is opposed to the high selectivity found at 200°C. NO remained the most abundant product while the N_2O yields were lower than 3%. The CO_2/CO ratios obtained showed significant changes depending on reductant type and feed concentration. Using 1- and 2-propanol, this ratio shows a strong peak at 250 ppm reductant while gradually increased using acetone and remained relatively constant, around 1.5-2.0, when using propene or propane.

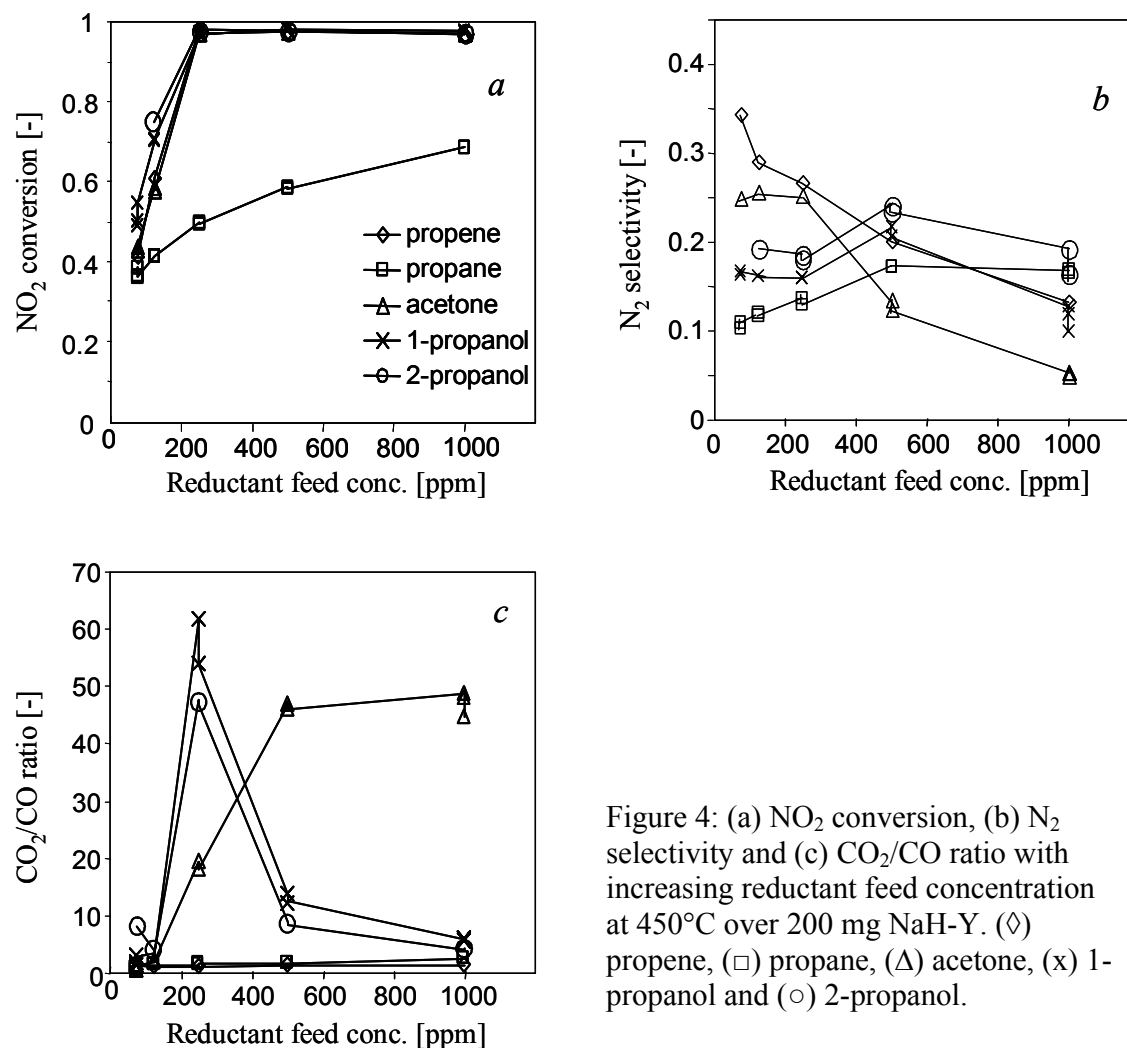


Figure 4: (a) NO_2 conversion, (b) N_2 selectivity and (c) CO_2/CO ratio with increasing reductant feed concentration at 450°C over 200 mg NaH-Y. (\diamond) propene, (\square) propane, (Δ) acetone, (\times) 1-propanol and (\circ) 2-propanol.

Chapter 4

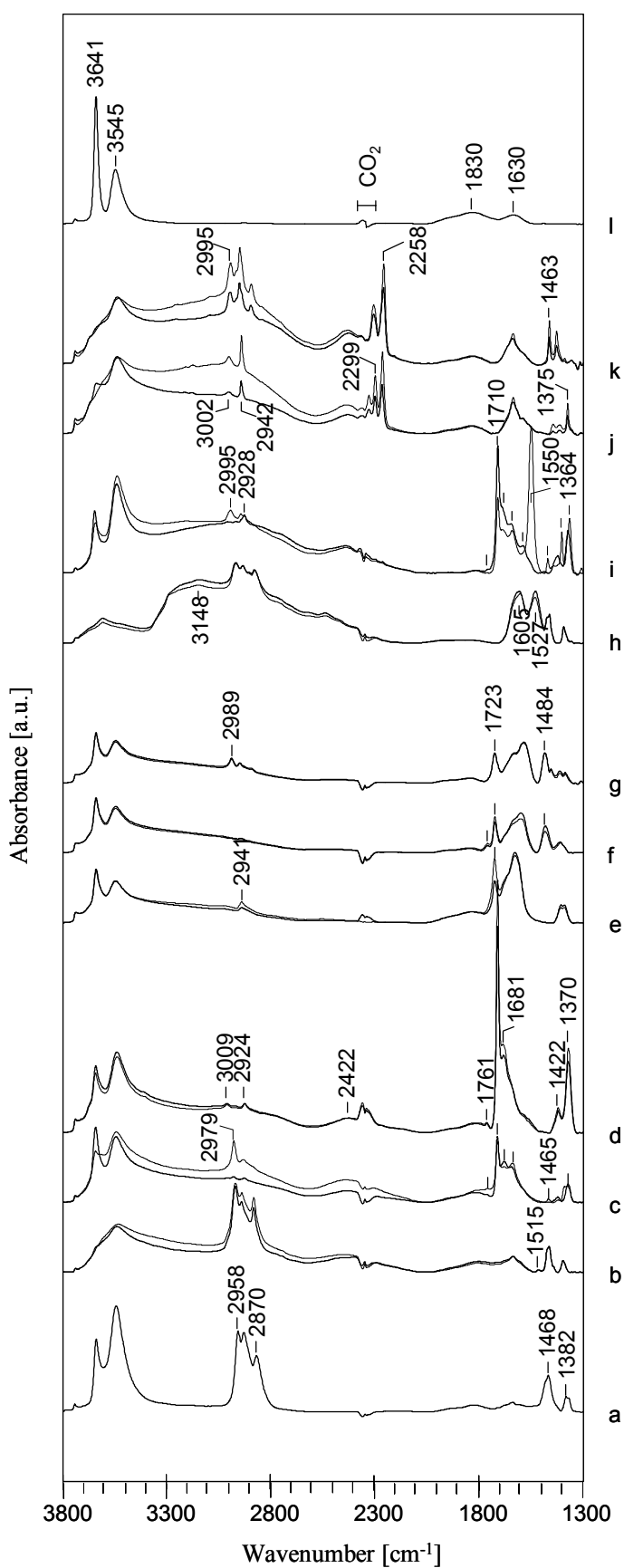
4.3.3 Characterization of adsorbed species by IR spectroscopy

Figure 5 shows spectra obtained after adsorption of some probe molecules on NaH-Y at 120°C. For the NaH-Y sample (Figure 5l), the bands at 3641 and 3548 cm^{-1} are assigned to bridging hydroxyl groups, located in the super cages (HF) and sodalite cages (LF), respectively. The bands at 1830 cm^{-1} (plus the shoulder at $\sim 1930 \text{ cm}^{-1}$) and 1630 cm^{-1} are overtones of the zeolite framework vibrations.

After adsorption of propene (Figure 5a), the HF band strongly decreased giving rise to a band at 3545 cm^{-1} , which coincides with the LF band. This red shift is attributed to coordinative bonds of propene oligomers to neighboring HF Brønsted acid sites (see Chapter 2). The bands at 2958, 2930 and 2870 cm^{-1} correspond to asymmetric CH_3 , asymmetric CH_2 and symmetric CH_2 stretching vibrations, respectively. The corresponding bands for deformation vibrations appeared at 1468 cm^{-1} (as.def. CH_3 , def. CH_2) and 1382, 1369 cm^{-1} (sym.def. CH_3). The group of bands around 1711 and 1640 cm^{-1} is mostly due to adsorption of carbonaceous deposits.

On adsorption of 1-propanol (Figure 5b), the HF band disappeared, while bands appeared at $\sim 3500 - 2600 \text{ cm}^{-1}$, around 2450 cm^{-1} and a small band around 1638 cm^{-1} . The combination of these three bands is typical for the formation of hydrogen bondings of polar compounds on the bridging hydroxyl group of the zeolite and are commonly referred to as the ABC bands [42-44] indicating different OH vibrations.

The spectra obtained on adsorption of 2-propanol (Figure 5c) differed markedly from the spectrum obtained after adsorption of 1-propanol. 2-Propanol is known to dehydrogenate readily to acetone or dehydrate to propene. The spectra obtained show strong resemblance with the spectra obtained after adsorption of acetone (Figure 5d) and, thus, suggest that 2-propanol has partly dehydrogenated to



acetone. Adsorption of acetone resulted in the appearance of a strong band at 1710 cm^{-1} which is assigned to the carbonyl group.

Figure 5: IR absorption spectra of adsorbed (a) propene, (b) 1-propanol, (c) 2-propanol, (d) acetone, (e) formic acid, (f) acetic acid, (g) propionic acid, (h) n-propylamine, (i) 2-nitropropane, (j) acetonitrile, (k) propionitrile and (l) activated NaH-Y at 120°C . Immediately after adsorption (thin line) and after flushing with He for 30 minutes (fat line).

Chapter 4

On adsorption of formic acid, (Figure 5e), bands appeared at 2941 (str. CH), 1723 (C=O), 1625 cm^{-1} with a shoulder at 1670 cm^{-1} (COO) and at 1408 and 1388 cm^{-1} (def. CH). On purging with He, the band at 1723 cm^{-1} decreased significantly, while COO and CH bands remained practically unchanged. Adsorption of acetic acid (Figure 5f) resulted in a similar spectrum with an extra small band at 1761 cm^{-1} . The presence of a CH_3 group resulted in the appearance of a band at 1484 cm^{-1} . After adsorption of propionic acid (Figure 5g) the band at 1761 cm^{-1} did not appear, while an extra band appeared at 1454 cm^{-1} , which is assigned to the CH_2 group. The COO bands shifted to lower wavenumbers as compared to formic (1670, 1625 cm^{-1}), acetic (1636, 1598 cm^{-1}) to propionic acid (1633, 1583 cm^{-1}).

On adsorption of 1-propylamine, bands appeared at 1527 and 1605 cm^{-1} , which are commonly observed on adsorption of amines and are attributed to NH deformation vibrations. The bands appearing at 2970-2877 cm^{-1} , 1467 and 1393 cm^{-1} are assigned to CH vibrations. Propylamine can decompose to ammonia and propene on Brønsted acid sites. The adsorption of ammonia is evident from the broad band appearing at $\sim 3300 - 2200 \text{ cm}^{-1}$ and indicates ammonia adsorbed on the Brønsted acid sites. The disappearance of the LF and HF Brønsted acid site bands indicates that ammonia is sufficiently small to enter the sodalite cages.

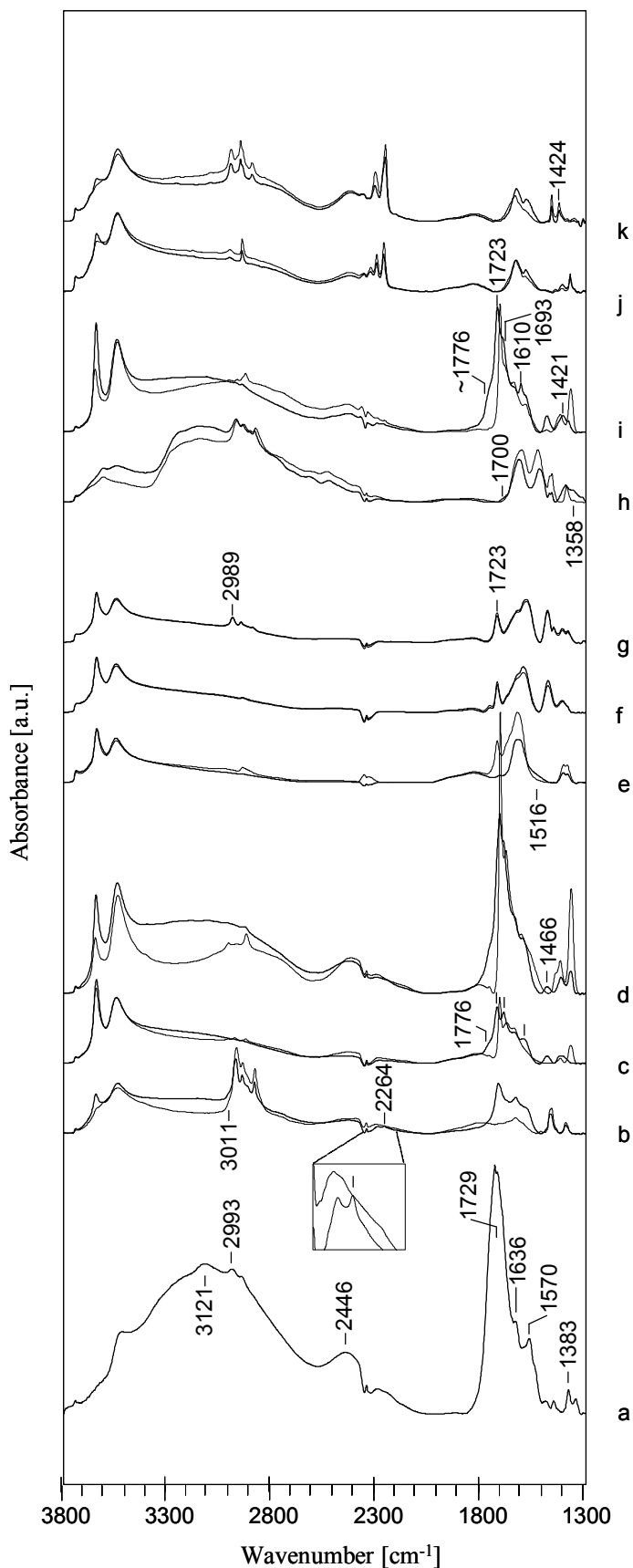
Adsorption of 2-nitropropane (Figure 5i) resulted in the bands at 1550, 1470, 1402 and 1364 cm^{-1} , which disappeared on flushing with He. These bands are assigned to the nitro group (1550 cm^{-1}) and CH deformation vibrations, respectively. After flushing with He, the spectrum showed large resemblance with the spectrum of adsorbed acetone. This indicates that nitro propane has decomposed to acetone over NaH-Y. Hydrolysis of 2-nitropropane is known to yield acetone and N_2O (*Nef* reaction). It is likely that some nitropropane had already decomposed before flushing with He, which thus explains the acetone bands observed in the spectrum obtained before the flushing. Note that the small

band at 1761 cm⁻¹ was also observed on adsorption of acetone, 2-propanol and acetic acid and may thus indicate the presence of an CH₃CO-R group.

Adsorption of acetonitrile (Figure 5j) and propionitrile (Figure 5k) resulted in complete disappearance of the HF band (3641 cm⁻¹) and the appearance of typical ABC bands indicating that both nitriles have formed hydrogen bonds to the bridging hydroxyl groups. In the spectrum of adsorbed acetonitrile, the bands at 2329, 2299 and 2264 cm⁻¹ are assigned to the nitrile group. The three bands indicate that acetonitrile has adsorbed on two different sites [45, 46]. It is likely that the sample contains extra framework aluminum and accessible Na⁺ cations. Sorption of acetonitrile on Lewis acid sites leads to the appearance of bands at 2335 and 2300 cm⁻¹, which partly overlap with the bands at 2299 and 2264 cm⁻¹ due to the adsorption on Brønsted acid sites. In the spectrum of adsorbed propionitrile, the nitrile bands appeared at 2306, 2258 cm⁻¹ indicating adsorption on Brønsted acid sites, while bands indicative for the adsorption on Lewis sites did not appear.

4.3.4 Reactivity of adsorbed species with NO₂

Figure 6 shows the spectra obtained after contacting the adsorbed probe molecules, (Figure 5), with gas phase NO₂ for 30 minutes and subsequently flushing with Helium for 10 minutes at 120°C. Figure 6a was obtained feeding a mixture of propene and NO₂ to simulate reaction conditions. The spectrum shows pronounced ABC structure of the bands indicating that adsorbed species form hydrogen bonds with the Brønsted acid sites as well as a band resembling that of adsorbed acetone. The strong ABC bands are tentatively assigned to adsorbed water, which is a product of the partial oxidation of propene by NO₂. The intensities of the acetone and water bands are relatively high and may mask the



bands of other species. The band at 1570 cm^{-1} is tentatively assigned to a primary nitro group [47].

Figure 6: IR absorption spectra of adsorbed (a) propene, (b) 1-propanol, (c) 2-propanol, (d) acetone, (e) formic acid, (f) acetic acid, (g) propionic acid, (h) n-propylamine, (i) 2-nitropropane, (j) acetonitrile and (k) propionitrile on NaH-Y after adsorption (thin line, Figure 5) and after contacting with NO_2 (fat line).

The other spectra presented in Figure 6 monitor the potential interaction of the various probe molecules with NO₂. On contacting sorbed 1-propanol with NO₂ (Figure 6b), the ABC bands appeared around 3500 – 2800 cm⁻¹, 2240 and 1640 cm⁻¹, which may indicate water. The HF band (3641 cm⁻¹) regained part of its intensity, while a small band appeared at 2263 cm⁻¹ and a group of bands at 1718, 1636 and 1574 cm⁻¹. The CH stretching (3011-2883 cm⁻¹) and deformation bands (1468, 1398 cm⁻¹) decreased. The resulting spectrum resembled a mixture of the spectra of adsorbed acetone and unreacted 1-propanol. Note that the extinction coefficients for carbonyl groups are significantly higher than those of CH bonds and, thus, only a small amount of 1-propanol is needed for the reaction to acetone and derivatives to result in such a spectrum. The small band at 2263 cm⁻¹ may indicate the presence of a cyanide group. Contacting adsorbed 2-propanol with NO₂ resulted in a spectrum similar to that of contacting adsorbed 1-propanol with NO₂, which suggests that both alcohols were dehydrogenated to acetone and/or partly oxidized to carboxylic acids. The spectrum obtained on contacting adsorbed acetone with NO₂ showed strong resemblance to that of 2-propanol/NO₂. This is not surprising, since earlier experiments (Figures 5c,d) showed that 2-propanol dehydrogenates to acetone upon sorption. A band at 1776 cm⁻¹ appeared as a shoulder in the spectra of 1-, 2-propanol and acetone.

After contacting adsorbed formic, acetic or propionic acid with NO₂ (Figures 6e-g), major changes are seen in the case of formic acid, while the spectra with the latter two compounds remained practically unchanged. In the case of formic acid, the band at 1723 cm⁻¹ disappeared completely and a small band at 1712 cm⁻¹ appeared. The COO bands (1670, 1625 cm⁻¹) are displaced and appear at 1622 cm⁻¹. The CH deformation bands at 1408 and 1388 cm⁻¹ decreased to about 50% of their original intensity. This is indicative of a reaction between NO₂ and formic acid. It is surprising that acetic and propionic acids do not seem to react with NO₂ under identical conditions.

Chapter 4

On contacting adsorbed propylamine with NO_2 (Figure 6h), the intensity of the band between $\sim 3640 - 2800 \text{ cm}^{-1}$ increased, while that between $2800 - 2200 \text{ cm}^{-1}$ decreased. Possibly, adsorbed ammonia, which was formed by the decomposition of propylamine upon adsorption on the Brønsted acid sites reacted with NO_2 resulting in a decrease of the very wide NH_4^+ stretching band. Ammonia is known to react easily with NO_2 over H-forms of zeolites producing N_2 , N_2O and water. The small band at 1700 cm^{-1} indicates that a very small amount of oxygenates was formed. The spectrum obtained on contacting adsorbed 2-nitropropene with NO_2 (Figure 6i) appeared practically identical to the spectrum obtained on contacting acetone with NO_2 , which may confirm that 2-nitropropane was partly decomposed to acetone upon adsorption.

On contacting adsorbed acetonitrile (Figure 6j) or propionitrile (Figure 6k) with NO_2 all bands for adsorbed nitrile decreased resulting in the appearance of the HF Brønsted acid site band at 3641 cm^{-1} . Besides this, a small increase in intensities is observed around 1586 and 1631 cm^{-1} , which may indicate the formation of nitrates possibly formed on adsorption of NO_2 on Lewis acid sites. These results suggest that aceto- or propionitrile adsorbed on NaH-Y zeolite did not react with gas phase NO_2 at 120°C but partly desorbed upon flushing with He.

4.3.5 IR spectroscopy of adsorbed species at 200°C

Following the exposure of the adsorbed probe molecules to NO_2 at 120°C , the temperature was increased by $10^\circ\text{C}/\text{min}$ to 450°C in the presence of NO_2 , while spectra were taken at intervals of 10°C . Figure 7 shows the spectra obtained at 200°C . In all spectra, the ABC bands ($\sim 3300 - 2600, 2450, 1638 \text{ cm}^{-1}$) decreased in intensity indicating that a significant amount of species, that previously were coordinatively bond to the Brønsted acid sites, desorbed or have reacted. A corresponding increase of the HF band (3641 cm^{-1}) was also observed.

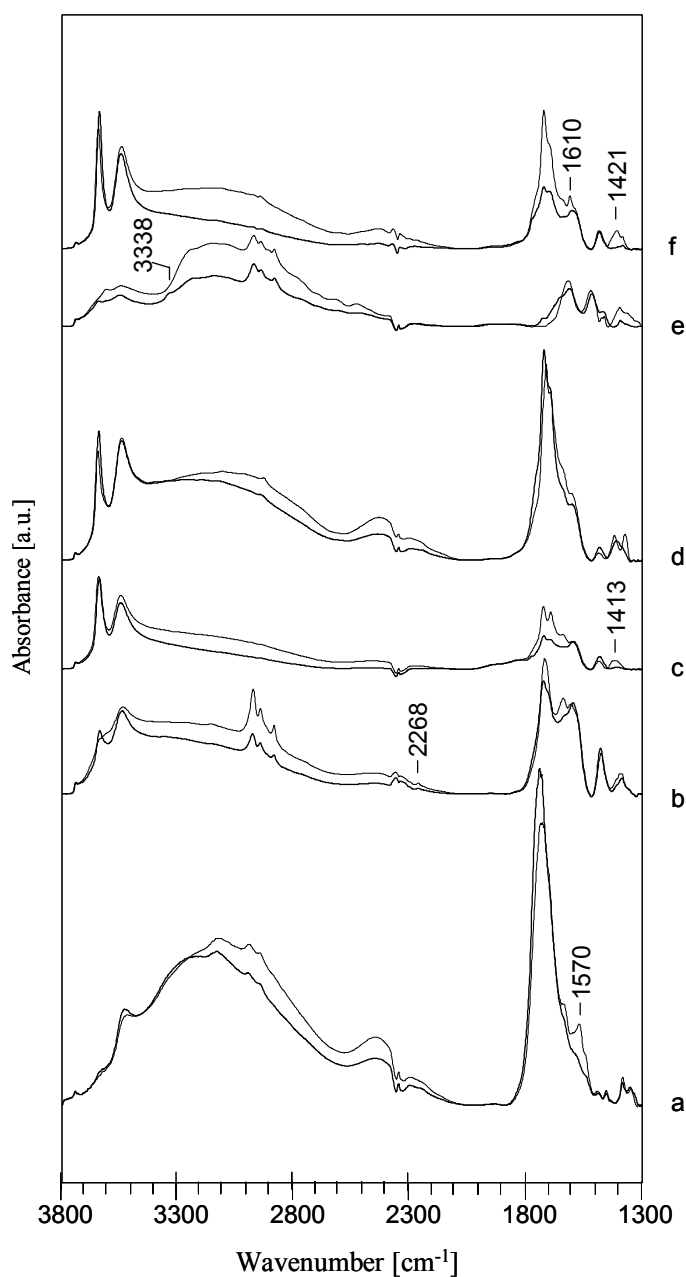


Figure 7: IR absorption spectra of adsorbed (a) propene, (b) 1-propanol, (c) 2-propanol, (d) acetone, (e) propylamine and (f) nitropropane on NaH-Y in contact with NO₂ at 120°C (thin line) and 200°C (fat line).

The spectra of propene (Figure 7a) and acetone (Figure 7d) showed similar changes. The shift of the very wide band (3300 - 2600 cm⁻¹) to slightly higher wave numbers (~3250 cm⁻¹) and the increase of the carbonyl band (1729 cm⁻¹) strongly suggest that acetone is a product of the reaction of propene and NO₂. The band at

Chapter 4

1570 cm^{-1} , previously assigned to a primary nitro compound, disappeared from the spectrum of propene, which suggest that these species are relative unstable.

The spectra of 1-propanol (Figure 7b) and 2-propanol (Figure 7c) showed large similarities and appeared to consist of a mixture of the alcohols and carboxylic acids. In the spectrum of 1-propanol, the band around 2268 cm^{-1} , previously assigned to a nitrile compound, remained practically unchanged while increasing temperature.

In the spectrum of propylamine, the band indicating adsorbed ammonia (3300 – 2400, 1358 cm^{-1}) was reduced significantly in intensity, while only minor changes occurred in the band indicating adsorbed propylamine (1605, 1527 cm^{-1}). This suggests that NO_2 reacts more easily with ammonia than with propylamine. A band appearing around 1723 cm^{-1} , also observed in the spectra of adsorbed carboxylic acids, indicates that a small amount of propylamine was oxidized to form a carboxylic acid. Note that the spectrum of nitropropane (Figure 7f), which, at 120°C, showed large similarity with the spectra of adsorbed acetone and propene/ NO_2 resembled, at 200°C, the spectra 1- and 2-propanol (Figures 7b,c). This could indicate that 2-nitropropane, as well as 1- and 2-propanol, were partly oxidized to carboxylic acids.

The spectra of formic-, acetic- and propionic acid are omitted, since they showed only the gradual decrease of the existing bands and thus apparently did not react with NO_2 . It should be noted that, a band indicating the presence of cyanide species was observed only in the spectra derived from adsorbed 1-propanol in contact with NO_2 . Further increase in temperature, to 450°C, did not lead to the appearance of cyanide or isocyanate bands in any of the experiments. In general, the bands gradually decreased in all spectra with increasing temperature and changed through a mixture of oxygenates and carbonaceous species to the spectrum of the fresh zeolite at 450°C.

4.3.6 Reactivity of adsorbed nitriles

Figure 8 shows spectra of adsorbed aceto- or propionitrile in contact with H₂O and a mixture of H₂O and NO₂. These spectra were recorded immediately after the adsorbed nitriles were exposed to NO₂ (Figures 6j,k and Figures 8a,d) and subsequently flushed with He. Contacting the adsorbed nitriles with H₂O (Figures 8b,e) did not result in a significant decrease of the CN bands (2667 and 2660 cm⁻¹). However, the increase of the band at 2450 cm⁻¹ shows that adsorbed water is present. On addition of NO₂ to the flow of H₂O/He, the CN bands showed again only minimal changes. However, when the feed of the nitriles was stopped, the intensity of the CN bands decreased gradually with time. The disappearance rate was not influenced by the introduction of NO₂, H₂O or the combination of both. This strongly suggests that these nitriles were not hydrolyzed under the applied conditions at 120°C.

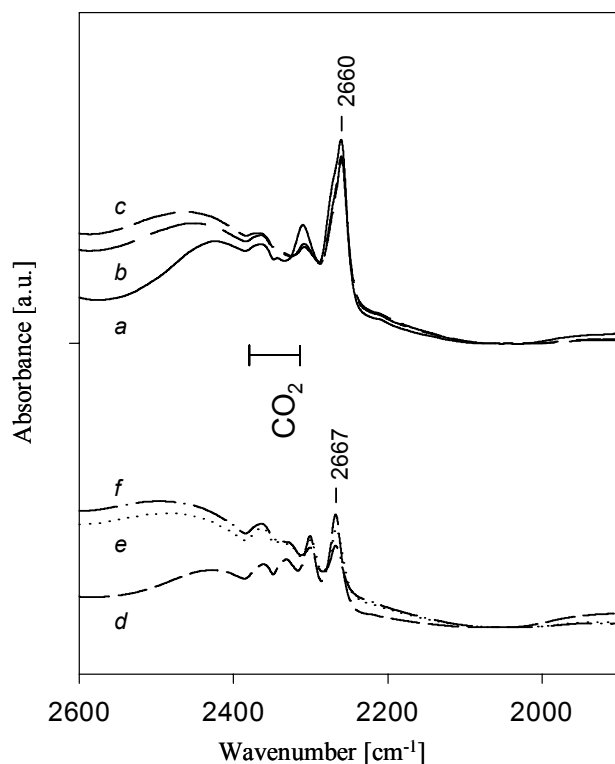


Figure 8: IR absorption spectra of (d, e, f) acetonitrile and (a, b, c) propionitrile (a, d) adsorbed on NaH-Y, (b, e) in contact with H₂O and (c, f) in contact with H₂O and NO₂ at 120°C.

Chapter 4

These spectra of Figure 9 were recorded immediately after the spectra of Figure 8. With increasing temperature, desorption of water was as an intensity decrease of the bands at 2450 and 1638 cm^{-1} . In the spectra of both acetonitrile and propionitrile, a pair of bands appeared at ~ 1580 and 1480 cm^{-1} and reached maximum around $\sim 260^\circ\text{C}$ after which they decreased and disappeared completely at 450°C . The bands at this position indicate the presence of carboxylic acids. These results thus show a clear indication for the hydrolysis of nitriles, since carboxylic acids are the typical products of hydrolysis.

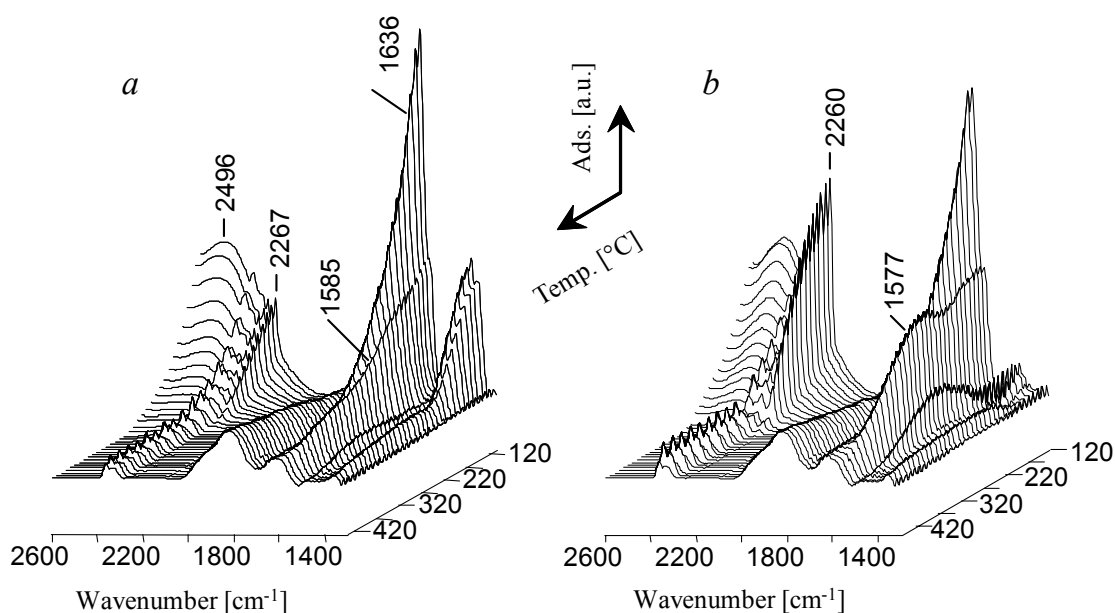


Figure 9: IR absorption spectra of (a) acetonitrile and (b) propionitrile adsorbed on NaH-Y in contact with H_2O and NO_2 with increasing temperature ($120 - 450^\circ\text{C}$).

4.4 Discussion

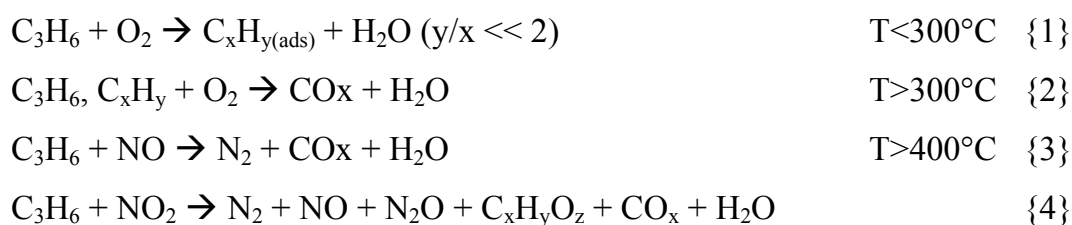
4.4.1 Formation of oxygenates during NO_x reduction

The NO_x present in exhaust gases is mainly NO ($>90\%$). During the reduction of NO by hydrocarbons in the presence of oxygen and over metal

supported catalysts, oxidation to NO₂ has been reported by many authors to be the initial step in the reduction of NO. Although NO₂ is thermodynamically favored over NO at lower temperatures, it is significantly more reactive as compared to NO. Transition metals (oxides) and even acidic zeolites, have been shown to catalyze the oxidation of NO to NO₂. Thus, the reduction of NO₂ represents an important part of the conversion of NO to N₂.

In the low temperature range (<375°C), propene oxidation over NaH-Y was not observed with either O₂ or NO+O₂. However, oxidation products were observed when NO₂ was present (Fig. 1b). It was also noticed that the O₂ pressure did not influence the N₂ formation rate during the reaction of NO₂ and C₃H₆. In Chapter 2 we showed by infrared spectroscopic measurements that the presence of O₂ led to extensive coke formation at lower temperatures (120°C), which partially deactivate the catalyst. At higher temperatures, oxygen helped in the combustion of this coke.

This indirectly suggests the role for NO₂ in oxidizing propene. This was observed, when the catalyst was contacted with propene and NO₂ (Fig. 6a). The resulting spectrum showed the presence of sorbed oxygenate species, resembling that of adsorbed acetone. The reactions of C₃H₆, O₂, NO and NO₂ is, thus, summarized as {1-4}:



Chapter 4

Therefore oxygenates are concluded to be feasible products of the reaction of propene and NO_2 and their possible role in the formation of N_2 is discussed below.

Table 1 summarizes the results shown in Figures 3 and 4 with 250 ppm of reductant. As seen from the results, the reduction of NO_2 with propene proceeds with reasonable efficiency over NaH-Y. The study aims at establishing the role of oxygenates (derived from propene or propane) in the reduction of NO_x to N_2 . The results of the reduction of NO_x (Figure 1) show that NO_2 is efficiently converted to N_2 at temperatures below 375°C , while NO is almost unreactive. The fact that NaH-Y is not very efficient for the oxidation of NO to NO_2 is in agreement with this observation.

Table 1: NO_2 conversion, N_2 selectivity and CO_2/CO ratio at 250 ppm reductant, 1000 ppm NO_2 , 5% O_2 (Figures 3 and 4).

Reductant	200°C			450°C		
	x. NO_2 [%]	s. N_2 [%]	CO_2/CO [-]	x. NO_2 [%]	s. N_2 [%]	CO_2/CO [-]
propane	2	-	-	50	14	1.7
propene	100	33	1.9	100	27	1.5
acetone	60	45	1.9	100	25	18
1-propanol	70	12	1.4	100	16	57
2-propanol	80	31	1.9	100	19	47

At 200°C , the oxidation of propene by O_2 was negligible (see Figure 1b) and if we assume similar behavior for the other reductants, CO and CO_2 produced is concluded to result from the oxidation by NO_2 . Therefore CO_2/CO ratio is used as an indication of the differences in the combustion characteristics of the reductants, which influences the selective reduction of NO_2 . The oxygenates (acetone, 1- and 2-propanol) exhibit a very high ratio, while for propene and propane this ratio remains practically constant around 1.5-2.5. The large difference between propene and the oxygenates strongly suggests that the oxygenates used

here are combusted much more easily and may not be involved in the reduction of NO₂ by propene at these higher temperatures.

However, at 200°C, all reductants used resulted in a CO₂/CO ratio of about 1.5-2.0, which remained nearly constant with increasing reductant feed concentration. A role for the oxygenates may, thus, play a significant role at lower reaction temperatures. The strong similarity of this ratio when using propene or propane (Figure 4c) suggests that the reaction pathway to the selective formation of N₂ may be similar. This implies that dehydrogenation of propane to propene is the primary and rate limiting step. The latter aspect is inferred from the low activity of propane for NO₂ reduction (Figures 3, 4).

4.4.2 Identification of adsorbed species

Kinetic experiments using oxygenates instead of propene showed that they were able to reduce NO₂ to N₂. Infrared measurements employing 1-, 2-propanol and acetone show that on adsorption of 2-propanol or acetone, the spectra are similar and correspond to sorbed acetone. 1-propanol sorbed without a chemical reaction. In contact with NO₂, 2-propanol and acetone resulted in the formation of sorbed carboxylic acid species and water. The spectra show remarkable resemblance with the spectrum obtained at reaction conditions, i.e., when feeding propene, (oxygen) and NO₂. This strongly suggests that acetone is a product in the reaction of propene and NO₂.

Assuming that propene also reacts with NO₂ to give a nitrated species, we carried out sorption of 2-nitropropane on NaH-Y. 2-nitropropane was not stable under reaction conditions indicating the formation of acetone (Figure 5i) upon adsorption.

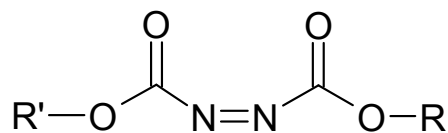
Aceto- and propionitrile appeared unreactive with NO₂ at 120°C in the absence of H₂O. In the presence of H₂O, the nitriles were removed relatively slow

Chapter 4

at elevated temperatures (around 260°C), while bands indicating carboxylic acids increased in intensity. Hydrolysis of nitrile compounds results in the formation of ammonia and carboxylic acids and thus enables the reaction of ammonia with NO₂ which is assumed to yield N₂. Of all probe molecules tested, only 1-propanol in contact with NO₂ resulted in a band indicating the formation of nitrile compounds. Of the tested carboxylic acids, only formic acid appeared to react with NO₂ while acetic acid and propionic acid appeared nearly inert to NO₂. These results indicate that the formation of nitrile species cannot account for the formation of N₂ at low temperatures, but may still contribute to the formation of ammonia and N₂ at higher temperatures.

On contacting adsorbed acetone (or 2-propanol or 2-nitropropane, all leading to acetone), a band at 1776 cm⁻¹ was observed, for which no assignment was made. Carboxylic compounds absorbing around this wavenumber are attributed to non-cyclic saturated anhydrides (1820-1750 cm⁻¹), linear carbonates (1780-1740 cm⁻¹), and lactones (1795-1747 cm⁻¹). Linear esters, ketons, aldehydes or carbamates absorb at wavenumbers below 1770 cm⁻¹ [48]. Anhydrides, organic carbonates and lactones (if formed) are likely to be easily hydrolyzed to form carboxylic acids, which show bands at lower wavenumbers (Figure 5 e-g). An alternative possibility might be an azo-diformate species of the type shown below [48]. In this case the R and R' are ethyl or n-propyl groups and the N=N band appears around 1775 cm⁻¹ [48]. Because an N=N group is already present in this species, decomposition of such a compound is likely to yield N₂. Note that the possibility of azo compounds as intermediates was also put forward by Hayes [50] for the reduction of NO by propene over Cu/ZSM5. For the formation of such azo compounds several possible steps are listed by March [49]. Organic nitro species may reduce to nitroso and hydroxylamine species. A condensation of the two yields an azoxy group, which can form an azo group *via* an internal rearrangement.

A detailed mechanism for the formation of organo nitro, nitroso or hydroxamic species from a reaction of acetone with NO₂ remains unclear.



R',R azo diformate

4.4.3 Mechanism of the reaction of NO₂ with C₃H₆ adsorbed on NaH-Y zeolite

In the reduction of NO_x with hydrocarbons, N containing intermediates such as -CN, -NCO, -CNO have been reported to be crucial for the selective conversion NO_x to N₂. The mechanisms proposed for the formation of these species are mostly based on result obtained using metal supported catalysts. Our results show that the formation of N₂ can be catalyzed by the Brønsted acid sites of NaH-Y zeolite at relatively low temperatures.

The formation of nitrogen containing species by a reaction of NO or NO₂ and propene is often believed to be initiated by the abstraction of a hydrogen radical from an allylic methyl group [5]. The obtained carbon radical can directly bond with the unpaired electron on the nitrogen atom of NO or NO₂ resulting in an allylic nitroso or nitro compound [34, 39]. Hayes *et al.* [50] proposed that NO₂ attacks the adsorbed allylic species (on Cu sites dispersed on ZSM5) forming nitro compounds which recombine to form nitroso or oxime species. This concept has, ever since, gained popularity and additional steps were proposed by several authors [31, 35, 51].

Figure 10 shows a possible mechanism for the reaction of NO₂ with propene over Brønsted acidic zeolites. On adsorption of propene on a Brønsted acid, site a propyl carbenium ion is obtained. Possibly, the propyl carbenium ion

Chapter 4

complex can somehow stabilize a primary carbon radical and thereby facilitates the abstraction of a hydrogen radical by NO_2 . The addition of the second NO_2 leads to the formation of a primary nitro group. Alternatively, NO_2 may perform a nucleophilic attack on the positively charged carbon to form a secondary nitrite or nitro group. Organic nitrite species are known to be extremely unstable and readily decompose to the corresponding keton or alcohol [52]. Although nitro compounds are more stable, IR measurements showed that 2-nitropropane spontaneously decomposed to acetone. This mechanism proposes a feasible route for the formation of oxygenated species by a reaction of NO_2 with adsorbed propene and the formation of primary nitro compounds. These primary nitro compounds are believed to enable the formation of ammonia *via* a complex sequence of nitrogen containing intermediates, such as proposed in Chapter 3.

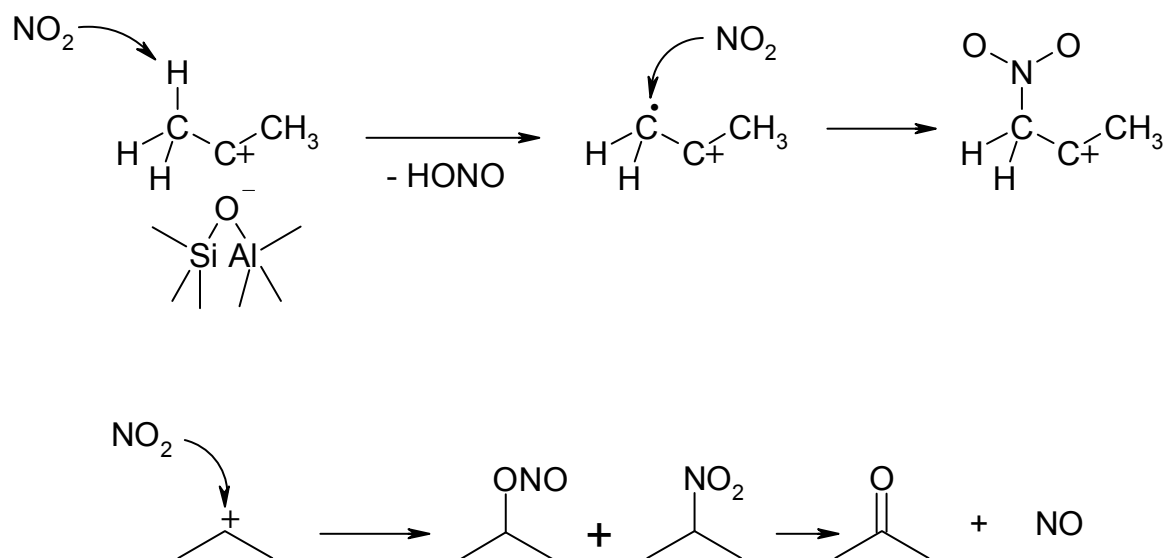


Figure 10: Mechanism of the reaction of NO_2 on a propyl carbenium ion leading to the formation of oxygenates and a primary nitro compound.

Figure 11 compiles the reaction scheme for the reaction of NO_2 and propene in the presence of excess oxygen over NaH-Y zeolite leading to the

formation of N₂. The reaction of NO₂ with a propyl carbenium ion leads to the formation of primary and secondary nitro compounds of which only the primary is believed to be stable enough to allow for the formation of nitrogen containing species. A sequence of rearrangements in combination with water enables the formation of oxime, hydroxamic acid, isocyanate and cyanide species which lead to the formation of ammonia on hydrolysis. A reaction of NO₂ (or NO) with ammonia selectively yield N₂. The secondary nitro and nitrite compounds are relative unstable and easily decompose to form acetone or alcohols. The results indicate that acetone is the most abundant product at low temperatures and a reaction with NO₂ leads to the formation of azo-diformate type species. Such compounds already include an N-N bond, which can decompose to yield N₂. The reaction of acetone and NO₂ shows only a relative high selectivity to N₂ at low temperatures, which indicates that the formation of N₂ *via* azo-diformate accordingly takes place only at low temperatures.

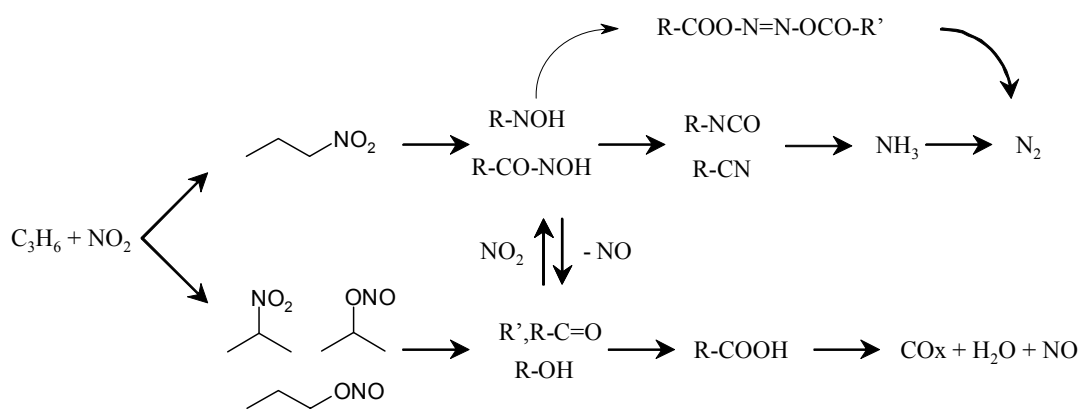


Figure 11: Reaction scheme for the formation of N₂ from a reaction of NO₂ with propene in the presence of oxygen via oxygenated intermediates as occurring in the SCR of NO₂ by propene over NaH-Y.

4.5 Conclusions

The role of oxygenate intermediates in the reduction of NO₂ by propene over H-Y zeolite catalysts has been explored by kinetic and infrared spectroscopic measurements. At low temperatures, propene is partially oxidized by NO₂ to acetone, probably *via* the formation of a 2-nitropropane like intermediate. Acetone, though less reactive towards NO₂ than propene, produces N₂ with a significantly higher selectivity. Acetone is a crucial intermediate in the formation of N₂ from the reduction of NO₂ by propene at low temperatures. The formation of acetone also limits the theoretical maximum selectivity to N₂.

An azo-diformate species may be an important nitrogen containing intermediate for the formation of N₂. At high temperatures, the reaction of propene and NO₂ yields N₂ with a higher selectivity as compared to any of the tested oxygenated reductants. Thus, we conclude that the overall reaction does not proceed *via* oxygenated intermediates under such reaction conditions, but probably involves nitrogen containing intermediates.

A mechanism is proposed for the reaction of NO₂ and propene over Brønsted acidic zeolites, *via* the abstraction of an allylic hydrogen radical leading to the formation of oxygenates and primary nitro compounds.

References

- 1 Iwamoto M., Yahiro H., Yu-u Y., Shundo S., Mizuno N., Shokubai 32 (1990) 430.
- 2 Held W., Konig A., Richetr T., Puppe L., SAE Tech. Paper Ser. 4 No. 900469, (1990) p.209.
- 3 Corma A., Forner V., Palomares E., Appl. Catal. B 11, 1997 233.

- 4 Witzel F., Sill G.A., Hall W.K., *J. Catal.* 149, 1994 229.
- 5 Cowan A.D., Dumpelmann R., Cant N.W., *J. Catal.* 151, 1995 356.
- 6 Maisuls S.E., Seshan K., Feast S., Lercher J.A., *Appl. Catal. B* 29, 2001 69-81.
- 7 Chen H.Y., Voskoboinikov T., Sachtler W.M.H., *J. Catal.* 180, 1998 171.
- 8 Garcia-Cortes J.M., Pérez-Ramírez J., Illan-Gomez M.J., Kapteijn F., Moulijn J.A., Salinas-Martinez de Lecea C., *Appl. Catal. B* 30, 2001 399.
- 9 Long R., Yang R.T., *Catal. Lett.* 52, 1998 91.
- 10 Descorme C., Gelin P., Lecuyer C., Primet M., *Appl. Catal. B* 13, 1997 185.
- 11 Li Y.L., Armor J.N., *Appl. Catal. B* 1, 1992 L31.
- 12 Li Y.L., Armor J.N., *Appl. Catal. B* 2, 1993 239.
- 13 Li Y.L., Armor J.N., *J. Catal.* 145, 1994 1.
- 14 Indovina V., Campa M.C., Rossi De S., Ferraris G., *Appl. Catal. B Env.* 8 (1996) 315.
- 15 Campa M.C., Iacono B., Pietrogiacomi D., Indovina V., *Catal. Lett.* 66 (2000) 81.
- 16 Miller J.T., Glusker E., Peddi R., Zheng T., Regalbuto J.R., *Catal. Lett.* 51 (1998) 15.
- 17 Hamada H., Kintaichi Y., Sasaki M., Ito T., *Appl. Catal. B Env.* 64 (1990) L1.
- 18 Sasaki M., Hamada H., Kintaichi Y., Ito T., *Catal. Lett.* 15 (1992) 297.
- 19 Hamada H., Kintaichi Y., Sasaki M., Ito T., *Appl. Catal.* 75 (1991) L1.
- 20 d'Itri J., Sachtler W.M.H., *Catal. Lett.* 15 (1992) 289.
- 21 Inui T., Iwamoto S., Kojo S., Yoshida T., *Catal. Lett.* 13 (1992) 87.
- 22 Bennet C.J., Bennet P.S., Golunski S.E., Hayes J.W., Walker A.P., *Appl. Catal. A Gen.* 86 (1992) L1.
- 23 Montreuil C.N., Shelef M., *Appl. Catal. B Env.* 1 (1992) L1.
- 24 Halasz I., Brenner A., Ng K.Y.S., Hou Y., *J. Catal.* 161 (1996) 359.
- 25 Tanaka T., Okuhara T., Misono M., *Appl. Catal. B* 4 (1994) L1.

Chapter 4

- 26 Myadera T., *Appl. Catal. B Env.* 2 (1993) 199.
- 27 Zuzaniuk V., Meunier F.C., Ross J.R.H., *Chem. Comm.* (1999) 815.
- 28 Cant N.W., Liu I.O.Y., *Catal. Today* 63 (2000) 133.
- 29 Cowan A.D., Cant N.W., Haynes B.S., Nelson P.F., *J.Catal.* 176 (1998) 329.
- 30 Centi G., Galli A., Perathoner S., *J. Chem. Soc., Faraday Trans.* 92 (1996) 5129.
- 31 Park S.-K., Park Y.-K., Park S.-E., Kevan L., *P.C.C.P.* 2 (2000) 5500.
- 32 Bamwenda G.R., Ogata A., Obuchi A., Oi J., Mizuno K., Skrzypek J., *Appl. Catal. B Env.* 6 (1995) 311.
- 33 Ukisu Y., Sato S., *Appl. Catal. B Env.* 2 (1993) 147.
- 34 Hayes N.W., Grunert W., Hutchings G.J., Joyner R.W., Shpiro E.S., *Chem. Comm.* (1994) 531.
- 35 Radtke F., Köppel R.A., Baiker A., *Appl. Catal. A* 107 (1994) L125.
- 36 Chen H.Y., Voskoboinikov T., Sachtler W.M.H., *Catal. Today* 54 (1999) 483.
- 37 Satsuma A., Enjoji T., Shimizu K.I., Sato K., Yoshida H., Hattori T., *J. Chem. Soc., Faraday Trans.* 94 (1998) 301.
- 38 Gerlach T., Baerns M., *Chemical Eng. Sci.* 54 (1999) 4379.
- 39 Gerlach T., Illgen U., Bartoszek M., Baerns M., *Applied Cat. B Env.* 22 (1999) 269.
- 40 Nanba T., Obuchi A., Akaratiwa S., Liu S., Uchisawa J., Kushiya S., *Chem. Lett* (2000) 986.
- 41 Nanba T., Obuchi A., Izumi H., Sugiura Y., Xu J., Uchisawa J., Kushiya S., *Chem. Comm.* (2001) 173.
- 42 Stepanov B.I., *Nature* 157 (1946) 808.
- 43 Claydon M.F., Sheppard N., *Chem. Comm.* 23 (1969) 1431.
- 44 Pelmeshnikov A.G., Van Santen R.A., *J. Phys. Chem.* 97 (1993) 10678.

- 45 Trombetta M., Busca G., Rossini S., Piccoli V., Cornaro U., Guercio A., Catani R., Willey R.J., *J. Catal.* 179 (1998) 581.
- 46 Krietenbrink H., Knözinger E., *J. Chem. Soc. Faraday Trans.* 72 (1976) 2421.
- 47 Shlyapochnikov V.A., Khrapkovskii G.M., Shamov A.G., *Russ. Chem. Bull. Int. ed.* 51 (2002) 940.
- 48 Coltrup N.B., Daly L.H., Wiberley S.E., "Intro. to Infrared and Raman Spectr.", 3rd ed., p. 289-325, 350-352, Academic Press Inc., Boston, 1990.
- 49 Smith B.M., March J., "March's Advanced Organic Chemistry", 5th ed., p. 818, 819, 1557, 1563, Wiley, New York, 2001.
- 50 Hayes N.W., Joyner R.W., Shpiro S.E., *Appl. Catal. B* 8 (1996) 343.
- 51 Y. Traa, B. Burger, J. Weitkamp, *Micro. Meso. Mat.* 30 (1999) 3-41.
- 52 J. March, "Advanced Organic Chemistry", 3rd ed., p. 739, Wiley, New York, 1985.

Chapter 4

Chapter 5

Kinetic study on the Reduction of NO using separated steps of oxidation and reduction

Abstract

The overall reduction of NO to N₂ in oxygen rich atmosphere has been studied as two separate steps, i.e., (1) oxidation of NO to NO₂ by oxygen and (2) reduction of NO₂ with the intermediate addition of propene to N₂. Using Pt/ZSM5 for the oxidation step and unmodified γ -alumina for the reduction step, high N₂ yields over a wide temperature range were obtained. The temperatures of both catalysts were independently varied and an optimum was obtained at around 300°C for the oxidation reaction and 450°C for the reduction to N₂. The dependence on NO₂ concentration for the reduction over γ -alumina was tested by applying a series of NO/NO₂ feed ratios. The conversion of NO was significantly enhanced by the presence of small amounts of NO₂. Possibly the conversion of NO at relative low temperatures is enabled by the formation of intermediates from the reaction of NO₂ with propene. The reductant efficiency, expressed in yield of N₂ per consumed propene, showed a maximum of nearly one. The combination of Pt/ZSM5 for the oxidation and γ -alumina for the reduction is found to be highly suitable.

5.1 Introduction

Increasing concerns about the environment have led governments worldwide to stringent restrictions of emissions such as CFC's, SO_x and NO_x. For the removal of NO_x, effective end-off-pipe methods such as selective catalytic reduction with ammonia or with hydrogen/CO mixtures have been developed. For the latter, the three-way catalyst is a well known example. The three-way catalyst is widely applied to reduce NO_x and CO emissions from auto gasoline engines working at stoichiometric conditions. However, lean-burn and diesel engines operate in oxygen rich conditions. Under these conditions the three-way catalyst is ineffective and, thus, other solutions are required. The reduction of NO_x using hydrocarbons (HC-SCR) is a promising route and is widely studied. However, until today a satisfactory solution is not available.

Numerous catalysts have been synthesized and tested so far, mostly based on transition metals supported on various oxides or zeolites [1-4]. In general, these studies attempt to simulate the activity of the three-way catalyst under oxygen rich conditions. Catalysts based on transition metals such as Pt [5, 6], Co [7, 8] or Fe [9,10], have been found to show high to moderate activities although they exhibit strong oxidation activity with increasing temperature and the reductant is consumed by unselective combustion. Many of these catalysts tend also to yield nitrous oxide (N₂O), which is an undesired side product. Mechanistic studies of the reduction of NO over such catalysts has indicated that NO is first partly oxidized to NO₂ (which is more reactive towards the hydrocarbons) and subsequently reduced to N₂ [11-15]. The two catalytic functions (oxidation and reduction) thus contribute to the effective conversion of NO to N₂.

A combination of oxidation and reduction functions on a single material has been reported by several authors [16-23] and high activities were obtained

although often the operating temperature window remained limited by the unselective combustion of the reductant.

A logical step is then to separate oxidation and reduction functions i.e., to use (i) a catalyst dedicated to the oxidation of NO to NO₂ and (ii) another dedicated to the reduction of NO₂. This way, the most active oxidation catalysts can be used in combination with the most active reduction catalyst. This can also dramatically simplify the catalyst design, while with catalysts that combine both functions none of them will operate under optimal conditions. In such an approach, the reductant should be prevented from contacting the oxidation function.

Hamada [24] and Bamwenda *et al.* [25] have stacked active catalysts to form a multiple staged catalyst beds in which a catalyst active at high temperatures is placed in front and followed by catalysts active at lower temperatures. Akaritawa *et al.* [26] applied a wash-coating of Pt/SiO₂ with a layer of H-, Ce- or Cu-ferrierite to restrict diffusion of reductant and minimize unselective combustion. Accordingly, Martens *et al.* [27] made use of the molecular sieving function of small pore zeolites (Chabazite) for the oxidation function and used a relative large reductant molecule (iso-octane). The oxidation of NO to NO₂ can also be achieved by using a plasma reactor, which according to Miessner *et al.* [28], showed increased NO₂ yields with increasing reductant (propene) feed concentration while the reductant was by itself oxidized to CO and CO₂ only to a very small extent. A disadvantage of this method is the relatively high amount of energy that is required for the plasma to enable an effective oxidation of NO to NO₂ (adiabatic heating of ~ 50-100°C at a space velocity of 20000 h⁻¹). Iwamoto *et al.*, [29, 30] completely separated the oxidation and reduction functions using two catalysts and added the reductant to the reaction mixture after the oxidation catalyst. For this, they placed

Chapter 5

both catalysts inside the same oven so that both were operating at the same temperature.

In practical applications, the catalysts may not necessarily operate at identical temperatures and thus using two ovens, allowing each catalyst to operate at its optimal temperature, may improve the results. In the present work, we present the application of separated oxidation and reduction catalysts with the intermediate addition of reductant using γ -alumina as the reduction catalyst. γ -alumina is known to show good activities for the reduction of NO_2 and shows low activities for the oxidation of hydrocarbons.

5.2 Experimental

5.2.1 Catalysts and reactants

For the oxidation of NO a 1 wt% Pt/ZSM5 was used. This catalyst was prepared by liquid-state ion exchange of ZSM5 (Zeolysts International, sample code CBV8014, which has a $\text{SiO}_2/\text{Al}_2\text{O}_3$ ratio of 80) using a highly diluted solution of $\text{Pt}(\text{NH}_3)_4(\text{OH})_2$ and ammonia. Details can be found in reference [31]. For the reduction of NO and NO_2 an unmodified γ -alumina (CONDEA, PURALOX) was used. For catalytic tests, the catalysts were pressed into tablets, crushed and sieved to obtain particles of 0.3-0.6 mm diameter. Gas mixtures used were 1.0% NO_2/He , 1.0% NO/He , 1.0% $\text{C}_3\text{H}_6/\text{He}$ and 100% O_2 and were all obtained from Messer Griesheim GmbH, Germany. The reactant feeds were directly mixed using BROOKS 5850S mass flow controllers.

5.2.2 Catalytic tests

For the catalytic tests using separated as well as single bed reactors, a flow system was used as shown in Figure 1. The system contains two tubular reactor ovens connected through a 6-port valve. This allows for the intermediate addition of the reductant and independent control of the temperatures. By switching the 6-way valve one is able to use either one or both reactants. For the tests using the intermediate addition of reductant, both reactors were filled with 200 mg of the corresponding catalyst. Prior to the catalytic test, the catalysts were activated *in situ* in He by heating with 10°C/min to 550°C (Pt/ZSM5) and 600°C (γ -alumina). After 1 hour, the temperature was lowered to 150°C (oven 1) and 350 or 450°C (oven 2). The feed was then switched to the reaction mixture of 5% O₂, 1000 ppm NO and He (total 95 ml/min) to oven 1, plus 5 ml/min 1% C₃H₆/He (1000 ppm) to oven 2. For experiments using a single reactor the 6 port valve was switched to bypass the second oven and mixtures of 5% O₂, 1000 ppm C₃H₆ and 1000 ppm NO_x were fed to oven 1. Analysis of the products CO, CO₂, N₂O, O₂, N₂ and CH₄ was performed using a HP 6960 gaschromatograph equipped with a MS-5A and a Porapack Q capillary columns. NO and NO₂ concentrations were measured using a Thermo Environmental model 42C chemiluminescence NO_x analyzer.

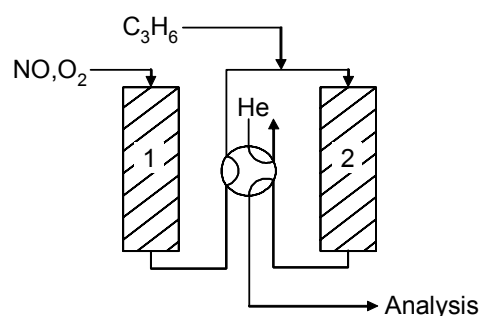


Figure 1. Schematic representation of the dual-reactor flow system.

5.3 Results and Discussion

5.3.1 Oxidation of NO and reduction of NO₂

Figures 2 and 3 show the activities of the oxidation and reduction catalysts used, respectively. Figure 2 shows activity for the oxidation of NO to NO₂ over both the oxidation and the reduction catalysts separately. For the oxidation of NO to NO₂ over Pt/ZSM5, a maximum NO₂ yield of ~70% was obtained at 300°C. At higher temperatures, the NO and NO₂ concentrations followed the limitations of the thermodynamic equilibrium ($\text{NO} + \frac{1}{2} \text{O}_2 \leftrightarrow \text{NO}_2$, at 1 bar, 1000 ppm NO_x and 5% O₂ in Helium). The NO₂ yield over γ -alumina remained around 5% over the whole temperature range showing clearly that γ -alumina hardly catalyzed this reaction.

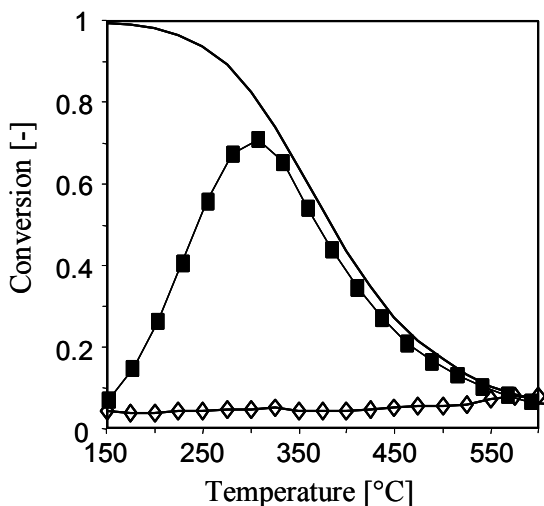


Figure 2. Oxidation of NO to NO₂ over (■) Pt/ZSM5 and (◇) γ -alumina and the thermodynamical equilibrium ratio of NO₂/NO (—).

Figure 3 shows the conversions and yields obtained over γ -alumina using a feed of 1000 ppm NO₂, 5% O₂ and 1000 ppm C₃H₆. The conversion of NO₂ (Figure 3a) reached 100% around 375°C with a high selectivity to N₂. The main side

product was NO, which reached a maximum of about 20% at 300°C. The N₂O yield remained below 5%, which is clearly an advantage of this catalyst over transition metal supported catalysts that commonly show relative high N₂O yields. The NO yield strongly increased at temperatures above 550°C, which is due to the strongly increasing unselective combustion of propene (see Figure 3b). The conversion of propene (Figure 3b) increased slower with increasing temperature as compared to the strongly increasing NO₂ conversion. This suggests that propene was used for the selective reduction of NO₂ rather than unselective combustion by oxygen. At higher temperatures methane was formed, which is a product of propene cracking and is relatively stable under these conditions. The deviations in the nitrogen and carbon balances never exceeded +/- 10 %.

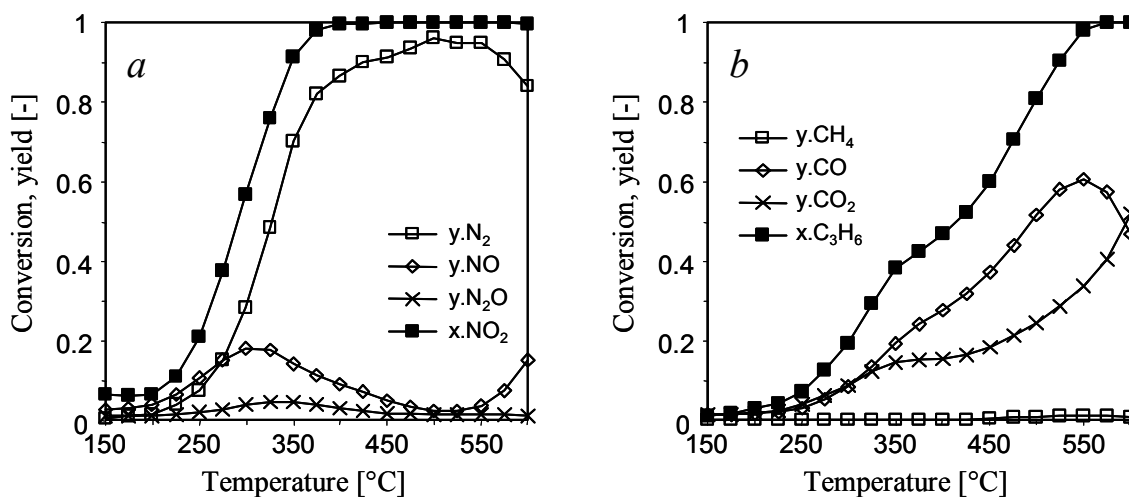


Figure 3. Conversions and yield of the reduction of NO₂ by propene over γ -alumina, (a) nitrogen compounds, (b) carbon compounds.

5.3.2 Catalytic tests using separated oxidation and reduction catalysts

Figure 4 shows the N₂ yield and propene conversion obtained using oxidation and reduction catalysts and the intermediate addition of propene, in the 2-reactor flow system (see Figure 1). Figure 4 compiles the results of two

experiments in which the temperature of the oxidation catalyst (Pt/ZSM5) was increased from 150 to 600°C, while the temperature of the reduction catalyst remained constant at 350°C or 450°C. It is clear that in both experiments good N₂ yields were obtained over a wide temperature range for the oxidation catalyst. With the temperature of the reduction catalyst at 350°C, the maximum N₂ yield was about 60%, while at 450°C a maximum yield of 90% was obtained. In both cases the maximum yield was obtained with the oxidation catalysts around 300°C. This, coincides (see Figure 3a) with the highest NO₂ concentration (~70%). With increasing temperature (>300°C) the NO₂ concentration decreased, which led to a decreasing N₂ yield and propene conversion. The conversion of propene followed the trend of the N₂ yield, indicating that propene was mainly consumed by the selective reduction of NO₂.

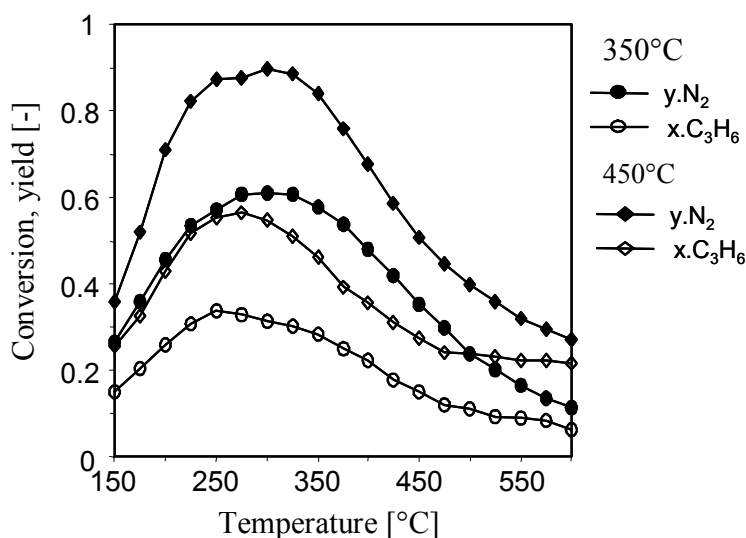


Figure 4. Yield of N₂ and propene conversion using two-reactor flow system with increasing oxidation catalysts temperature and constant reduction-catalyst temperature.

5.3.3 Reduction of NO/NO₂ mixtures over γ -alumina

The maximum N₂ yields obtained in these experiments remained below those obtained by feeding NO₂, as shown in Figure 3a. This may be attributed to the incomplete oxidation of NO to NO₂ over Pt/ZSM (see Figure 2). In order to probe the hypothesis, feed mixtures with different NO/NO₂ ratios were tested with a constant amount of propene and oxygen over γ -alumina. Figures 5a-c show the NO_x conversion, C₃H₆ conversion and selectivities to N₂ obtained from feeding mixtures of NO and NO₂. The concentration of NO₂ was increased stepwise by 250 ppm and the NO concentration was accordingly lowered to retain a constant NO_x feed concentration. The NO_x conversions of all mixtures, except NO/(NO+NO₂) = 1, increased almost simultaneously until about 300°C. Above this temperature, the differences in NO_x conversions widened, but the final conversions at 600°C were all around 80±5%. The propene conversions appeared to follow similar trends although conversions increased initially far slower, while in all mixtures 100% conversion was obtained at 575°C. The N₂ selectivity increased almost linearly to reach nearly 100% at 375°C. Upon further temperature rise it remained around 95% until 600°C.

Between 200°C and 575°C, the NO_x conversion increased strongly in parallel with the NO₂ concentration up to 250 ppm and kept increasing with smaller increment up to a feed of 1000 ppm NO₂ (0 ppm NO). For instance, at 300°C the NO_x conversion reached only ~5% with a feed of 1000 ppm NO, but increased to ~33% when feeding 250 ppm of NO₂ (NO/(NO+NO₂) = 0.75). For N₂ and N₂O similar yields were obtained as shown in Figure 3a, which in all cases resulted in a selectivity to N₂ of nearly 100% at temperatures above ~375°C. For the situation in which NO and NO₂ conversion occurs completely independently, the total NO_x conversion of a NO/NO₂ mixture can be described by the proportional sum of the

Chapter 5

conversions obtained feeding the pure components, as given in Equation (1).

$$x.\text{NOx}(\text{mix}) = \alpha \cdot x.\text{NO} + (1 - \alpha) \cdot x.\text{NO}_2 \quad (1)$$

where α is the fraction of NO, $\alpha = \text{NO}/(\text{NO}+\text{NO}_2)$ and $x.\text{NO}$, $x.\text{NO}_2$ are the conversions of NO and NO_2 obtained when feeding pure NO or NO_2 ($\alpha = 1, 0$), respectively.

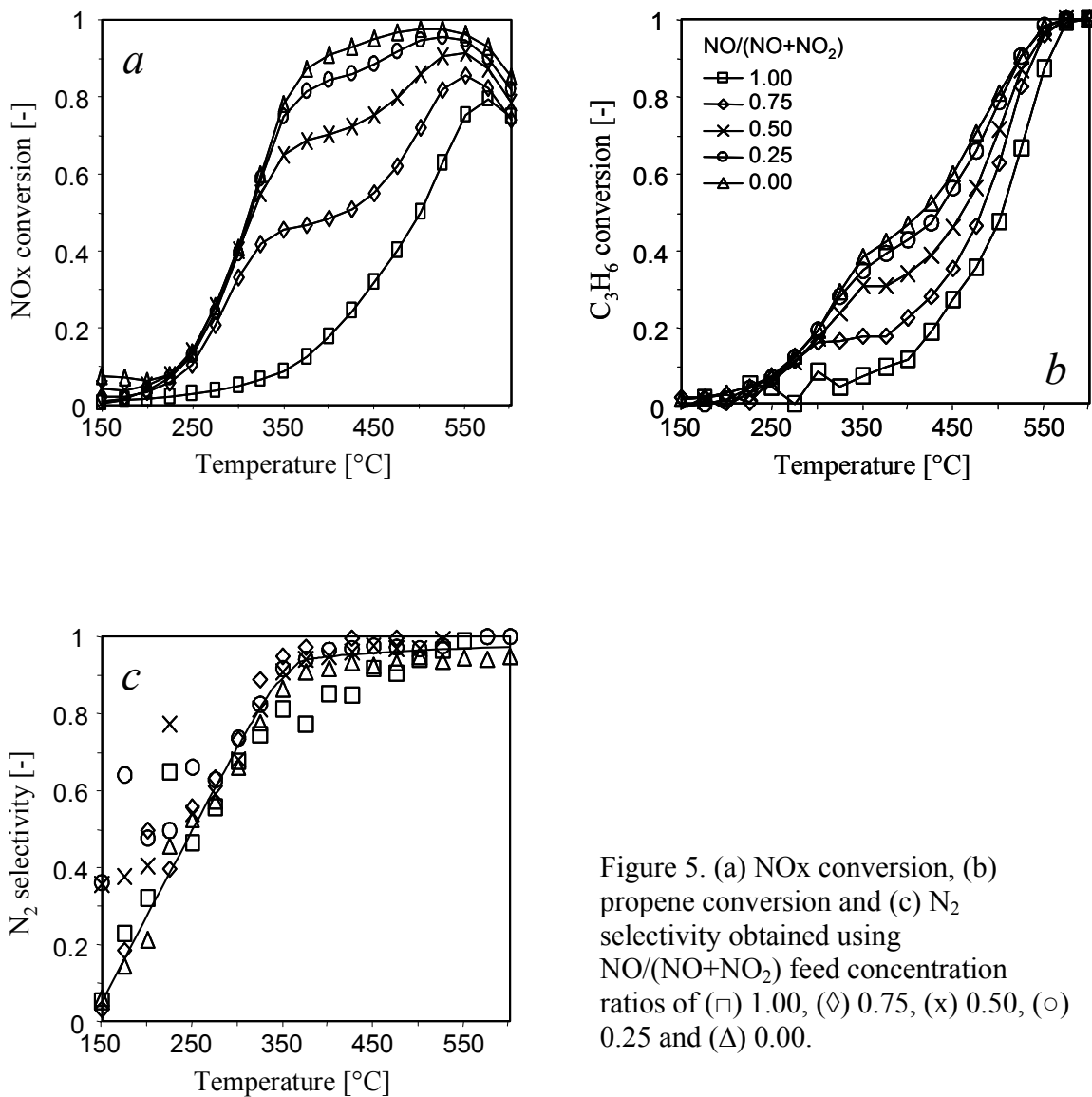


Figure 5. (a) NO_x conversion, (b) propene conversion and (c) N₂ selectivity obtained using NO/(NO+NO₂) feed concentration ratios of (□) 1.00, (◇) 0.75, (×) 0.50, (○) 0.25 and (△) 0.00.

Figure 6 shows the difference between the obtained NO_x conversion and proportional NO_x conversion calculated according to equation (1). The NO_x conversions obtained for NO/NO₂ mixtures were up to ~23% higher than what would be expected from a proportional contribution. All mixtures studied show a similar trend with maxima around 325°C and 500°C. This suggest that NO and NO₂, when fed as a mixture, do not convert completely independently, but reactions take place, which involve both NO and NO₂ and, thus, suggest a synergetic conversion of NO and NO₂. Although the total conversion of a mixture never exceeded that of pure NO₂, this synergy, apparently, enables significantly higher NO conversions as compared to feeding pure NO.

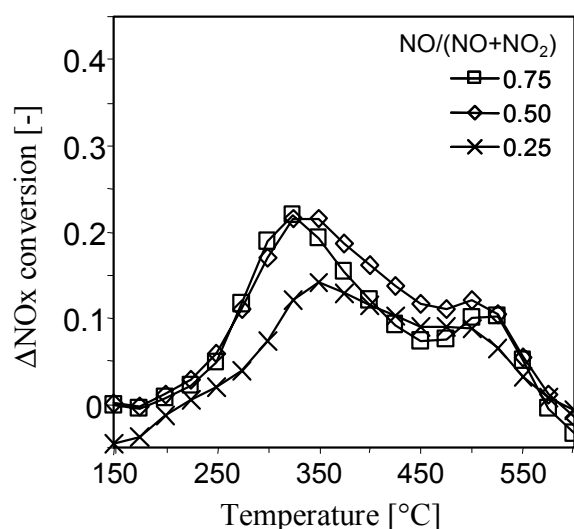


Figure 6. Difference between NO_x conversion measured with NO/NO₂ mixtures and calculated from proportional contributions of NO and NO₂.

The synergetic conversion of NO and NO₂ is also reported in NH₃-SCR related literature [32] and labeled “fast-SCR reaction”. Note that reaction mechanisms of NH₃-SCR involve the reduction and oxidation of the catalysts (usually vanadia or vanadyl complexes on titania). It is unlikely that alumina can be reduced by propene under the given conditions. This prevents the adoption of

Chapter 5

the “fast SCR-reaction” mechanism to the present observations. It is more likely that reactions of NO₂ and propene produce intermediates with which NO can react more easily as compared to propene and so enable the conversion of NO at lower temperatures.

5.3.4 Reductant efficiency

With the separation of the oxidation and reduction functions, a strong decrease in unselective combustion of the reductant was aimed for in order to enable high N₂ yields over a wide temperature range. Figure 3b shows that γ -alumina had a low activity for the unselective combustion of propene. The utilization of propene in the selective catalytic reduction of NO can be expressed by Equation 2 [30]

$$E_{\text{HC}} = \text{amount of NO reduced to N}_2 / \text{amount of C}_3\text{H}_6 \text{ consumed} \quad (2)$$

Figure 7 shows the changes in E_{HC} with increasing temperature for all NO/NO₂ mixtures used in Figure 5. All the mixtures which contained NO₂ showed a similar volcano type curve. For the mixtures containing NO₂, the maximum value for E_{HC} of 1.8 was obtained at 375°C. Below 375°C the yields of N₂ and conversions of propene were relatively low and, thus, a larger error in the ratio may exist. Above 375°C, yields and conversion are relative high and it is clear that all mixtures show identical propene utilization. The fact that this ratio increased until 375°C indicates that propene is consumed in another reaction below this temperature. The possibilities include the formation of carbonaceous deposits by dehydrogenation or partial oxidation or the preferentially conversion to N₂O. At temperatures above 375°C, the increasing unselective combustion of propene is concluded to cause the decrease in the reductant efficiency.

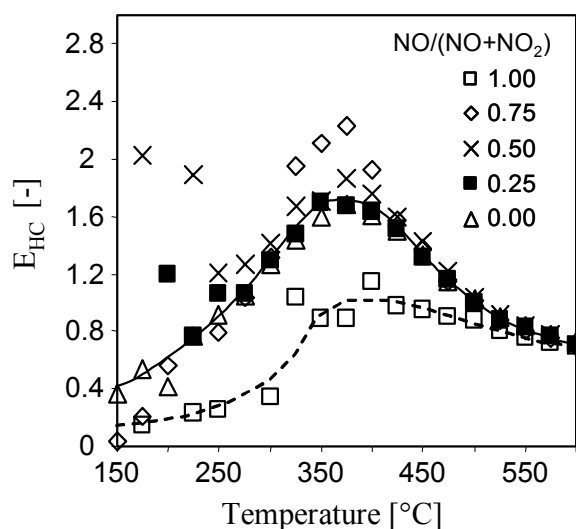


Figure 7. Reductant utilization (Eq. (2)) for the reduction of mixtures of NO/NO₂ by propene over γ -alumina.

The reduction of NO by oxidation and reduction with the intermediate addition of reductant was also applied by Iwamoto *et al.* [30]. For this, they used a Pt/ZSM5 as oxidation catalyst and a series of impregnated MFI catalyst for the reduction and ethene as reductant. The highest number for the $E_{HC} = \sim 2$ was obtained using a Zn/ZSM5 as reduction catalysts. An E_{HC} value close to 2 suggests that the formation of N₂ proceeds with a single reductant molecule so that interactions between reaction intermediates are concluded not to take place. In mixtures of NO₂ and NO, it is possible that a reaction of NO₂ with the reductant leads to a nitrogen containing intermediate, which is able to react with NO to enable the formation of N₂. Possibly, the reaction mechanisms of the reduction of NO_x with ethene and propene are largely similar so that in both cases one N₂ is formed per reductant molecule.

Chapter 5

5.3.5 Effectiveness of intermediate addition of reductant

Iwamoto *et al.* [30] showed, by comparing the N₂ yield and reductant efficiency of a series of metal exchanged ZSM5 catalysts, that the intermediate addition of reductant is an effective method to improve N₂ yields only when the reduction catalyst is (i) inactive for the oxidation of NO to NO₂ and (ii) inactive for the direct reduction of NO in the presence of O₂. The first constraint relates to the oxidation activity of the catalysts. A catalyst that is active for the oxidation of NO to NO₂ is likely also to be active for the unselective oxidation of the reductant. Catalysts that are already active for the reduction of NO by hydrocarbons will not profit from a prior oxidation of NO to NO₂ and, thus, are unsuitable. γ -alumina satisfies both requirements, as it is active for the reduction of NO₂, while significantly less active for the reduction of NO and exhibits a low activity for the oxidation of propene. Thereby it combines a high NO_x conversion with high N₂ selectivity over a wide temperature range.

5.4 Conclusions

The reduction of NO in the presence of excess O₂ *via* the oxidation to NO₂ and subsequent reduction with the intermediate addition of propene was studied. For the oxidation of NO, Pt/ZSM5 was used and unmodified γ -alumina for the reduction. The method proved to be very effective, as high N₂ yields were obtained over a wide temperature range.

The oxidation of NO to NO₂ showed a maximum conversion of 70% and, thus, implies that the feed to the reduction catalysts contains a mixture of NO and NO₂. On the reduction catalyst, a moderate activity for the reduction of NO is present. The influence of NO₂ concentrations was tested by applying different NO/NO₂ concentrations for the reduction. It was found that the presence of small

amounts of NO₂ significantly enhanced the conversion of NO. Possibly, NO reacts with intermediates of a reaction of NO₂ and propene and, thus, allows for the conversion of NO at low temperatures. The efficiency with which propene was consumed relative to the amount of N₂ formed showed a limit of ~0.85 N₂ formed per propene consumed. It was argued that a value close to unity suggests that N₂ formation occurs using a single adsorbed reductant molecule.

Applying the system of intermediate addition of reductant, the reduction catalyst should have (i) a low oxidation activity in order to prevent the unselective combustion of the reductant and (ii) a relative low activity for the direct reduction of NO. γ -alumina satisfies both requirements and Pt/ZSM5 shows good NO to NO₂ conversions. The combination of these catalysts leads, thus, to a suitable solution. γ -alumina is known to be easily deactivated by SO_x and water and, thus, unsuitable for realistic conditions. An effective catalyst for this method, therefore, needs to combine the properties of γ -alumina (high activity for NO₂ reduction, high selectivity to N₂, low oxidation activity) with the resistance to deactivation by SO_x and water.

References

- 1 Y. Traa, B. Burger, J. Weitkamp, *Micro. Meso. Mat.* 30 (1999) 3.
- 2 R. Burch, J.P. Breen, F.C. Meunier, *Appl. Catal. B Env.* 39 (2002) 283.
- 3 M.D. Amiridis, T.J. Zhang, R.J. Farrauto, *Appl. Catal. B Env.* 10 (1996) 203.
- 4 V.I. Parvulescu, P. Grange, B. Delmon, *Cat.Today* 46 (1998) 233-316.
- 5 R. Burch, P.J. Millington, A.P. Walker, *Appl. Catal. B Env.* 4 (1994) 65.
- 6 M.D. Amiridis, K.L. Roberts, C.J. Pereira, *Appl. Catal. B* 14 (1997) 203.
- 7 Y. Li, J.N. Armor, US Patent 5 149 512, assigned to Air Products and Chemicals Inc., 22 September 1992.

Chapter 5

- 8 S.E. Maisuls, K. Seshan, S. Feast, J.A. Lercher, *Appl. Catal. B Env.* 29 (2001) 69.
- 9 X. Feng, W.K. Hall, *Catal. Lett.* 41 (1996) 45.
- 10 H.-Y. Chen, W.M.H. Sachtler, *Catal. Lett.* 50 (1998) 125.
- 11 C. Descorme, P. Ge'lin, M. Primet, C. Lécuyer, *Catal.Lett.* 41 (1996) 133.
- 12 J.-Y. Yan, H.H. Kung, W.M.H. Sachtler, M.C. Kung, *J. Catal.* 175 (1998) 294.
- 13 E. Kikuchi, M. Ogura, I. Terasaki, Y. Goto, *J. Catal.* 161 (1996) 465.
- 14 J.T. Miller, E. Glusker, R. Peddi, T. Zheng, J.R. Regalbuto, *Catal. Lett.* 51 (1998) 15.
- 15 C. Yokoyama, M. Misono, *Catal. Today* 22 (1994) 59.
- 16 Y. Nishizaka and M. Misono, *Chem. Lett.* (1993) 1295.
- 17 Y. Nishizaka and M. Misono, *Chem. Lett.* (1994) 2237.
- 18 C.J. Loughran and D.E. Resasco, *Appl. Catal. B* 7 (1995) 113.
- 19 A.P. Walker, *Catal. Today* 26 (1995) 107.
- 20 R. Burch, S. Scire, *Appl. Catal B Env.* 3 (1994) 295.
- 21 E. Kikuchi, M. Ogura, I. Terasaki, Y. Goto, *J. Catal.* 161 (1996) 465.
- 22 Y. Li, T.L. Slager, J.N. Armor, *J. Catal.* 150 (1994) 388.
- 23 B.J. Adelman, T. Beutel, G.D. Lei, W.M.H. Sachtler, *J.Catal.* 158 (1996) 327.
- 24 H. Hamada, *Cat. Surv.Japan* 1 (1997) 53-60.
- 25 Bamwenda GR, Obuchi A, Ogata A, Oi J, Kushiyama S, Mizuno K, *React. Kin. Catal. Lett.* 63 (1998) 53.
- 26 S. Akaratiwa, T. Nanba, A. Obuchi, J. Okayasu, J.-O. Ochisawa, S. Kushiyama, *Top.Catal.* 16/17 (2001) 209.
- 27 J.A. Martens, A. Ceuvel, F. Jayat, S. vergne, E. Jobson, *Appl. Catal. B Env.* 29 (2001) 299.
- 28 H. Miessner, K.-P. Francke, R. Rudolph, *Appl. Catal. B Env.* 36 (2002) 53.

- 29 M. Iwamoto, A.M. Hernandez, T. Zengyo, Chem. Commun. (1997) 37.
- 30 M. Iwamoto, T. Zengyo, A.M. Hernandez, H. Araki, Appl. Catal. B Env. 17 (1998) 259.
- 31 G.D. Pirngruber, K. Seshan, J. A. Lercher, J. Catal. 186 (1999) 188.
- 32 M. Koebel, G. Madia, F. Raimondi, A. Wokaun, J. Catal. 209 (2002) 159.

Chapter 5

Chapter 6

Summary

6.1 Summary

The emission of NO_x in the atmosphere causes a series of significant environmental problems such as acid rains, photochemical smog, ozone depletion and green house effect. Roughly three quarters of the global production of NO_x is due to anthropogenic activity of which combustion of fossil fuels account for more than half. Combustion of fossil fuels is in general used to free energy for the propulsion of cars, trucks, trains, boats, airplanes and to generate electricity in power plants or heat for industrial processes. During combustion NO_x can be formed by oxidation of nitrogen containing organic compounds, oxidation of HCN or oxidation of N_2 present in the air (Thermal NO_x). Nitrogen can efficiently be removed from organic fuels by hydro-treating while HCN is only formed in fuel rich flames leaving the oxidation of N_2 as the major source of NO_x . To achieve reduction of NO_x emissions governments world wide have installed restrictive legislations such as in 1971 the 'clean air act' in the USA and the Euro I-V norms in Europe which initiated the development of NO_x reducing technologies. The development of the NH_3 -SCR process in the 70's enables the efficient reduction of NO_x from stationary sources. Thermal NO_x can efficiently be reduced by CO and H_2 (three-way catalyst) in car exhausts containing stoichiometric O_2 levels. Exhausts of Diesel and Lean burn engines contain excess of O_2 and thus is the development of new technologies required. The use of hydrocarbons for the reduction of NO_x appears a promising technique and a wealth on research results on this topic has been reported in the last 20 years what until today did not result in a satisfactory solution.

Brønsted acid sites in metal exchanged zeolites have been believed to significantly improve the catalysts performance. A detailed knowledge on the influence of Brønsted acid sites is important for the development of more effective

NO_x reduction catalysts. The aim of this work was to obtain insight in the role of Brønsted acid sites for the reduction of NO_x and in particular NO₂ by light hydrocarbons.

In chapter 2, the reduction of NO₂ by propene over H-Y zeolite and steamed H-Y zeolite has been studied by *in situ* infra red spectroscopy and kinetic measurements. H-Y zeolite is a very active catalyst for this reaction, converting all NO₂ at temperatures between 150 and 600°C. At lower temperatures C₃H₆ readily reacts with NO₂ to oxygenates, CO, CO₂, water and nitrogen containing organic compounds such as oximes, isocyanates or cyanides and organo-nitro species. The presence of O₂ primarily enhances the formation of carbonaceous deposits and unselective combustion of C₃H₆. Results indicate that O₂ does not play a crucial role in the formation of N₂. Optimal N₂ yields were obtained feeding NO₂ and C₃H₆ is a stoichiometric ratio of 4 to 1. The selectivity to N₂ is determined by the competitive reactions of NO₂ with coke, formation of coke by oxygen, partial oxidation of C₃H₆ by NO₂ and selective formation of N₂. Results indicate that an optimal selectivity to N₂ is obtained at infinite low C₃H₆ feed concentration. Extrapolation of N₂ selectivity indicates a maximum N₂ selectivity of 50% can be obtained using an infinite low propene feed concentration.

In chapter 3, the reduction of NO₂ by C₃H₆ and C₃H₈ over H-Y, H-USY, H-MOR and H-ZSM5 has been investigated. This optimal feed concentration ratio for propene and NO₂ of 1:4 was independent of the zeolite type. At C₃H₆ to NO₂ feed concentration ratios below 1:4 the selectivity to N₂ remained practically constant but was different for the different zeolites. In these conditions H-MOR showed the highest selectivity to N₂, closely followed by H-ZSM5 while H-Y and H-USY showed a significantly lower selectivity. The selectivity was related to a combination of three competitive reactions; formation and removal of hydrogen

Chapter 6

poor coke species, hydrolysis of organo nitro compounds and selective formation of N_2 . A mechanism for the reduction of NO_2 by C_3H_6 is proposed in which H-form zeolites catalyze the formation of primary nitro compounds which through a sequence of rearranging steps produce iso-cyanates, cyanides, amines, amides and ammonia and finally N_2 . The reduction of NO_2 by C_3H_8 proceeds via the initial activation of C_3H_8 through the formation of carbenium ion complex at a Brønsted acid site after which the mechanism proceeds in a similar way as proposed for C_3H_6 .

In chapter 4, the role of oxygenate intermediates in the reduction of NO_2 by propene over H-Y zeolite catalysts has been studied. At lower temperatures, selective oxidation of propene can lead to oxygenates formation. These together with NO_2 form azo type intermediates, where N-N coupling has occurred and further decomposition of these lead to the formation of N_2 . At higher temperatures, such intermediates derived from oxygenates are not stable. Hydrolysis of N containing residue on the catalyst surface leads to ammonia and NO_x reduction is achieved in a typical ammonia NO_x reaction.

In chapter 5, the overall reduction of NO to N_2 in oxygen rich atmosphere has been studied as two separate steps, i.e., (1) oxidation of NO to NO_2 by oxygen and (2) reduction of NO_2 with the intermediate addition of propene to N_2 . Using Pt/ZSM5 for the oxidation step and unmodified γ -alumina for the reduction step, high N_2 yields over a wide temperature range were obtained. The temperatures for the oxidation and reduction catalysts were independently varied and an optimum was obtained at around 300°C for the oxidation reaction and 450°C for the reduction to N_2 . The dependance of NO_2 concentration for the reduction over γ -alumina was tested by applying a series of NO/ NO_2 feed ratios. The conversion of NO was significantly enhanced by the presence of small amounts of NO_2 . Possibly,

the conversion of NO at relative low temperatures is enabled by the formation of intermediates from the reaction of NO₂ with propene. The reductant efficiency, expressed in yield of N₂ per consumed propene, showed a maximum of nearly 1, which is similar to the maxima reported in literature.

6.2 Samenvatting

The uitstoot van stikstofoxides (NO_x) in de atmosfeer veroorzaakt serieuze problemen voor het milieu, zoals zure regen, fotochemische smog, afbraak van de ozonlaag en broeikas effect. Grofweg drie kwart van de globale uitstoot aan NO_x wordt door menselijk handelen veroorzaakt waarvan meer dan de helft bij de verbranding van fossiele brandstoffen. De energie die vrijkomt bij de verbranding van fossiele brandstoffen wordt in het algemeen gebruikt voor de voortbeweging van auto's, treinen, boten en vliegtuigen alsmede voor de opwekking van elektrische energie en verwarming voor industriële processen. Tijdens de verbranding kan NO_x gevormd worden door oxidatie van stikstof houdende organische verbindingen, oxidatie van HCN en oxidatie van N₂ (thermische NO_x) dat in de lucht aanwezig is. Stikstofhoudende verbinding kunnen efficiënt van stikstof ontdaan worden d.m.v. hydrogenering, HCN wordt alleen gevormd in zeer zuurstof arme verbranding condities waarmee de vorming van thermische NO_x overblijft als belangrijkste bron van NO_x. Om vermindering van NO_x uitstoot te bereiken zijn wereldwijd wettelijke restricties ingesteld zoals de 'clean air act' in the vereenigde staten van amerika en de EURO I-V normen in Europa. De invoer van deze regels heeft de ontwikkeling van NO_x reductie technologieën sterk versneld. De ontwikkeling van de NH₃-SCR technologie in de 70er jaren maakte het mogelijk om efficiënt de NO_x uitstoot van stationaire bronnen te reduceren. Thermische NO_x kan efficiënt worden gereduceerd met CO en H₂ (drie-weg katalysator) in auto uitlaatgassen welke een stoichiometrische verhouding aan

Chapter 6

zuurstof bevatten. Uitlaatgassen van Diesel of 'Lean Burn engines' (arme verbrandings motor) bevatten een sterke overmaat aan zuurstof en dus is de ontwikkeling van nieuwe technologieën noodzakelijk. Het gebruik van koolwaterstoffen voor de reductie van NO_x is een veel belovende techniek en een weelde aan onderzoeksresultaten is gepubliceerd op dit onderwerp in de laatste 20 jaar, wat helaas tot op heden nog niet tot een tevredenstellende technologie heeft geleid.

Aan de Bronsted zure groepen van met metaal uitgewisselde zeolieten worden gunstige eigenschappen toegewezen voor de prestaties van de katalysator. Een gedetailleerde kennis van de invloed van de Bronsted zure groepen is belangrijker voor de ontwikkeling van effectievere NO_x reductie katalysatoren. Het doel van dit werk was om inzicht te vergaren in de rol die de Bronsted zure groepen spelen tijdens de reductie van NO_x door koolwaterstoffen.

In hoofdstuk 2 wordt de reductie van NO_2 door propaan over H-Y zeoliet en gestoomde H-Y zeoliet bestudeerd door middel van *in situ* infra rood spectroscopie en kinetische activiteit metingen. Alle NO_2 werd geconverteerd binnen het temperatuur bereik van 150 tot 600°C wat aantoonde dat H-Y zeoliet een erg actieve katalysator voor deze reactie. Op relatief lage temperaturen reageerde NO_2 met propaan waarbij CO , CO_2 , water, zuurstofhoudende organische verbindingen en stikstofhoudende verbindingen gevormd zoals oximen, iso-cyanaten, cyanides en organische nitro verbindingen. De aanwezigheid van O_2 versnelde de vorming van koolwaterstof houdende afzettingen en niet-selectieve verbranding van propaan. Resultaten geven de indruk dat O_2 geen cruciale rol speelt bij de vorming van N_2 . Een optimum N_2 opbrengst werd verkregen wanneer NO_2 en propaan in de verhouding 4 : 1 aan de katalysator geleid werden. De selectiviteit voor N_2 wordt bepaalde door competitieve reacties van NO_2 met coke, vorming van coke door

zuurstof, partiele oxidatie van propene door NO_2 en de selectieve vorming van N_2 . De resultaten geven aan dat bij een oneindig lage voedings concentratie van propene de hoogste selectiviteit voor N_2 (50%) behaald kan worden.

In hoofdstuk 3 wordt de reductie van NO_2 door propene en propaan over H-Y, H-USY, H-MOR en H-ZSM5 bestudeerd. De optimum verhouding voor propene en NO_2 voedings concentraties van 1:4 blijkt onafhankelijk van het type zeoliet. Bij voedingsconcentratie verhoudingen beneden 1:4 blijft de N_2 selectiviteit constant maar is verschillend voor de verschillende type zeolieten. The hoogste selectiviteit werd behaald met H-MOR, gevolgd door H-ZSM5 terwijl H-Y en H-USY een aanzienlijk lagere N_2 selectiviteit opleverde. De selectiviteit wordt gerelateerd aan een combinatie van drie competitieve reacties; vorming en verwijdering van waterstof arme coke verbindingen, hydrolyse van organische nitro verbindingen en de selectieve vorming van N_2 . Een mechanisme voor de reductie van NO_2 door propene is voorgesteld waarin H-vorm zeolieten de vorming van primaire nitro verbindingen katalyseert welke door een aaneenschakeling van reacties via iso-cyanaten, cyanides, amines, amides en ammonia de vorming van N_2 mogelijk maakt. The reductie van NO_2 door propaan volgt via de activering van propaan door middel van de vorming van carbonium anion op een Brønsted zure groep waarna het mechanisme eenzelfde route volgt als voorgesteld voor propene.

In hoofdstuk 4 wordt de rol van zuurstof houdende koolwaterstoffen in de reductie van NO_2 over H-Y zeoliet bestudeerd. Zuurstof houdende koolwaterstoffen worden gevormd bij relatief lage temperaturen. Deze kunnen samen met NO_2 leiden tot de vorming van azo type verbindingen waarbij reeds de N-N verbinding is gevormd en welke door decompositie leidt tot de vorming van N_2 . Zulke intermediären zijn instabiel bij hogere temperaturen. Hydrolyse van

Chapter 6

overige stikstof houdende verbindingen op het oppervlak leid to de vorming van ammonia welke eenvoudig met NO_x reageerd.

In hoofdstuk 5 de reductie van NO via de oxidatie naar NO_2 en vervolgens de reductie to N_2 is bestudeerd waarbij de katalysatoren voor beide reacties gescheiden werden en de reductant (propeen) na de oxidatie reactie aan de reactie stroom werd toegevoegd. Gebruik makend van Pt/ZSM5 voor de oxidering van NO en een ongemodificeerde γ -alumina voor de reductie van NO_2 werden hoge N_2 opbrengsten over een breed temperatuur bereik behaald. De temperatuur van beide katalysatoren kon onafhankelijk worden geregeld waarbij een optimum conditie werd bereikt bij $\sim 300^\circ\text{C}$ voor de oxidatie reactie en $\sim 450^\circ\text{C}$ voor de reductie. De afhankelijkheid voor de reductie van de NO_2 concentratie werd getest gebruik makend van verschillende NO/NO_2 verhoudingen. De omzetting van NO werd beduidend verbeterd bij de aanwezigheid van een lage concentratie NO_2 . Wellicht, wordt de omzet van NO bij relatief lage temperaturen mogelijk gemaakt door de aanwezigheid van intermediären van de reactie van NO_2 en propaan. De efficiency waarmee de reductant werd geconsumeerd relatief tot de hoeveelheid N_2 gevormd vertoonde een maximum van bijna 1, wat overeenkomt met de maximum waardes in de literatuur.

6.3 Zusammenfassung

Atmosphärische Stickoxidemissionen verursachen eine ganze Reihe von Umweltproblemen wie zum Beispiel saurer Regen, photochemischer Smog, Abbau der Ozonschicht und Verstärkung des Treibhauseffektes. Etwa drei Viertel der globalen NO_x Emissionen sind anthropogenen Ursprungs, davon stammt mehr als die Hälfte aus der Verbrennung fossiler Brennstoffe. Verbrennung fossiler Rohstoffe wird vorwiegend genutzt zur Energieerzeugung in Kraftwagen, Zügen,

Schiffen und Flugzeugen, zur Stromerzeugung in Kraftwerken und zur Wärmeproduktion für industrielle Prozesse. NO_x entstehen während der Verbrennung durch Oxidation von stickstoffhaltigen Verbindungen, Oxidation von HCN oder Oxidation von Luftstickstoff (thermales NO_x). Stickstoff in organischen Verbindungen kann effektiv durch Hydrotreating entfernt werden, während HCN erst in brennstoffreichen Flammen erzeugt wird, so dass N_2 die Hauptquelle für NO_x Emissionen darstellt. Um die NO_x Emissionen zu reduzieren, wurden weltweit Gesetze erlassen, wie zum Beispiel der „Clean Air Act“ in den USA 1971 und die Euro I-V Normen in Europa, die die Entwicklung von NO_x reduzierenden Technologien erzwangen. Die Entwicklung des NH_3 -SCR Prozesses in den 70er Jahren erlaubte die effiziente NO_x Reduzierung aus stationären Quellen. Thermales NO_x in Autoabgasen kann durch CO und H_2 (3-Wege-Katalysator) bei stöchiometrischen O_2 Konzentrationen reduziert werden. Diesel und Magermotor Abgase und enthalten überschüssiges O_2 , was die Entwicklung neuer Technologien erforderlich macht. Der Einsatz von Kohlenwasserstoffen zur NO_x Reduktion ist eine viel versprechende Technologie, über die eine große Zahl von Studien in den letzten 20 Jahren veröffentlicht wurden, die aber noch keine befriedigenden Ergebnisse erzielte.

Von Brønsted Säurezentren in Metall-ausgetauschten Zeolithen wird angenommen, dass sie die katalytische Wirkung der Katalysatoren entscheidend verbessern. Eine genaue Kenntnis des Einflusses von Brønsted Säurezentren ist wichtig für die Entwicklung besserer NO_x Reduktionskatalysatoren. Das Ziel dieser Arbeit war, eine genauere Kenntnis des Einflusses von Brønsted Säurezentren auf die NO_x Reduktion, insbesondere von NO_2 , durch Kohlenwasserstoffe zu erlangen.

In Kapitel 2 wurde die Reduktion von NO_2 durch Propen über Zeolith H-Y und dampfbehandeltem H-Y durch *in situ* Infrarot-Spektroskopie und kinetische

Chapter 6

Studien untersucht. H-Y ist ein sehr aktiver Katalysator für diese Reaktion, der zwischen Temperaturen von 150°C bis 600°C NO_2 vollständig umsetzt. Bei niedrigeren Temperaturen reagiert C_3H_6 leicht mit NO_2 zu Oxygenaten, CO, CO_2 , Wasser und stickstoffhaltigen organischen Verbindungen wie Oxime, Isocyanate oder Cyanaten und organischen Nitroverbindungen. Die Anwesenheit von Sauerstoff verstärkt hauptsächlich die Bildung von kohlenstoffreichen Rückständen und die unselektive Oxidierung des Propens. Die Ergebnisse legen nahe, dass O_2 keine wichtige Rolle in der Bildung von N_2 spielt. Die besten N_2 Ausbeuten wurden mit einem stöchiometrischem $\text{NO}_2/\text{C}_3\text{H}_6$ Verhältnis von 4 erzielt. Die Selektivität zu N_2 wird bestimmt durch die kompetitiven Reaktionen von NO_2 mit dem Koks, die Bildung von Koks durch Sauerstoff die partielle Oxidation von C_3H_6 durch NO_2 und die selektive Bildung von N_2 . Die Ergebnisse legen nahe, dass die höchste N_2 Ausbeute bei sehr kleinen Propen Einsatz Konzentrationen liegt. Eine Extrapolation der N_2 Selektivität zeigt, dass bei sehr geringer Propen Einsatz Konzentration eine maximale N_2 Selektivität von 50% erreicht werden kann.

In Kapitel 3 wurde die Reduktion von NO_2 durch C_3H_6 und C_3H_8 über H-Y, H-USY, H-MOR und H-ZSM5 untersucht. Das optimale Konzentrationsverhältnis zwischen Propen und NO_2 war unabhängig vom Zeolithtyp 1:4. Bei kleineren Verhältnissen war die N_2 Selektivität praktisch konstant, mit unterschiedlichen Werten für die einzelnen Zeolithe. Unter diesen Bedingungen zeigte H-MOR die höchste N_2 Selektivität, gefolgt von H-ZSM5, während H-Y und H-USY eine signifikant niedrigere Selektivität aufwiesen. Die Selektivität hängt ab von einer Kombination aus drei kompetitiven Reaktionen: Bildung und Abbau von wasserstoffarmem Koks, Hydrolyse von organischen Nitroverbindungen und die selektive Bildung von N_2 . Es wird ein Mechanismus zur Reduktion von NO_2 durch C_3H_6 vorgeschlagen, in dem die H-Form der Zeolithe die Bildung von primären Nitroverbindungen katalysieren, die durch eine

Folge von Umlagerungsschritten Isocyanate, Cyanate, Amine, Amide und Ammoniak produzieren. Die Reduktion von NO_2 durch C_3H_8 verläuft über die Aktivierung des C_3H_8 durch die Bildung eines Carbeniumionenkomplexes auf einem Brønsted Säurezentrum. Danach läuft die Reaktion weiter wie mit C_3H_6 vorgeschlagen.

In Kapitel 4 wurde die Rolle der sauerstoffhaltigen Zwischenprodukte während der Reduktion von NO_2 durch Propen über H-Y Zeolithen durch kinetische Studien und Infrarot Spektroskopie untersucht. Bei niedrigen Temperaturen kann die selektive Oxidation von Propen zu sauerstoffhaltigen Verbindungen führen. Diese bilden zusammen mit NO_2 Azo-Verbindungen, in denen N-N Kupplungen stattfinden und diese durch weiteren Abbau zur Bildung von N_2 führen. Bei höheren Temperaturen sind diese Zwischenprodukte instabil. Hydrolyse von stickstoffhaltigem Rückstand auf der Katalysatoroberfläche führt zur Bildung von Ammoniak, so dass die NO_x Reduktion auf konventionellem Weg über Ammoniak NO_x Reduktion stattfindet.

In Kapitel 5 wurde die Gesamtreaktion von NO zu N_2 in einer sauerstoffreichen Atmosphäre in zwei Stufen: (1) Oxidation von NO zu NO_2 durch Sauerstoff und (2) Reduktion von NO_2 durch Zusatz von C_3H_6 untersucht. Mit Pt/ZSM5 für den oxidativen Schritt und unmodifiziertem γ -Alumina für den Reduktionsschritt konnten hohe N_2 Ausbeuten über eine weite Temperaturspanne erzielt werden. Die Temperaturen für die Oxidations- und Reduktionskatalysatoren wurden unabhängig voneinander variiert. Als Optimum wurde für die Oxidation eine Temperatur von 300°C und für die Reduktion von 450°C gefunden. Die Abhängigkeit der NO_2 Konzentration für die Reduktion über γ -Alumina wurde anhand einer Reihe unterschiedlicher NO/NO_2 Einsatzverhältnisse untersucht. Der Umsatz von NO wurde signifikant erhöht durch die Anwesenheit kleiner Mengen

Chapter 6

an NO_2 . Möglicherweise wird die Umsetzung von NO bei niedrigen Temperaturen erst durch die Bildung von Zwischenprodukten durch NO_2 initiiert. Die Effektivität des Reduktionsmittels, ausgedrückt durch die Ausbeute an N_2 pro umgesetzttem Propen, wies ein Maximum bei ungefähr 1 auf, was in etwa dem Literaturwert entspricht

6.4 Résumé

L'émission de NO_x dans l'atmosphère cause différents problèmes environnementaux tels que les pluies acides, le smog photochimique, la destruction de la couche d'ozone et l'effet de serre. Approximativement trois-quarts de la production totale de NO_x sont dus à des activités anthropogènes, parmi lesquelles la combustion de combustibles fossiles représente plus de 50%. La combustion de combustibles fossiles est en général utilisée pour fournir l'énergie nécessaire à la propulsion d'automobiles, de camions, de trains, de bateaux, d'avions et pour générer de l'électricité dans les centrales électriques ou de la chaleur dans les procédés industriels. Au cours d'une étape de combustion, les NO_x sont formés par oxydation de composés organiques azotés, de HCN ou par oxydation du N_2 présent dans l'air (NO_x thermiques). L'azote peut être efficacement éliminé des composés organiques présents dans les carburants par hydro-traitement, tandis que HCN est uniquement produit lorsque le milieu de combustion est riche en carburant; par conséquent, l'oxydation de N_2 est la principale source de NO_x . Afin de réduire les émissions de NO_x , les gouvernements du monde entier ont installé de nouvelles législations, telles que le "clean air act" de 1971 aux USA ou les normes européennes Euro I-IV qui ont initié le développement de technologies de réduction des NO_x . Le développement, dans les années 70, du procédé de réduction catalytique sélective utilisant NH_3 , a permis la réduction des NO_x provenant de sources fixes. Les NO_x thermiques peuvent être efficacement éliminés des gaz d'échappement contenant des quantités stoechiométriques d' O_2 par réduction avec

le CO ou l'H₂ (catalyseur 3 voies). Les gaz d'échappement des véhicules à moteur diesel contiennent un excès d'O₂ ce qui nécessite le développement de nouvelles technologies. L'utilisation d'hydrocarbures pour la réduction de NO apparaît prometteuse et une recherche considérable a été menée dans cette direction ces 20 dernières années, sans résultat satisfaisant cependant jusqu'à présent.

Les sites acides de Brønsted des zéolites échangées avec des métaux sont considérés avoir une grande influence sur l'amélioration des performances catalytiques de tels matériaux. Une connaissance approfondie de l'influence de ces sites de Brønsted est importante pour le développement de catalyseurs plus efficaces dans la réduction des NO_x. Le but de cette recherche était d'obtenir des informations sur le rôle des sites acides de Brønsted dans la réduction des NO_x et plus particulièrement sur la réduction de NO₂ par des hydrocarbures légers.

Au chapitre 2, la réduction de NO₂ par le propène sur des zéolites H-Y et H-Y traitées à la vapeur a été étudiée par spectroscopie Infra-rouge *in situ* et grâce à des mesures cinétiques. Les zéolites H-Y sont très actives pour cette réaction, convertissant tout le NO₂ présent à des températures entre 150 et 600°C. A basses températures, C₃H₆ réagit facilement avec NO₂ pour former des composés oxygénés, CO, CO₂, H₂O et des composés organiques azotés tels que des oximes, des isocyanates, des cyanures ou des composés nitro-organiques. La présence d'O₂ accroît la formation de dépôts de carbone et la combustion non-sélective de C₃H₆. Les résultats indiquent que O₂ ne joue pas un rôle crucial dans la formation de N₂. Des rendements optimaux de N₂ ont été obtenus quand un rapport stoechiométrique de 4 à 1 était utilisé entre NO₂ et C₃H₆. La sélectivité en N₂ est déterminée par la compétition entre la réaction de NO₂ avec le coke, la formation du coke par O₂, l'oxydation partielle de C₃H₆ par NO₂ et la formation sélective de N₂. Les résultats indiquent qu'une sélectivité optimale en N₂ est obtenue pour des concentrations en

Chapter 6

C_3H_6 extrêmement basses. Une extrapolation de la sélectivité en N_2 indique qu'un maximum de 50% peut être obtenue en utilisant une concentration en propène extrêmement basse.

Au chapitre 3, les résultats concernant l'étude de la réduction de NO_2 par C_3H_6 et C_3H_8 en utilisant H-Y, H-USY, H-MOR et H-ZSM5 sont reportés. Des expériences de spectroscopie Infra-rouge *in situ* et des mesures cinétiques ont été menées. En augmentant la concentration de C_3H_6 et en gardant la concentration de NO_2 et la température constantes, NO_2 et C_3H_6 réagissent dans un rapport stoechiométrique de 4 NO_2 pour 1 C_3H_6 . Ce rapport est indépendant de la nature du matériau zéolitique utilisé. Pour des rapports $C_3H_6:NO_2$ inférieurs à 1:4, la sélectivité en N_2 reste quasiment constante pour un type de matériau donné mais varie suivant le type de zéolite étudié. Dans ces conditions, H-MOR avait la plus haute sélectivité en N_2 , suivie de près par H-ZSM5, alors que H-Y et H-USY avaient une sélectivité sensiblement plus faible. La sélectivité était liée à une combinaison de trois réactions concurrentielles: la formation et l'élimination de coke appauvri en hydrogène, l'hydrolyse de composés nitro-organiques et la formation sélective de N_2 . Un mécanisme de réduction de NO_2 par C_3H_6 est proposé: zéolites H catalysent la formation de composés nitro-organiques primaires, qui se réarrangent par une série de réactions et forment des isocyanates, des cyanures, des amines, des amides et de l'ammoniaque. La réduction de NO_2 par C_3H_8 se passe par une activation initiale du propane qui forme un complexe ionique carbenium à niveau d'un site acide de Brønsted. Après cette activation, la réaction se poursuit suivant un mécanisme similaire à celui proposé pour la réduction de NO_2 par C_3H_6 .

Au chapitre 4, le rôle d'intermédiaires oxygénés de la réduction de NO_2 par le propène sur des catalyseurs zéolitiques H-Y est étudié par spectroscopie Infra-rouge et par mesures cinétiques. Aux plus basses températures, l'oxydation

sélective du propène conduit à la formation de composés oxygénés. Ces derniers réagissent avec NO_2 pour former des espèces intermédiaires de type azo, dans lesquels une liaison N-N s'est formée et qui se décomposent consécutivement pour former N_2 . Aux plus hautes températures, de tels intermédiaires dérivés de produits oxygénés ne sont pas stables. L'hydrolyse de résidus contenant de l'azote à la surface des catalyseurs conduit à la formation de NH_3 et la réduction des NO_x est alors accomplie par la réaction conventionnelle des NO_x avec NH_3 . La consommation non-sélective de l'hydrocarbure réducteur se produit par l'intermédiaire de composés oxygénés qui réagissent pour former des oxydes de carbone; l'efficacité de cette réaction influence l'efficacité d'ensemble de la transformation des NO_x en N_2 .

Au chapitre 5, la réduction totale de NO en N_2 en présence d'un large excès d'oxygène a été étudiée en deux étapes séparées: (1) l'oxydation de NO en NO_2 par O_2 et (2) la réduction de NO_2 en N_2 avec l'addition intermédiaire de propène. En utilisant Pt/ZSM5 comme catalyseur de l'étape d'oxydation et $\gamma\text{-Al}_2\text{O}_3$ pour l'étape de réduction, un haut rendement en N_2 a pu être obtenu pour une large gamme de températures. La température des catalyseurs d'oxydation et de réduction était variée indépendamment et un rendement optimal a été obtenu pour une température d'oxydation de 300°C et une température de réduction de NO_2 en N_2 de 450°C . L'influence de la concentration en NO_2 (étudiée en variant le rapport NO/NO_2) sur la réduction de NO a été testée sur $\gamma\text{-Al}_2\text{O}_3$. La conversion de NO était considérablement augmentée par la présence de petites quantités de NO_2 . Il est suggéré que la conversion de NO aux basses températures est activée par la formation d'intermédiaires résultant de la réaction de NO_2 avec le propène. L'efficacité du réducteur, exprimée par le rendement en N_2 par molécule de propène consommée, a un maximum proche de 1, ce qui est en accord avec les maxima reportés dans la littérature.

Curiculum Vitae

Martin Lucas Smidt was born on the 9th of October 1971 in Apeldoorn, The Netherlands. In 1989 he finished high school with a distinction in Mathematics, Physics and Chemistry. He continued at the Hogeschool Enschede where he studied Chemical Technology with the distinction in Material Sciences and Process Engineering which he finished in 1993 after which he continued his studied in the same area of interest at the University of Twente which he completed in 1997 with a doctoral project on “Partially exchanged Mordenite for the synthesis of ethylamines” in the group of professor J. A. Lercher. In 1998 he accepted a PhD position in the group of professor J. A. Lercher, initially at the University of Twente, later moving to the Technische Universität München where he started a research on the reduction of NO_x from diesel and lean burn engines of which the results are described in this thesis.

List of Publications

Veefkind, V. A., **Smidt, M. L.**, Lercher, J. A., “On the role of strength and location of Bronsted acid sites for ethylamine synthesis on mordenite catalysts”, Applied Catalysis A - General 194 (2000) 319-332.

Maisuls, S. E., Lefferts, L., Seshan, K., Furusawa, T., Aika, K., Mosqueda-Jimenez, B. I., **Smidt, M. L.**, Lercher, J. A., “Selective reduction of NO_x with propylene in the presence of oxygen over Co-Pt promoted H-MFI and H-Y”, accepted in Catalysis Today 2003.

Smidt, M. L., Schenkel, R., Seshan, K., Lercher, J. A., “Reduction of NO₂ by propene over parent and steamed NaH-Y zeolite“, in preparation.

Smidt, M. L., Seshan, K., Lercher, J. A., “Reduction of NO₂ by C₃H₆ and C₃H₈ over H-form zeolites “, in preparation.

Smidt, M. L., Seshan, K., Lercher, J. A., “Role of oxygenated intermediates in the reduction of NO₂ over NaH-Y zeolite“, in preparation.

Smidt, M. L., Seshan, K., Lercher, J. A., “Kinetic study on the reduction of NO using separated oxydation and reduction catalysts“, in preparation.